1969

A model of accommodative-pupillary dynamics

Stanley Gordon Day
Iowa State University

69-15,607

DAY, Stanley Gordon, 1939-

A MODEL OF ACCOMMODATIVE-PUPILLARY DYNAMICS.

Iowa State University, Ph.D., 1969
Engineering, electrical

University Microfilms, Inc., Ann Arbor, Michigan

A MODEL OF ACCOMMODATIVE-PUPILLARY DYNAMICS

by

Stanley Gordon Day

A Dissertation Submitted to the

Graduate Faculty in Partial Fulfillment of

The Requirements for the Degree of

DOCTOR OF PHILOSOPHY

Major Subject: Electrical Engineering

Approved:

Signature was redacted for privacy.

In Charge of Major Work

Signature was redacted for privacy.

Head of Major Department

Signature was redacted for privacy.

Dean of Graduate College

Iowa State University
Of Science and Technology
Ames, Iowa

1969

TABLE OF CONTENTS

DEDICATION

This dissertation is dedicated to

Sandra R. Day

and

Dr. and Mrs. Luther W. Day

and in memory of

Dr. and Mrs. Walter G. Day

and

Dr. and Mrs. Isaac H. Day

INTRODUCTION

In electrical engineering, systems theory has provided new methods usable in engineering analysis. Systems theory can be subdivided into linear and nonlinear theory, the former being a subclass of the latter. Linear systems theory is well established since it is based on the theories of linear differential equations. Nonlinear systems theory is a very dynamic area and remains a challenge to engineers and mathematicians alike. Nonlinear systems are more difficult to analyze due to the small number of constraints. They are, however, more representative of the systems that one would encounter in the physical and biological world.

Linear systems theory is well developed and therefore a basic tool in analysis. Many engineers have tried to apply these techniques to the analysis of biological systems. In many biological systems it is difficult to find a suitable input or test signal to the system which will not disturb the normal anatomy and physiology of the system. The examination of a biological system may or may not alter its function. The experimental results must be modified in order to account for the effects of the testing procedure.

The human eye is an ideal biological system for study. If light is used as an input and pupillary diameter as an output, the pupillary response of the eye to light can be measured without the use of drugs or surgical intervention. Light levels can be controlled so that no retinal or lenticular damage results. The pupil of the eye is then responding to a controlled light level. The control signal used to investigate a biological system must be chosen so that input and output information

will lead to the determination of the system's characteristics. For example, the controlled signal might be an impulse, a step, a ramp, a double step, a sine wave, a square wave, a random variable or some other test signal.

The determination of the proper input is dependent on the nature of the system being examined. For example, if a subject tries to focus on a target whose distance from his eye is varying sinusoidally, his eye will easily fatigue. For a linear system, the same information obtained from a series of sinusoidal waveforms can be obtained from a single response where the input is a step function. In either case the system must be observed until it reaches a steady-state. The step input is less taxing to the subject than the sinusoidal input. If the input were an impulse function, the subject might never have a chance to respond even if the duration of the impulse were equal to one-fifth of the shortest time constant of the system. The problem is that many biological systems do not respond immediately to a step function due to a voluntary or involuntary time delay, the latter resulting from limited signal velocities over neurological pathways. Many times the time delay will be longer than the duration of the impulse.

This dissertation is an attempt to use linear systems theory to obtain an understanding of one phase of the human visual system; the dynamics of the accommodative-pupillary system. The investigations demonstrated that this system is highly nonlinear. Several nonlinearities which are considered are the static relationship between the pupillary diameter and the accommodative level, the asymmetry in the constrictive

and dilatative dynamics and the nonlinearities in the constrictive and dilatative dynamics. The resulting mathematical model is a functional approximation to the living system and does not have a one-to-one correspondence with its anatomical structure. This model is a first step in the understanding of the accommodative-pupillary system. The model has not been simulated and tested with other inputs such as a ramp function. It is possible that the response of the accommodative-pupillary system to a ramp input would demonstrate a significant change in the basic parameters of the system and thus require a more complex model to account for this difference.

The IBM 1800 digital computer was a fundamental part of this research project. It was used in conducting the sequencing of experimental maneuvers and in analyzing the resulting data.

REVIEW OF LITERATURE

The following review of literature includes selected articles covering historical and modern aspects of the accommodative-pupillary system. The review is presented in five parts: The Accommodative System, The Pupillary System, The Accommodative-Pupillary System, Related Physiology, and Engineering Methods of Analysis.

The Accommodative System

The optical characteristics of the eye change during the act of focusing. The act of focusing is defined as accommodation.

Two excellent references on the structure and function of the eye are by Davson (26) and Duke-Elder (27). Classic works on accommodation can be found in Allen (2), Alpern (6), Duke-Elder (27), Fincham (31), and Morgan (46). Current information on accommodation can be found in Adler (1), Alpern (6), Guyton (36), Ruch and Patton (53), and Westheimer (71).

Stimuli to accommodation

There is controversy concerning valid stimuli to accommodation. Fincham (30) conducted experiments to determine whether or not chromatic aberration and spherical aberration are stimuli to accommodation. Of the fifty five subjects tested, sixty per cent lost the normal reflex in the absence of chromatic aberration. The remaining forty per cent were deprived of spherical aberration and continued to possess a normal reflex. Fincham concludes that chromatic aberration is useful to some subjects as a stimulus to accommodation.

Campbell (16) states that the conscious awareness of an object assists in correcting accommodation. He also states that accommodation can be changed without knowledge of the object distance from the eye by placing before the eye a low power negative lens. This change of vergence of light occurs rapidly without conscious effort of the subject. Campbell then states that this reaction may be classed as a reflex. Allen (5) conducted experiments minimizing all accommodation cues except blur. When the eye is not focused on an object, the retinal image is blurred. An appropriate change in the dioptric power of the flexible lens of the eye will reduce this blur until the object is in focus. Blur can be defined as the magnitude of dioptric correction needed by the eye to achieve an acceptable focus upon an object. This definition will apply to the word "blur" as it is used throughout the dissertation.

The experiments of Allen (5) did not allow the targets to change size, color, brightness, or lateral position and no binocular parallax was present. He concludes that retinal blur must be an accommodative stimulus. Due to different reaction times involved in correcting an error, a conscious effort and not a reflex is indicated. Campbell and Westheimer (19) conducted experiments designed to evaluate current theories concerning accommodative stimuli. They conclude that chromatic aberration helps some subjects to detect the direction of blur. They demonstrate that monochromatic light causes subjects to make errors. They conclude that the asymmetry of bidirectional blur, when astigmatism is present, also acts as a clue. They also found that the responses of subjects deprived of spherical and chromatic aberration are not always

correct. Ripps et al. (52) demonstrate that if an artificial pupil whose diameter is equal to or less than 1.5 mm is placed in front of the eye, the accommodative and convergence responses decrease. Alpern (7) concludes that refractive fluctuations might act as an accommodative stimulus. In summary, chromatic aberration, blur, and astigmatism are important clues to accommodation.

Fluctuations of accommodation

A sensitive optometer demonstrates that the refractive state of the eye is in constant fluctuation. Alpern (7) investigated these fluctuations and concludes that their limits are proportional to the retinal change in light intensity divided by the initial intensity. Campbell et al. (17) state that when a young adult subject fixates on a near target, the refractive power constantly fluctuates. These fluctuations disappear when the subject views a target at infinity or when a cycloplegic agent is administered. Harmonic analysis shows that for the small pupil, the dominant frequency components are in the 0-0.5 Hz. region and with a large pupil, in one or more narrow bands near 2.0 Hz. Campbell (15) demonstrates that random fluctuations in the right and left eyes are highly correlated. He concludes that most of the residual tremor must arise at, or central to, the point where the two oculomotor nerves are functionally conjoint.

Analysis of accommodation

Carter (20) and Warshawsky (70) applied servoanalysis to the accommodative system. Carter concludes that the accommodative response is approximately exponential and follows a time delay. He does not succeed in deriving a transfer function for the system. Warshawsky presents a model of the accommodation system. He concludes that accommodation error is detected through the integrated response of derivative photoreceptors in the bouquet of cones.

Stark et al. (66) used automatic control theory to study the accommodative control system. They modelled the system as a nonlinear, unity feedback control system using blur as the error signal. Brodkey and Stark (12, 13) studied the accommodative convergence system and modelled it as a nonlinear, unity feedback control system.

Basic accommodative dynamics

Stimulation of the accommodative system does not produce immediate response due to time delays in the retina, neuropathways, and the intrinsic ocular muscles. Allen (4) demonstrates that the smooth muscle tissue of the ciliary body has a time delay in the order of 0.1 to 0.2 second or more. He states that the time delay of the internal rectus muscle is negligible, being of the order of 0.001 second. Allen (2) gives an excellent review of the classical experiments concerning time characteristics of accommodation. Allen (3) discusses the equipment used and the results obtained in a study concerning the speed of accommodation. He concludes that the time delay is 0.3 second for accommodation and 0.2 second for convergence. In all instances, up to two diopters (D) of

accommodation occur within one second. Allen (5) reestablished the accommodative time delay as 0.343 second. Campbell and Westheimer (18) report that the time delay for an accommodative response to a near stimulus is 0.31 second. They also state that the maximum velocity recorded during a 2.0D response is about 10.0D per second. Carter (20) states that the initial accommodative response to an optical step of 1.0D, either positive or negative, follows a time delay of up to 0.425 second. The corresponding value for repetitive data is 0.24 second for positive accommodation and 0.2 second for negative accommodation. He reports that the transient accommodative response is approximately exponential and that the time constant for positive accommodation is approximately 0.275-0.325 second. The corresponding range for negative accommodation is 0.250-0.346 second. Stark et al. (66) determined the time delay for far-to-near accommodation as 0.36 second and for near-to-far accommodation as 0.38 second. O'Neill and Stark (51) state that the time delay for a 5.0D to 8.0D stimulus is 0.43 second and for an 8.0D to 5.0D stimulus the time delay is 0.4 second. In summary, little information is available concerning the dynamics of the accommodative response to an accommodative stimulus. The current value of the accommodative time delay is in the neighborhood of 0.4 second.

The Pupillary System

Classical and modern information

The pupil of the human eye is formed by the inner border of the pigmented iris. It serves three main functions: it controls the amount

of light entering the eye, it increases the depth of focus of the eye by decreasing the aperture of the optical system and it reduces chromatic and spherical aberrations.

The normal pupillary diameter varies between two and eight millimeters. With the use of drugs these limits can be extended to 1.3 mm (miosis) or to 10 mm (mydriasis).

Information on the pupil can be found in Lowenstein and Lowenfeld (41) and Duke-Elder (27). Current information on the pupil can be found in Adler (1), Ruch and Patton (53), Guyton (36) and Westheimer (71).

Stimuli to the pupil

Light is a familiar stimulus to the pupil. Jones (38) states that fear, emotion, eye irritation and accommodation act as additional stimuli to the pupil. Naquin (49) states that Father Paul of Venice (17th Century) is usually given credit for discovering the light reflex. He also states that Douglas Argyll Robertson (1869) reported a series of cases in which there was loss of the reflex to light stimuli but preservation of constriction to accommodative convergence. Young and Biersdorf (68) discuss the light reflex.

Pupillary fluctuations

The pupillary diameter undergoes constant fluctuations. Stark et al. (63) demonstrate that pupillary fluctuations of the right and left eye are highly correlated. Stanten and Stark (58) examine these fluctuations and conclude that they have Gaussian characteristics. A

model is given and high correlation of the right and left pupillary fluctuations is shown.

Analysis of the pupillary reflex to light

Stark and Sherman (65) discuss the open- and closed-loop characteristics of the pupillary reflex to light. A transfer function is derived and a time delay of 0.18 second is established. Additional work on this system is reported by Stark (59, 60, 61), Stark and Baker (62) and Stark and Cornsweet (64). Electronic Associates, Inc. (28) demonstrate how to simulate the above transfer function on an analog computer. Clynes (22) develops differential equations describing the pupillary response to light and introduces the concept of unidirectional rate-sensitivity. He also demonstrates nonlinearities in this system. Baker (10) examines the light reflex using double-pulse stimulation and applies nonlinear analysis to the system.

Basic pupillary dynamics

The simulation of the transfer function deduced by Stark and Sherman (65) leads to characterization of pupillary responses in the time domain. The dynamics of the pupillary reflex to light can be obtained from these responses. Each response will contain a time delay of 0.18 second. Campbell and Westheimer (18) report time delays of 0.24-0.26 second for the pupillary reflex to light. O'Neill and Stark (51) cite the unpublished work of Troelstra and state that he recorded time delays of about 0.24 second for the pupillary reflex to light. It should be

noted that the time delay for the pupillary reflex to light is shorter than the 0.4 second time delay for the accommodative response to an accommodative stimulus.

The Accommodative-Pupillary System

Classical and modern information

The purpose of this research is to investigate a specific input-output relationship of the accommodative-pupillary system. The static and dynamic relationships between the pupillary diameter and the accommodative level are investigated. The nature of the pupillary response to an accommodative change suggests that it is a reflex action. This response is called the "near reflex" of the eye although it is questionable as to whether or not it is a true reflex. Marg and Morgan (42) discuss the history of the near reflex and state that it was first noted by Christorphoro Scheiner in 1619. They conclude from their experiments that it is dependent on accommodation and not on convergence. Fry (33) discusses the history of the near reflex and its relation to accommodation and convergence. He cites classical papers by Weber (1851), Cramer, Donders (1864) and Le Conte (1869) and states that other investigations of this type are referred to by Duke-Elder: Borthern (1892), Guillery (1892), Seggel (1895) and Moderow (1905). Fry's experiments indicate that changes in pupillary size induced by accommodation are not as great as when accommodation is accompanied by changes in convergence. He concludes that pupillary constriction, accommodation and accommodative convergence are all related. Duke-Elder (27) discusses the near reflex

and concludes that the pupillary reaction may occur with either accommodation or convergence with the other excluded, but of the two, the pupillary reaction is more nearly associated with convergence. Naquin (49) cites historical references on the near reflex and states that pupillary constriction to accommodative convergence was described by Porterfield (1759). Lowenstein and Lowenfeld (41) conclude that accommodation, convergence and pupillary constriction are associated, synchronized and controlled by supranuclear connections; they are not caused by one another. Additional discussions on the near reflex can be found in Adler (1), Campbell and Westheimer (18), Ruch and Patton (53), Guyton (36) and in Westheimer (71).

Static relationships of the accommodative-pupillary system

The static relationship of the accommodative-pupillary system involves pupillary diameter as a function of accommodative level. This relationship must be determined for a fixed level of light since light is a stimulus to the pupil. Knoll (39) studied the nonlinear relationship between the pupillary diameter and accommodation resulting from experiments in a dark room. Alpern et al. (8) established a static curve for the accommodative-pupillary system using normal room illumination. This curve is reprinted by Alpern (6). Similar curves for presbyopes are given by Alpern and Jardinico (9).

Dynamics of the accommodative-pupillary system

Campbell and Westheimer (18) discuss the dynamics of accommodation and of the pupil. They state that the time delay in the pupillary

response to light is 0.26 second and for eye movements it is 0.12 second. They also discuss the physiology of accommodative apparatus. For example, they state that the pupillary response to light is predominately if not entirely due to contraction of the sphincter muscle of the iris. It has a close affinity to the far-to-near accommodation response in the neural and muscular aspects of the effector system. They state that both responses are mediated by the third nerve parasympathetic pathways via the ciliary ganglion. They also discuss the near reflex of the pupil and conclude that while the pupillary light reflex follows an uncomplicated pathway involving the pretectal area, the near response of the pupil shares a central pathway with the accommodative and convergence reactions. The complete neurological pathways involved require further characterization. They conclude that one would expect the pupillary response to shift to a near target to have a time delay longer than that of the simple pupillary reflex to light. In fact, it would have a time delay comparable to that of the accommodative response to a near target. They conducted experiments on the near reflex using optical switches with equal light intensity and found a mean time delay of 0.32 second for the pupillary response to a near target and a mean time delay of 0.30 second for an accommodative response to a near stimulus. Pupillary responses to light measured on the same subject at the same session had a mean time delay of 0.24 second. They conclude that the difference in time delay between the two kinds of pupillary responses indicates that the pupillary response to a near target involves a longer central component. The time delay for a convergence response was 0.20 second and they concluded that if conver-

gence, accommodation and pupil responses to a near target share the same afferent, and most of the central pathways, then the longer time delay of the last two responses is a consequence of a long time delay component in the peripheral accommodative and pupillary effector mechanisms. These experiments were conducted under conditions of monocular vision. They also state that the maximum velocity recorded during a 2.0D response was 10.0D per second.

Related Physiology

The following is a brief discussion of the neuroanatomy and neurophysiology of accommodation, pupillary constriction and dilatation. Additional information can be found in Adler (1), Alpern (7), Duke-Elder (27), Guyton (36), Lowenstein and Lowenfeld (41) and Ruch and Patton (53).

Accommodation

Adler (1) states that changes in the refractive power of the lens (accommodation) are caused by changes in the length of the ciliary muscle. He states that there are three groups of muscle fibers which make up the whole of the ciliary muscle. These are the meridional bundle, a radial portion and a circular portion. He states that the ciliary muscle is innervated by parasympathetic fibers running in the oculomotor nerve and that the cells serving this muscle probably lie in the Edinger-Westphal nuclei. In addition, he states that evidence is available to support the involvement of the sympathetic nervous system in the innervation of the ciliary muscle and that since involuntary muscles

are involved, the parasympathetic and sympathetic nervous systems might be mutually antagonistic. Many organs in the body are innervated in this reciprocal manner. For example, stimulation of parasympathetic fibers to the heart causes cardiac deceleration whereas stimulation of the sympathetic fibers innervating the heart causes cardiac acceleration. In conclusion, he states that the iris is innervated by the sympathetic and parasympathetic systems, the latter supplying the sphincter pupillae muscle and the former the dilator pupillae muscle. He also concludes that the ciliary muscle should not be an exception to the general finding of dual innervation of unstriated muscle in the body.

Alpern (7) states that the ciliary muscle is richly supplied with nerves, probably from both the sympathetic and parasympathetic division of the autonomic nervous system. He also states that when the eye focuses at infinity, part of the ciliary muscle innervated by the parasympathetic nervous system is relaxed. In addition, he states that impulses in these nerves cause the release of acetylcholine which in turn initiates the contraction of the ciliary muscle. Adler (1) and Alpern (7) give excellent discussions concerning the historical aspects of accommodation. It is established that the ciliary muscle complex is responsible for accommodative changes in the human eye.

Pupillary constriction and dilatation

The iris is composed of two basic muscles, the sphincter pupillae muscle and the dilator pupillae muscle. Adler (1) states that the sphincter pupillae muscle is a typical sphincter muscle composed of

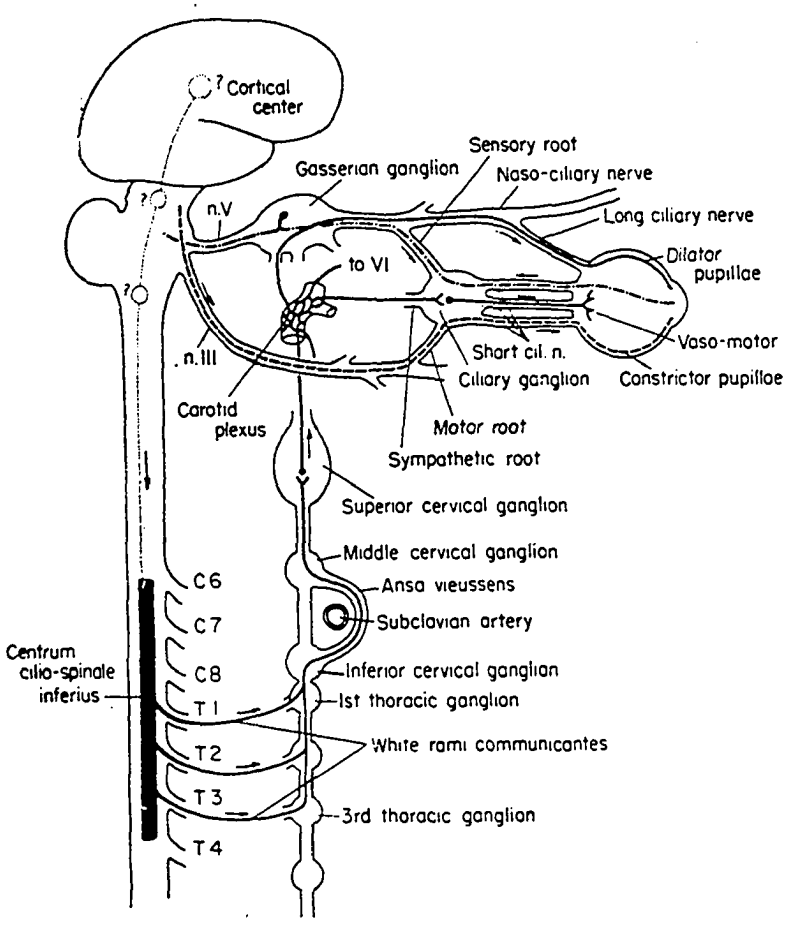

Figure 1. The neuropathways for pupillary constriction and dilatation (Adler 1, p. 194)

unstriated fibers. It lies in the posterior iridal stroma just in front of the pigmented epithelium and next to the margin of the pupil. When fully constricted, the normal pupil may be 1.5 mm in diameter and with maximal dilatation it may be 8 mm in diameter. The sphincter muscle is supplied by a branch of the oculomotor nerve. This branch runs to the ciliary ganglion and from there to the eyeball. The short ciliary nerves leaving the ciliary ganglion contain only postganglionic parasympathetic fibers.

The dilator pupillae muscle extends from the ciliary border of the sphincter muscle to the root of the iris. These muscles are innervated by sympathetic fibers. Adler (1) states that centers for the origin of sympathetic impulses are probably located in the hypothalamus. Fibers then extend down the spinal cord as far as the eighth cervical and first thoracic nerve roots. Fibers leave the cord with these roots and proceed as white rami communicantes to the superior thoracic ganglion. The fibers then ascend the sympathetic chain as far up as the superior cervical ganglion forming a synapse with the cells of this ganglion. Adler (1) states that fibers then proceed to the dilator muscle by two routes. First of all, fibers run from the superior cervical ganglion to the gasserian ganglion and join the nasal branch of the ophthalmic division. Then they follow the nasal branch to the point where the two long ciliary nerves are given off. Here they follow the long ciliary nerves and penetrate the sclera, entering the suprachoroidal space where they form a plexus from which fibers proceed to the dilator muscle. In the second pathway fibers given off from the superior cervical ganglion run to the various plexi on the branches of the internal carotic

artery. One of these is the cavernous plexus which sends a fine branch to the ciliary ganglion. Sympathetic fibers run to the ciliary ganglion and enter the eyeball with the short ciliary nerves along with the fibers destined for the sphincter muscle. Adler (1) continues by noting that the sphincter and dilator muscles are antagonistic and have generally been thought to exhibit reciprocal innervation. He states that some authors do not accept the concept of this reciprocal relationship. Figure 1 illustrates the neuropathways for pupillary constriction and dilatation.

This is a brief discussion on the physiology of the pupil and accommodation. A description of the nervous innervation of the ciliary and iridal muscles is given. As indicated, further research is needed to identify unequivocally these pathways and their methods of operation.

Engineering Methods of Analysis

Linear systems analysis

The accommodative-pupillary system is a nonlinear system. It does not conform to the most basic theorem of linearity which is the principle of superposition. The principle of superposition requires that if $ac_1(t)$ is the response to $ar_1(t)$ and $bc_2(t)$ to $br_2(t)$, then the response to $ar_1(t)+br_2(t)$ is $ac_1(t)+bc_2(t)$ for all a and b. In addition, if a linear system is excited by a sinusoidal signal of a given amplitude and frequency, the system output will be a sinusoidal signal of the same frequency, but it may have a different amplitude and phase. The sine wave is important as an input since it can be subjected to linear operations such as differentiation, integration, multiplication by a

constant, addition of a constant, etc., and retain its sinusoidal nature. Brown and Nilsson (14) state that if the input to a linear system whose transfer frunction is $Y(s)$ is $r(t) = A\sin(\omega t+\theta)$, the system steady-state output will be $c(t) = A|Y(j\omega)|\sin(\omega t+\theta+\phi(\omega))$ where $\phi(\omega)$ is by definition the phase angle of $Y(j\omega)$. Note that the frequency of the output and input sine waves are identical. The output of a linear system cannot contain components at frequencies not present in the input.

Truxal (67) states that the stability of a linear system is clearly defined. The system is either stable or unstable. The unexcited stable system eventually comes to rest whereas the output of the unstable system grows without bound, either exponentially or in an oscillatory mode with the envelope of the oscillations increasing exponentially. The driving functions and the initial conditions have no effect on the stability of a linear system. The above statements are characteristic of a linear system and can be used to determine whether or not an unknown system is linear or nonlinear. Kuo (40) states that all physical systems are nonlinear to some extent and that the ideal linear system does not exist. He also states that it is only for the sake of the mathematics involved that the linear equivalence of a physical system is introduced.

Nonlinear systems analysis

The nonlinear system is more representative of the physical world. The mathematical treatment of nonlinear systems is difficult and in some cases impossible. A great deal can be learned about a nonlinear system

by testing it as if it were a linear system. For example, a nonlinear system does not obey the principle of superposition and frequency components present in the output may not be those of the input. Gibson (34), Kuo (40) and Truxal (67) discuss these and other factors useful in identifying a nonlinear system.

In this present investigation three different tests were used to examine the nonlinearities in the accommodative-pupillary system. The first test examined the DC relationship between pupillary diameter and the accommodative level. This led to the determination of the nonlinear DC response of the system. The second test examined the system response to "on" and "off" step inputs. This test examined the asymmetry in the response dynamics. The third test examined changes in the response dynamics as a function of blur. It should be noted that a 4.0D step will cause a retinal blur which can be represented as 4.0D of blur. These three methods will be discussed in more detail in later sections.

Application of nonlinear analysis to biological systems

Two useful approaches to the analysis of nonlinear systems are describing-function and phase-plane analyses. These methods are discussed by Clark (21), Gibson (34), Kuo (40), Seifert and Steeg (56), Sridhar (57) and Truxal (67). Stark et al. (66) applied describing-function analysis to the accommodation system. They modelled this system as a unity feedback control system utilizing blur in diopters (D) as the error signal. Brodkey and Stark (12, 13) applied describing-function analysis to the accommodative convergence system. This system was also

modelled as a unity feedback control system utilizing blur in diopters (D) as the error signal.

EQUIPMENT AND METHODS

The TV Pupillometer

The TV Pupillometer[1] is a research tool developed to study the pupillary responses of the eye. It was developed by Dr. Lawrence Stark while at the Presbyterian-St. Luke's Hospital in Chicago, Illinois.

Figure 2 shows a picture of a prototype pupillometer which was used throughout the research project. The pupillometer has been used to study the pupillary responses of cats and humans, but actually can be used on all animals exhibiting pupillary dynamics.

The pupillometer was used on several human subjects. The experimental data presented in this dissertation was obtained from one human subject. The male subject (J. L., 20 years old) was trained for two weeks. He made few errors during the experiment. The subject responded to step changes in accommodation. Binocular vision was permitted throughout the experiments.

The stimulus presented to the subject was a moving illuminated target mounted on the pen-holder bracket of an X-Y recorder[2]. This recorder was mounted up-side-down in front of the subject in a position elevated slightly above his head. The X-axis of the recorder was disabled. Only Y-axis motions were allowed. The stimulus target travelled thru a distance

---

[1] Information on current models of the TV Pupillometer can be obtained from Lawrence Stark, M.D., Professor of Physiological Optics, University of California, Berkeley, California 94720.

[2] Moseley Autograph Model 2DR-2, Hewlett-Packard Company, 1501 Page Mill Road, Palo Alto, California 94304.

Figure 2. An overall view of the experimental setup

of 25.4 cm on the Y-axis of the recorder. Its closest target distance from the eye was 10 cm. Its farthest distance from the eye was 35.4 cm. This range allowed accommodative stimulus levels in the range of 3.0D-10.0D. The line-of-travel of the stimulus target was directly toward and away from the right eye. Throughout this target range the right eye did not undergo nasal or temporal movement. The left eye was required to undergo lateral rotation since its line-of-sight was 10.5 cm to the left of the stimulus target line-of-travel.

The response time of the X-Y recorder was acceptable for steps requiring the stimulus target to travel thru a distance of 0-13 cm on the Y-axis of the recorder. Large steps requiring 13-25.4 cm of travel produced trapezoidal stimulus target responses with respect to the step input due to the velocity-limited servomechanisms of the recorder. The recorder response was initially considered to be a problem. The stimulus levels selected were such that only one set of stimuli (3.0D to 9.0D and 9.0D to 3.0D) required large excursions of the plotter pen-holder assembly. These levels produced a trapezoidal response. All subjects felt that the trapezoidal response was acceptable and that a true step would have little effect on their response. No attempt was made to correct this error.

The stimulus target was a one square centimeter section of a 35 mm slide, chosen so as to encourage critical focusing over the 3.0D-10.0D range. It was illuminated by a small light[3] operating from a direct current voltage source. A one square centimeter piece of ground glass

---

[3] General Electric Miniature Lamp Type 40, General Electric Company, Miniature Lamp Department, Nela Park, Cleveland, Ohio 44112.

was placed between the section of the 35 mm slide and the light source to produce uniform lighting of the stimulus target. The intensity of the light source was adjusted to the desired level by a rheostat. The desired level was the lowest level that allowed critical focusing on the stimulus target over the 3.0D to 10.0D range. The intensity of the light source was reduced to this minimum level in order to minimize changes in the light or dark adaptative processes of the eye. A bright stimulus target would cause retinal adaptation. This would cause the pupillary diameter to drift slowly to a new level. The pupillary diameter would then be a function of two stimuli: the external light level and the level of accommodation. The experimental apparatus was adjusted to minimize the effect of the light stimulus and to establish the accommodative stimulus as the major stimulus to the system.

Davson (26) states that the retina is not as sensitive to red light as it is to white light. Moderate levels of red light have little effect on pupillary diameter compared to moderate levels of white light. For this reason a red lamp was used to allow the experimenter sufficient room illumination to operate the equipment. The subject was allowed 10-15 minutes to undergo dark adaptation to the low level of red light. A black cloth was placed around the back and sides of the X-Y recorder to prevent the subject from observing ambient light or extraneous movements.

The right eye was illuminated with infrared (IR) light. IR light does not act as a light stimulus to the pupil. An IR filter[4] was placed over

---

[4]Kodak Infrared Filter # 87C, Eastman Kodak Company, 343 State Street, Building 205, Rochester, New York 14650.

the light source[5]. The light source was placed in front of the left eye, but directed toward the right eye. It did not interfere with binocular visualization of the stimulus target. The subject's head was supported by a head and chin rest[6]. The right eye was viewed by an infrared TV camera[7] equipped with a modified telephoto lens[8,9]. The focal length of the telephoto lens was decreased by placing a plano-convex lens[9] in front of the telephoto lens. The camera was placed in front of and to the right of the subject's right eye. The TV image of the right eye was then displayed on a 12 inch portable TV set[10] as shown in Figures 2 and 3.

When viewing the television set from the front, the electron beam

---

[5]American Optical Model 359 Universal Illuminator, American Optical Company, 5405 Milton Parkway, Rosemont, Illinois 60018.

[6]Adjustable Head and Chin Rest # 71-91-10, Bausch and Lomb, Inc., 635 St. Paul Street, Rochester, New York 14602.

[7]Sony CVC-2000 Infrared TV Videcon Camera, Sony Corporation of America, 516 W. Florence Avenue, Inglewood, California 90301.

[8]Kern-Paillard Macro-Yvar 100 (F.L.=100 mm, 1:2-8), Paillard, Inc., 1900 Lower Road, Linden, New Jersey 07036.

[9]Plano-Convex Lens (F.L.=187 mm, Dia.=41 mm), American Science Center, Inc., 5700 N. Northwest Highway, Chicago, Illinois 60646.

[10]General Electric Model M150CWH Portable TV, General Electric Company, Vacuum Products Business Section, 1 River Road Building 28-4, Schenectady, New York 12305.

exciting the phosphorescent screen moved from left-to-right. An electronic device was designed to differentiate the beam signal. This produced a signal accenting contrast edges. This signal was rectified allowing only those changes resulting from a decrease in beam intensity to pass. The rectified output passed to a threshold detector which produced an output only if its input had an amplitude equal to or greater than the manually set threshold level. This signal was differentiated and added to the video signal. Changes caused by increases in the beam intensity were not used. The system was in effect, then a unilateral edge detector. The edge detector voltage was then integrated and smoothed.

The regions undergoing sharp changes in contrast were outlined by a bright dot on the scan line. This occurred where the beam intensity decreased to a level acceptable to the threshold detector. For example, assume that the camera is viewing a life-sized artificial pupil. Without the unilateral edge detector, only the pupil will be displayed on the TV screen. It will appear as a dark annular area surrounded by a uniform gray area, the dark area appearing in the center of the screen. One millimeter of the artificial pupillary diameter will be displayed as 0.5 inch on the TV screen. An 8 mm pupil will be displayed as a 4.0 inch pupil on the TV screen. If the unilateral edge detector is used and the threshold control set at a high level (to eliminate noise), one will see the artificial pupil plus a dotted "C" which will occur along the left edge of the pupil from 180° to 360°. This is illustrated in Figure 3.

The smoothed edge detector voltage was proportional to the number of dots forming the "C". A calibration curve relating the pupil diameter

to the resulting voltage was established.

The TV Pupillometer measured the vertical diameter of the pupil. The pupil diameter was independent of peripheral irregularities. The calibration curve was slightly nonlinear and approximated by a straight line. The sensitivity of the pupillometer to pupillary changes was dependent on the number of horizontal lines forming the TV picture (425 lines per 10 inches). This system could detect pupillary changes in the order of several hundredths of a millimeter. The bandpass of the TV Pupillometer was many orders of magnitude greater than that required to monitor the responses of the slow accommodative-pupillary system.

The variation in the pupillometer voltage for a 2 mm to 8 mm pupillary diameter change was 0.4 volt. This output voltage contained 60 Hz. interference. The 60 Hz. interference and other low frequency noise was attenuated by two cascaded, low pass, third-order Butterworth filters. These active filters were simulated on Philbrick analog equipment[11]. The first stage of active low pass filtering had an attenuation of -3db at a frequency of 20 Hz. The second stage of active low pass filtering had an attenuation of -3db at a frequency of 10 Hz.

The interface equipment between the pupillometer and the digital computer used six Philbrick operational amplifiers. The pupillometer output voltage was presented to the first operational amplifier which

---

[11] Philbrick Model 6009, Rack Mounting Operational Manifold and Philbrick Model R-300, Rack Mounting Dual Power Supply, George A. Philbrick Researches, 127 Clarendon Street, Boston, Massachusetts 02116.

Figure 3. The image of the right eye on the TV screen. Note the dotted "C" appearing at the left edge of the pupil

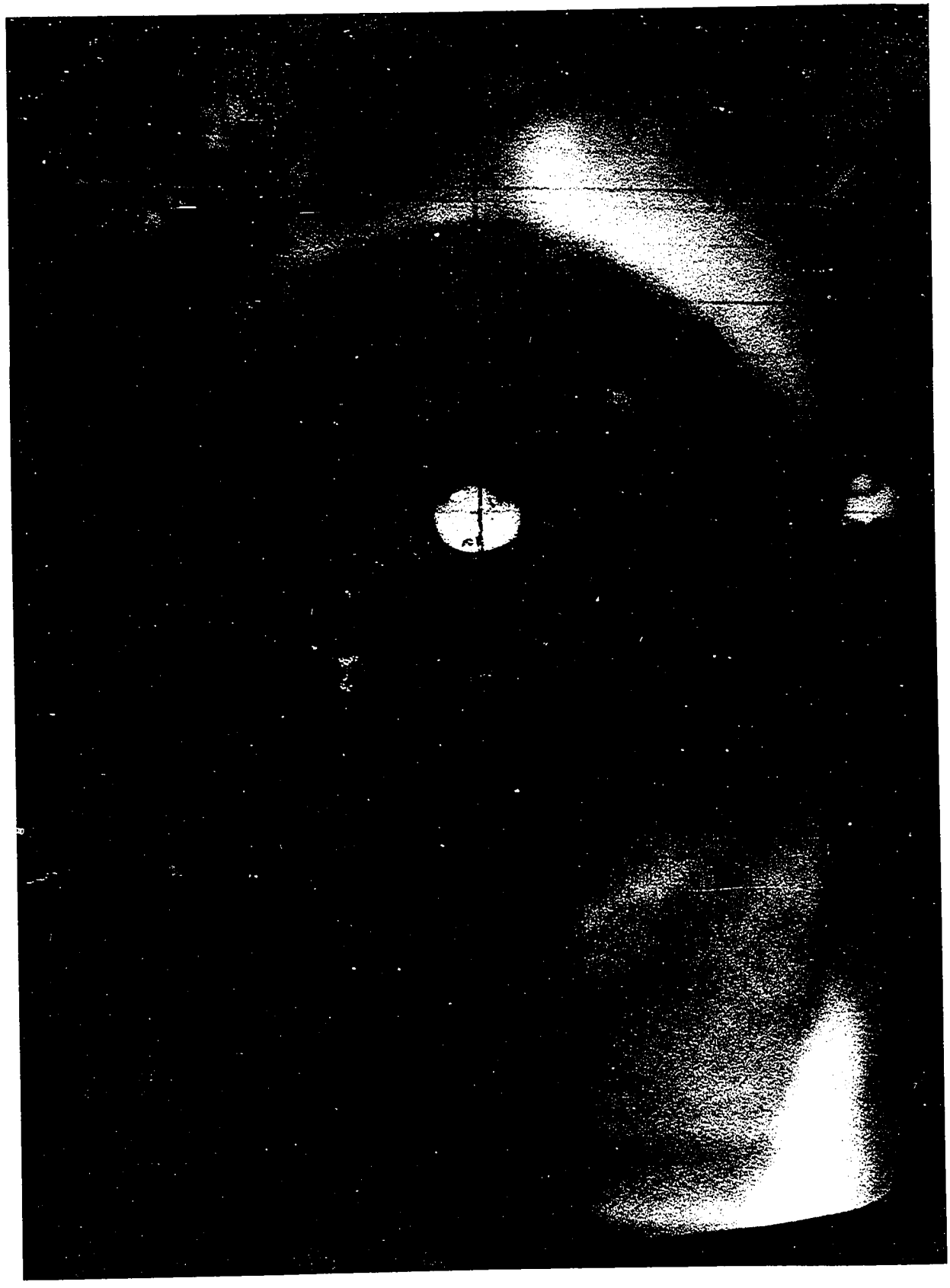

simulated an emitter follower. The output of the emitter follower entered the first stage of active filtering. The simulation of this filter utilized one operational amplifier. The output of this filter was amplified, its bias level was changed and it was again amplified. This required two operational amplifiers. The new output went to the second stage of active filtering. The simulation of this filter utilized one operational amplifier. The output of the second stage of active filtering was amplified. This utilized the sixth operational amplifier.

For a range of 2-8 mm in pupillary diameter, the interface equipment produced an output voltage in the range of 0-5 volts. The interface equipment filtered the pupillometer output and adjusted the voltage levels to a range compatible with the analog-to-digital (A/D) conversion equipment. This range was -5.0 to +5.0 volts. A Bode plot illustrating the frequency response of the interface equipment is given in Figures 7-9. The insert in the lower left-hand corner of the Bode plot shows the step stimulus input and the response output periodic functions. The interface system has an attenuation of -4db at a frequency of 8.0 Hz. This characteristic is acceptable since the pupillary information is restricted to a bandwidth of 0-4.0 Hz. Corrections for the interface phase error are shown in Figures 44-46.

Calibration Technique

The TV Pupillometer was calibrated in the following manner. A four centimeter square piece of millimeter grid paper was placed in the pupillary plane and viewed by the TV camera. The magnified grid was then

displayed on the TV screen. One millimeter on the paper was displayed as 0.5 inch on the TV screen. A black felt pen was used to outline this grid on the face of the TV screen. This is shown in Figure 3. When the subject's pupil appeared on the screen, the scaled grid was superimposed on top of the pupil. It was used to measure the pupillary diameter.

The edge of the pupil rarely fell on a grid line. This made it difficult to measure the pupillary diameter. This problem was avoided by first measuring the diameter of the pupil using calipers and then transferring this measurement to the grid to obtain the pupillary diameter in millimeters. The measurements of pupillary diameter were recorded on magnetic tape by the digital computer. A two-point calibration scheme was used. The calibration was done with the aid of a Teletype and the IBM 1800 digital computer.

A Teletype was placed in the laboratory. Long cables connected the laboratory area and the Teletype to the IBM 1800 digital computer room. The Teletype allowed "on-line" use of the digital computer while the experimenter remained in the laboratory. These connections are illustrated in Figure 6.

The calibration was performed as follows. The Teletype was used to instruct the digital computer to position the X-Y recorder at a stimulus level of 3.0D. Focusing on this stimulus level caused the subject's pupil to dilate. While the subject focused on the 3.0D stimulus, his pupillary diameter was quickly measured with the calipers. A key was simultaneously depressed on the Teletype keyboard and the output voltage of the interface equipment was recorded by the computer. The caliper measurement was then

converted (using the TV grid) to pupillary diameter in millimeters and entered into the computer via the Teletype. The prerecorded interface voltage level was now related to a specific pupillary diameter. A similar measurement was taken at a second stimulus level of 9.0D. This stimulus level caused the subject's pupil to constrict. This calibration technique entered two voltage levels and two corresponding pupillary diameters into the computer. The computer used these values to determine a linear equation between the interface voltage and the pupillary diameter.

The Use of the Digital Computer to Generate the Stimuli

The stimulus used throughout these experiments was accommodation. Focusing on the stimulus target caused changes in accommodation. Changes in the accommodative level of the eye resulted in pupillary changes. The stimulus target moved in a step-function manner and was controlled by a voltage generated by the digital computer. The digital computer voltage was discrete. It passed thru a digital-to-analog (D/A) converter before passing over the trunk lines to the laboratory and to the Y-axis of the X-Y recorder.

Outlets were provided for Teletypes in each laboratory such that "on-line" experiments using the digital computer could be conducted from the laboratory. A maximum of ten stimulus levels could be entered to the digital computer via Teletype. The digital computer would then generate a voltage for each stimulus level such that the recorder stimulus target would move to the corresponding position. For a stimulus level of 10.0D the digital computer would generate a voltage of 7.9 volts which would

move the recorder pen assembly to 25.4 cm. The stimulus target was 10 cm from the right eye. Ten diopters of accommodation were required to focus on the stimulus target. If a 5.0D stimulus level was entered via Teletype, the digital computer would generate 5.9 volts which would move the pen assembly to 15.4 cm. The target was then 10 cm plus 10 cm or 20 cm from the eye. This position required 5.0D of accommodation in order to focus on the stimulus.

If the stimulus waveform was a square wave switching between two accommodative levels D_1 and D_2, the subject would realize that the stimulus was periodic and would soon memorize the period and levels of the stimulus function. This would allow the subject to predict when a change in stimulus levels would occur. This prediction could remove the neurological time delay in the system. A response under these conditions would not be a natural response. If the duty cycle of the square wave stimulus was randomized, the subject could no longer predict when the stimulus level would switch from D_1 to D_2 or vice-versa. The natural time delays of the system would then be present in the responses. The subject would know the next stimulus level. To prevent this at least three stimulus levels were used. When these levels were entered via Teletype, a latin-square subroutine was used in the digital computer. This subroutine required a value for the stimulus duration time. The value of this time was entered via Teletype. The subroutine then checked to see what value of time delay was entered via teletype. It then checked the number of stimulus levels entered via Teletype. When the command was given by Teletype, the digital computer generated the

stimulus waveform as follows. It randomly selected one of the stimulus levels and moved the stimulus target to that position on the Y-axis of the X-Y recorder. It simultaneously began recording the pupillary response resulting from this accommodative step (assuming the former target position and that chosen by the computer are different). If the stimulus duration time was four seconds and the time delay was three seconds, the digital computer recorded data for four seconds on magnetic tape. Since a time delay of three seconds was entered, the duration of the stimulus at this level was randomly chosen from 4, 5, 6 or 7 seconds. The stimulus duration time was always at least four seconds. At the end of the stimulus duration time (4 seconds) plus the randomly selected time delay (0, 1, 2 or 3 seconds), the latin-square subroutine randomly chose a new stimulus level from the three entered levels. The stimulus target stepped to the new level and the concomitant pupil response was recorded on magnetic tape for four seconds. The stimulus waveform was thus a continuous function with random switching times and levels. This is illustrated in Figure 4.

In this set of experiments it was desired to do all testing about a fixed mean of 6.0D. Three separate experiments were conducted. The first experiment used levels of 3.0D, 4.0D and 9.0D with a time delay of three seconds and a data recording interval of four seconds. The time delay and recording interval were the same for all experiments. The subject was instructed to blink when the stimulus had the following changes: 3.0D to 4.0D, 4.0D to 3.0D, 4.0D to 9.0D, and 9.0D to 4.0D. Blinking moistens the sclera and the cornea of the eye. The subject then concentrated on the present stimulus level and prepared to immediately focus on the next level.

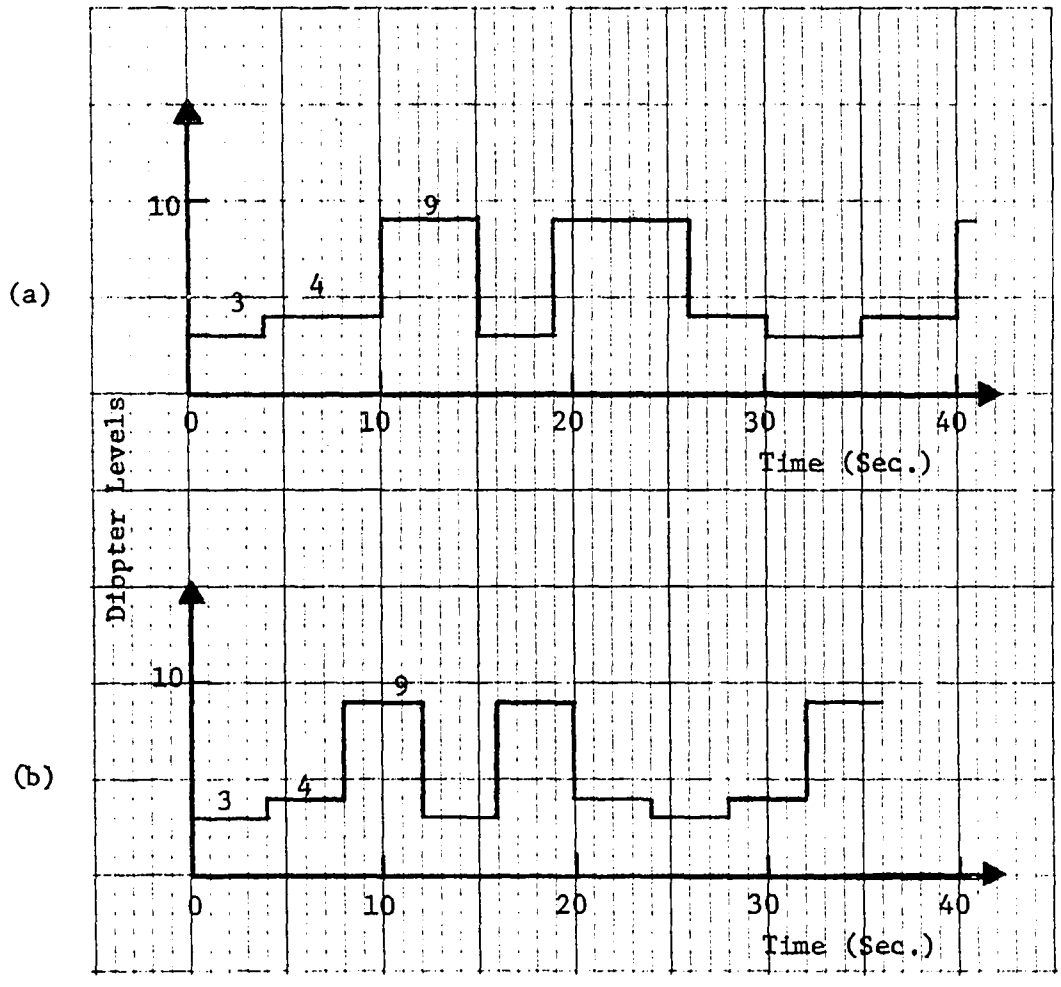

Figure 4. The random stimulus generated by the digital computer and the ideal pupillary response recorded on magnetic tape

(a) The computer generated random stimulus
(b) The ideal response recorded on magnetic tape

The second experiment used levels of 4.0D, 5.0D and 8.0D. The subject was trained to blink only during the following changes: 4.0D to 5.0D, 5.0D to 4.0D, 5.0D to 8.0D, and 8.0D to 5.0D. The third experiment used levels of 5.0D, 7.0D, and 8.0D. The subject blinked during the following changes: 5.0D to 8.0D, 8.0D to 5.0D, 7.0D to 8.0D, and 8.0D to 7.0D. The intervals of interest were 3.0D to 9.0D, 9.0D to 3.0D, 4.0D to 8.0D, 8.0D to 4.0D, 5.0D to 7.0D and 7.0D to 5.0D. A mean of 6.0D was common to all intervals of interest.

In a linear system, the Bode plot is invariant with changes in input amplitude. If the system is nonlinear, different input amplitudes will result in different Bode plots. For example, if the system has an amplitude nonlinearity (also called a no-memory nonlinearity), the phase of any resulting Bode plot will be the same. The amplitude plots will be different and dependent on the amplitude of the input.

The Use of the Digital Computer for Analysis

Use of the digital computer

The IBM 1800 digital computer generated stimuli, recorded the concomitant responses on magnetic tape and reduced the data to a form suitable for the application of linear systems theory. One objective was to transform the time response into the form of a Bode plot. This form was used to examine the low pass characteristics of the nonlinearities and to obtain the order of the system involved.

Converter

The A/D converter sampled each response 400 times. Both the number of samples and the sampling rate could be varied. A response sampled 400 times at a rate of 100 samples per second thus had a record length of four seconds. Bracewell (11) discusses the sampling theorem. This theorem states that a sampling rate of 100 samples per second is high enough to represent frequencies up to 50 Hz. For the accommodative-pupillary system, 5.0 Hz. was an upper limit.

The dynamic response of the pupil usually ceased after three seconds. The latter part of the response was free from dynamics. It represented the new DC pupillary level plus pupillary noise.

The time delay

When light is used to stimulate the pupil, the responses are involuntary. The subject has no control over this response. The time delay in this system was demonstrated by Stark and Sherman (65) to be 0.18 second and by Campbell and Westheimer (18) as 0.26 second. When accommodation is used as the stimulus, the response is voluntary. If the subject does not respond immediately, the response will appear to have a large time delay preceding the dynamics. That point at which the voluntary time delay ends and the time delay due to neurological signal transit begins is difficult to determine. The voluntary time delay can be reduced to an insignificant level by using a well trained subject. This subject should respond immediately to changes in stimulus levels.

In a linear system, an ideal time delay affects only the phase of the systems Bode plot. Its presence or absence has no affect on the ampli-

tude plot. If too much time delay is removed, a change will be noted in the amplitude of the Bode plot indicating that part of the dynamic response was removed with the time delay. This method can be used to separate the time delay from the dynamic response.

A second method for determining the physiological time delay would be the following. If the linear system was of small order, i.e., first or second, and if the Bode plot was extended to contain frequencies such that the amplitude and phase plots were stationary (asymptotic limits have been approached), and if the time delay was included in the plot, a plot of phase versus frequency on a linear scale would produce a straight line at high frequencies. The slope of this line would be the true time delay.

Another method of obtaining the time delay is to simply measure this delay from the time responses. This method may be just as accurate as the other two methods.

Editing the responses

Editing of the responses is necessary in order to identify (and discard) those responses due to blinks, eye movements, and inattention. The first step in editing the recordings of the responses is to instruct the computer to locate the data episode of interest on the magnetic tape. Two stimulus levels of interest are entered into the computer thru the IBM 1816 printer-keyboard. The computer then searches the magnetic tape for responses to these levels of stimulation.

Due to the experimental equipment, long lines to the computer, etc., a certain amount of electrical noise was superimposed on each single

response. This noise was random and reduced by signal averaging. The signal-to-noise ratio of the response was improved by the $\sqrt{n}$, if n responses were added. One must be careful before adding the responses. The voluntary time delay presents a problem for, if different time delays are present and the responses are added, this will result in erroneous dynamics as discussed by Cook and Stark (24).

The next step is to examine each response, improve those with unusual time delays by adjusting the time delay and to delete those responses having artifacts. As each response is edited, those that are saved are averaged. The final average is displayed on an oscilloscope and the average time delay that was removed is saved. This final average is stored on another magnetic tape for further analysis. If the dynamics and time delays of the responses are similar, the responses can be averaged without any adjustments. This direct averaging was used on all responses and is exemplified by Figures 12-17.

The Bode plot

After an experiment has been edited and the final average stored on another magnetic tape, a Bode plot is calculated relating the input stimulus and the output response. In obtaining the Bode plot, one basic assumption is made. Since the recorded response to the step stimulus has a duration of four seconds, the assumption is made that the response dynamics (transients) have ceased by the end of 3.4 seconds.

The analysis proceeds as follows. The four second stimulus (400 data points) and its resulting response are extended in time length to eight

seconds or 800 points. This extension occurs at the 340th point, or 3.4 seconds. The duration of the step stimulus is extended to 8.0 seconds. The value of this step at 3.4 seconds is used to extend its time length to 800 points.

The extension of the response is difficult since its time derivative may be erratic in the neighborhood of the 340th point. This makes it difficult to join a horizontal line to the response at the 340th point. If needed, an interpolation subroutine is used to smooth this transition. This smoothing subroutine interpolates between 20-40 points to the left of the 340th point. The value of the 340th point is used as the extention value for the 341st point to the 800th point. The smoothness of the final average response depends on the number of single responses available for averaging. If the experimental data is of high quality (smooth), the smoothing subroutine is not used. In addition, if the values for all time delays are reasonably close, they are not removed and are included in the final average response. A larger number of single responses will produce a smoother final average.

The extension forces the experimental data to assume a constant level at 3.4 seconds. If the slope of the experimental data is not zero in the neighborhood of the 340th point, the extension process produces an error beyond this point. Recall that all subsequent points (341-800) are assigned a value equal to that of the 340th point. This error will be present in the Bode plot. The final averages given in Figures 18-20 indicate that this error will occur only for the dilatative data (7.0D to 5.0D, 8.0D to 4.0D and 9.0D to 3.0D). The three constrictive responses

(average) reach a constant level before 3.4 seconds. The reason for this extension from 340 to 800 points will be discussed later.

If a linear system is driven by a square wave whose period is T, and if the transients have ceased before the square wave switches (T/2), the second half of the period can be constructed to a good approximation from the first half. Using this assumption, consider the two functions in Figure 5. The square wave represents the stimulus function. The other function is the response, f(t). The next step is to mathematically construct g(t) from f(t). The function f(t) represents the 800 point average response between two dioptric levels. It is defined over the interval $0 \leq t \leq T/2$. The function g(t), $T/2 \leq t \leq T$, is constructed as shown in Equation 1.

$$g(t) = -f(t-T/2) + f(T/2) + f(0) \qquad (1)$$

Notice that g(t) is the response to the second half of the square wave. The assumption has been made that any transients of f(t) are negligible after three seconds of data. In addition, a horizontal line segment is added at 3.4 seconds and extends the response length to 800 points or eight seconds. Thus T/2=8 seconds. Any transients beyond 3.4 seconds are being forced to the value of the response at 3.4 seconds. The function g(t) is then constructed from f(t) by the above relationship. This forms the periodic function where T=16 seconds. The absence of this extension produces a normal periodic function where T=8. The full response, f(t)+g(t), is constructed. The response is now the result of the given square wave stimulus. It is not the result of the random stimulus shown in Figure 4. This method of analysis was used due to the asymmetry in the system response to "on" and "off" step functions.

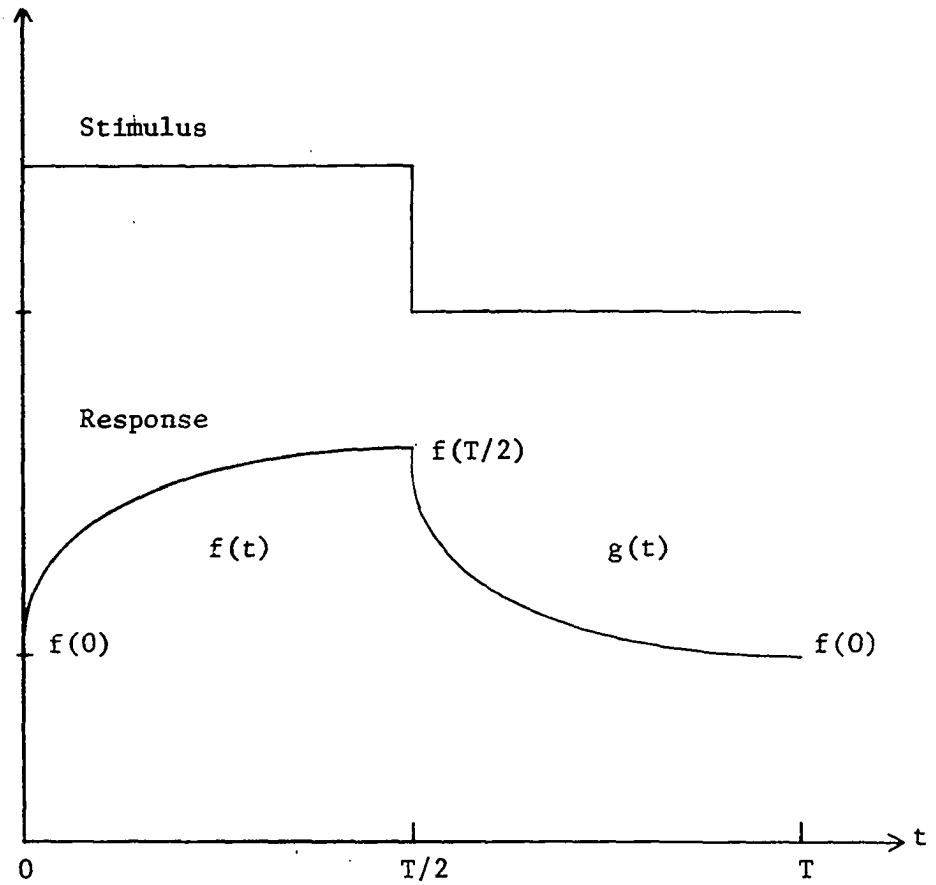

Figure 5. The synthesis procedure for the construction of the periodic function

The average value of the periodic function is $\overline{f(t)+g(t)}=(f(0)+f(T/2))/2$. By choosing T=16, the frequency of the 19th odd harmonic, which is 39 times the fundamental, is 39/16 Hz. or 2.44 Hz. The majority of energy of the response waveform is contained in the frequencies below 3.0 Hz. If T=8 were chosen, the 19th odd harmonic would be 4.88 Hz. Those points beyond 3.0 Hz. would be of little use. As the higher harmonics are computed, the accuracy of the computations decreases.

The stimulus and the response functions are now in the form of two periodic functions. From Fourier analysis, any function that is periodic, single valued and having a finite number of finite discontinuities can be represented by a Fourier series. Usually the periodic functions are such that they do not possess even or odd symmetry and the Fourier series representing these functions will contain both sine and cosine terms. The sine and cosine terms can be combined to yield a sine or cosine series having a phase angle and a magnitude. Both periodic functions were represented by a sine series. For a given harmonic, the sine term of the stimulus and response series contained a magnitude and a phase angle. The ratio of the response magnitude to the stimulus magnitude was used to construct the amplitude portion of the Bode plot. The difference of the response and stimulus phase angles was used to construct the phase portion of the Bode plot. The computer program selected the fundamental and the nineteen odd harmonics of the stimulus and response sine series as the frequencies in the Bode plot.

When the stimulus and response functions are extended the average value of the resulting periodic function is identical to the average

value of the normal periodic function. The extension does not alter the Bode plot of the system. It changes the set of frequencies comprising the Bode plot and the distribution of the energy. Bracewell (11) states that the envelope of the power spectrum of the extended (T=16) and the normal (T=8) periodic functions is the same.

The accuracy of the Bode analysis routine was checked as follows. A first-order function was simulated in the digital computer. The time constant of this function was 0.333 second. A Bode plot of this first-order system was made by the computer. An attenuation of -3db should have occurred at a frequency of 0.478 Hz. The results of this test are given in Figures 10 and 11. There was no significant error in the analysis routine.

RESULTS AND DISCUSSION

The pupillary responses to accommodative steps are shown in Figures 12-17. Figure 12 shows an ensemble of eleven responses to a 5.0D to 7.0D stimulus. The heavy line is the average value of the ensemble. The smoothness of the heavy line indicates that the slow variations appearing in each response are random and can be removed by averaging. These responses are the result of the random stimulus function shown in Figure 4.

The random stimulus function was allowed to continue until 60 stimuli had occurred. The stimulus function randomly switched between the three levels of accommodation entered to the digital computer via Teletype. For Figure 12, the three levels of accommodation were 5.0D, 7.0D and 8.0D. Sixty responses were recorded on magnetic tape for each experimental run. Each response had a duration of four seconds. When the 60 responses were edited the first 5.0D to 7.0D response was located. It was viewed on an oscilloscope and examined for acceptability with respect to time delay, dynamics and absence of artifacts. If the response was acceptable, it was plotted as in Figure 12. The second response was located, viewed and if acceptable, plotted. The editing procedure located all 5.0D to 7.0D responses contained in the experimental run. This particular run (Experiment 107, Run 006) produced eleven acceptable 5.0D to 7.0D responses. As each subsequent response was plotted, it was clear that the initial value of pupillary diameter was random. Figure 12 indicates that the maximum and minimum pupillary diameters were 6.2 mm and 5.1 mm respectively. The average pupillary diameter was approximately 5.5 mm. The random variation in initial pupillary diameter occurred for all stimulus levels of interest.

The levels of interest are discussed in the Equipment and Methods section and are shown in Figures 12-17.

The final average responses for the stimulus levels of interest are shown in Figures 18-20. These figures indicate that the constrictive responses (5.0D to 7.0D, 4.0D to 8.0D and 3.0D to 9.0D) occur more rapidly than the dilatative responses (7.0D to 5.0D, 8.0D to 4.0D and 9.0D to 3.0D). Events occurring close to the body constitute more of a threat than those occurring at a safe distance. This might account for the faster constrictive mechanism.

Figures 19 and 20 show a slight depression occurring in the dilatative data (8.0D to 4.0D and 7.0D to 5.0D). This depression occurs at the end of the time delay and precedes the dynamic response. It is the result of a vertical movement of the eye which occurred when a close stimulus target stepped to a distant position. Realignment of the subject with respect to the experimental equipment did not eliminate this "reflex-like" movement. This error is present in the dilatative Bode plots.

Figures 18-20 indicate that the constrictive responses reach a constant level shortly after three seconds. These responses are smooth and exponential in form. The dilatative responses are not smooth and are not exponential in form. Figure 19 indicates that a significant change in the 8.0D to 4.0D dynamic response occurs at about 1.75 seconds. Figure 20 shows a similar change in the 9.0D to 3.0D response. It occurs at approximately 2.0 seconds. It appears that the basic parameters of the dilatative dynamics change at around two seconds. This change does not occur in the constrictive responses. It is concluded that the

dilatative system is more complicated than the constrictive system. Figures 18-20 indicate that the dilatative responses do not reach a constant level by the end of four seconds.

The Equipment and Methods section stated that the Bode plot of each average dilatative response would contain an error. The error is the result of an interpolation and extension routine used to form a response periodic function. The extension routine forces the dilatative dynamics to cease at 3.4 seconds. This error does not occur in the Bode plots of each average constrictive response since each of these responses reaches a constant value before 3.4 seconds.

Figures 21-31 represent Bode plots of the constrictive-accommodative pupillary system. Figure 21 represents a Bode plot of this system based on an accommodative step of 5.0D to 7.0D. This step produces a retinal blur which requires the eye to produce 2.0D of positive (an increase in accommodative power) correction in order to eliminate the blur. Recall that Allen (5) and Campbell and Westheimer (19) stated that blur was one of the main stimuli to accommodation. A 7.0D to 5.0D step produces 2.0D of blur. The eye must produce a negative correction of -2.0D in order to eliminate the blur. Since the constrictive and dilatative dynamics will be separated into two models, the blur (B) will always be considered as a positive number. The blur will be in diopters (D) and can be calculated by taking the absolute value of the difference between the two levels of the accommodative step.

All Bode plots are composed of 20 frequencies. The fundamental frequency occurs at 0.0625 Hz. The 19 subsequent frequencies are odd

harmonics. The gain portion of the Bode plot was normalized. The fundamental frequency was adjusted such that its gain was always 0.0db. This adjustment was applied to the 19 odd harmonics. This normalizing process was necessary due to the limited plotting field of the IBM 1627 plotter.

No time delay has been removed from Figure 21. This can be seen from the insert in the lower left-hand corner. The phase portion of the Bode plot contains not only the phase shift due to the dynamics, but also contains the phase shift due to the time delay (e^{-sT}) which is ϕ(degrees)=-360fT where f is the frequency in Hz. and T the time delay in seconds. It can be seen from Figure 21 that the latter portion of the phase has exceeded -360°. This occurred for the 13th-20th "pluses" in the phase portion of the Bode plot. A value of -360° must be added to each of these points to determine the correct phase. Figures 22-24 illustrate the removal of 0.29, 0.41 and 0.51 second of time delay respectively. Theoretically, the removal of the time delay should affect only the phase data. The gain portion of the Bode plots in Figures 21-24 is similar to that of a second-order system having a double pole at a frequency of 1.0 Hz. The phase angle of this second-order system should have a value of -90° at a frequency of 1.0 Hz. Figures 21-24 do not exhibit the correct phase since the time delay phase and the interface phase error are included.

O'Neill and Stark (51) reported an accommodative-pupillary time delay of 0.4 second. Figures 18-20 indicate that the time delay is in the neighborhood of 0.4 second. Based on the above, a time delay of 0.4

second was extracted from the phase of Figure 23. Figure 44 is identical to Figure 23 except that the interface phase error has been removed. The Bode plots of the interface equipment are given in Figures 7-9. The heavy curved lines in Figure 44 represent the gain and phase curves for the second-order system having a double pole at a frequency of 1.0 Hz. The heavy curved phase line also represents the corrected phase curve after the phase effects of a time delay of 0.41 second and the interface phase error have been removed. The linear second-order system is a good approximation to the experimental data.

The slanted straight line in Figure 44 is the -40db/dec. asymptote of the second-order transfer function. Since Figure 44 involves a blur of 2.0D, it is conjectured that this small signal will allow the accommodative-pupillary system to operate as a linear system and that blurs of 4.0D and 6.0D will drive the system into nonlinear regions. The system will then be linear for blurs less than 2.0D. The Bode plots of Figures 45 and 46 are smooth compared to Figure 44. It is conjectured that a small blur requires the accommodative-pupillary system to involve more complicated mechanisms in order to maintain focus.

If a system is linear, the Bode plot is invariant with changes in the amplitude of the input. Figures 45 and 46 indicate that this is not the case with the accommodative-pupillary system. Figures 45 and 46 indicate that higher blur levels of 4.0D and 6.0D increase the low pass filtering in the system causing the response to be more sluggish. This is indicated in Figures 18-20. Since the low pass filter characteristics of the constrictive system change with increasing blur, a nonlinearity in

the dynamics is demonstrated. This nonlinearity was removed by first correcting the phase portions of Figures 45 and 46 for the interface phase error. The gain and phase portions of Figures 45 and 46 were then adjusted to those of the second-order system of Figure 44. The removal of the nonlinearity resulted in the curve shown in Figure 47. Figure 47 indicates a complex nonlinearity. Both the amplitude and the phase are dependent on the magnitude of the blur. An earlier assumption stated that the constrictive system was linear for blur levels of 2.0D or less. Figure 47 indicates that there are no phase or gain affects for blurs of 2.0D or less. Figures 44 and 47 represent Bode plots of the constrictive dynamics.

A curve displaying the static relationship between the accommodative level in diopters (D) and the pupillary diameter in millimeters is needed. This curve is shown in Figure 52. It was derived from Figures 18-20 by measuring the static pupillary diameter as a function of accommodative level. This curve is in excellent agreement with the curve given by Alpern et al. (8). Alpern's curve was obtained with normal room illumination. The curve in Figure 52 was obtained in a closed room having only a low level red light source. The pupil diameter is limited in both constriction and dilatation. With the light level present in these experiments, the maximum pupil diameter was approximately 7.1 mm and the minimum diameter was approximately 3.3 mm. The curve in the central region (1.5D-9.0D) is approximately linear. A piecewise mathematical description of the curve is indicated on the graph.

Figures 44, 47, and 52 were used to define the nonlinear model shown

in Figure 53. There are two inputs to this model: blur (B_1) in diopters and the static pupil diameter in millimeters as a function of accommodative level in diopters ($P_S(D)$). B_1 is always a positive step input that starts at zero. The characteristics of the nonlinear portion of the dynamics (NL_1) are given in Figure 47. The linear portion of the dynamics is given in Figure 44 and $P_S(D)$ is given in Figure 52. The time delay is T=0.4 second and a_1=6.28 [1/second]. If the system could be simulated, a gain $K_1(B_1)$ would be needed to keep the units consistent. It is conjectured that this gain will be a function of the blur level B_1. Since this model is difficult to simulate, a linear model is defined.

The linear model neglects the nonlinearity (NL_1) in the dynamics. This reduces the nonlinear model of Figure 53 to the linear model of Figure 58. The pupillary output can now be represented by Equation 2.

$$P(t)=P_S(D)-\frac{B_1K_1(B_1)}{a_1^2}U(t-T)[1-e^{-a_1(t-T)}(a_1(t-T)+1)] \qquad (2)$$

Each curve in Figures 18-20 was composed of 400 data points. The numerical values of these points was calculated and displayed in tabular form. The time interval between two adjacent data points was 0.01 second. A computer program was written which selected the 3rd, 6th, 9th, 12th, ..., 399th points and punched their values on IBM cards. This reduced the number of data points representing one experimental curve from 400 to 133. The time interval between two adjacent data points was now 0.03 second. The first point occurred at 0.03 second and the 133rd point occurred at 3.99 seconds. Since there are three experimental constriction curves as shown in Figures 18-20, three sets of data cards were punched for the

three levels of blur: 2.0D, 4.0D and 6.0D. All data cards were punched by the IBM 1442 card punch unit.

A computer program was written to fit Equation 2 to the experimental data. The values of B_1, T and $P_s(D)$ were fixed. The values of a_1 and $K_1(B_1)$ were varied until the absolute error was minimized. The absolute error was defined as the absolute value of the maximum vertical error between the computed and experimental curves plus the absolute value of the endpoint error which was the difference between the computed and experimental values for the 133rd point. An arbitrary decision was made to apply this method to the 4.0D to 8.0D data since it was the intermediate stimulus range. The value of a_1 was started at 2.0. The value of K_1 was started at 1.0 and increased by this amount 19 times. Then a_1 was reset to 2.1. The parameter a_1 was varied from 2.0 to 9.0 in increments of 0.1. For the 4.0D to 8.0D data, the absolute error was minimized when a_1=3.3 [1/second] and $K_1(B_1)$=5.0 [mm/D-second^2], B_1=4.0D. The maximum vertical error was +0.147 mm (the computed curve was above the experimental curve by this amount) and the endpoint error was -0.033 mm (the computed curve was below the experimental curve by this amount). A plot of the experimental and computed curves is given in Figure 56. The computed curve is the dashed curve. The numbers appearing in parentheses are the computed values. The numbers without the parentheses are experimental values. The left-hand set of numbers represent the pupil diameter in millimeters at 0.03 second. These values also represent $P_s(D)$. The right-hand values represent the pupil diameter in millimeters for 3.99 seconds. All intermediate values are available in tabular form.

Equation 2 was now fitted to the experimental constrictive data

having blurs of 2.0D and 6.0D. The value of a_1=3.3 [1/second] was used for all three blur levels of 2.0D, 4.0D and 6.0D. Equation 2 was fitted to the 5.0D to 7.0D experimental data by varying $K_1(B_1)$, B_1=2.0D, in the same fashion. For the given a_1, the value of $K_1(2)$ that minimized the endpoint error was K_1=5.0 [mm/D-second^2]. The maximum vertical error was +0.252 mm and the endpoint error was +0.000 mm. The computed curve is illustrated by the dashed line in Figure 55.

Equation 2 was fitted to the 3.0D to 9.0D experimental data by varying $K_1(B_1)$, B_1=6.0D, in the same fashion. For the given a_1, the value of $K_1(6)$ that minimized the endpoint error was K_1=5.0 [mm/D-second^2]. The maximum vertical error was -0.405 mm and the endpoint error was -0.237 mm. The computed curve is illustrated by the dashed line in Figure 57.

The dashed lines for the computed constrictive curves in Figures 55-57 are the result of fitting a linear equation (Equation 2) to nonlinear data. The middle stimulus level of 4.0D to 8.0D was chosen for the best fit. For this level, the minimum absolute error resulted in values of a_1=3.3 [1/second] and $K_1(4)$=5.0 [mm/D-second^2]. The value of a_1 was then fixed and K_1 was varied to achieve a minimum endpoint error in the 5.0D to 7.0D and 3.0D to 9.0D experimental data. K_1 had a value of 5.0 for all three levels.

The errors indicate that Equation 2 might match the experimental data better if a_1 was a function of B_1. This would suggest that the gain and time constant of the constrictive dynamics are functions of the blur level. Since $K_1(B_1)$ had a constant value for all blur levels, Equation 2 remained linear. Figure 58 represents the linear model of the constric-

tive system. This model is proposed because of its simplicity. Only a nonlinear model will truly describe the constrictive system. Neither model accounts for the fact that retinal blur eventually returns to zero due to refocusing.

An identical approach was taken for the dilatative system. The ensembles of responses for 7.0D to 5.0D, 8.0D to 4.0D and 9.0D to 3.0D accommodative steps are shown in Figures 13, 15, and 17. The heavy curves represent the ensemble averages. The ensemble average for the 7.0D to 5.0D accommodative step was formed from 15 single responses. The ensemble average for the 8.0D to 4.0D accommodative step was formed from 20 single responses and the ensemble average for the 9.0D to 3.0D accommodative step was formed from 15 responses. These averages are plotted in Figures 18-20. The Bode plots of these averages are shown in Figures 32-43.

The Bode plots of the dilatative system indicate that this system is extremely nonlinear compared to the constrictive system. They also suggest that the dilatative system is probably of a higher order than that of the constrictive system.

Figures 34, 38 and 42 represent Bode plots where approximately 0.4 second of time delay has been removed. The heavy curved lines of Figure 48 represent the Bode plot of a linear transfer function which has a third-order pole at a frequency of 0.48 Hz. The attenuation at this frequency is -9db and the phase angle is -135^{o}. It was felt that correction for interface phase error would be of little value. Figures 49 and 50 were adjusted to the linear third-order system given in Figure 48. This resulted in the extraction of the nonlinearity indicated in Figure 51. If Figure 51 is compared to Figure 47, it appears that the

nonlinearity in the dilatative dynamics has a lower pass characteristic than that of the constrictive system. This nonlinearity is also complex since both the phase and amplitude portions of the Bode plot are functions of blur. The assumption is made that the dilatative system is linear for blur levels of 2.0D or less. Figure 51 indicates that there are no phase or gain affects for blurs of 2.0D or less. Figures 48 and 51 represent Bode plots of the dilatative dynamics. Figure 52 represents the static characteristics.

Figures 48, 51 and 52 were used to define the nonlinear model shown in Figure 54. There are two inputs to this model: blur (B_2) in diopters and the static pupil diameter in millimeters as a function of accommodative level in diopters ($P_s(D)$). B_2 is always a positive step input starting at zero. The characteristic of the nonlinear portion of the dynamics (NL_2) is given in Figure 51. The linear portion of the dynamics is given in Figure 48 and $P_s(D)$ is given in Figure 52. The time delay is T=0.4 second and a_2=3.0 [1/second]. If the system could be simulated, a gain of $K_2(B_2)$ would be needed to keep the units consistent. It is conjectured that the gain will be a function of the blur level B_2. Since the model is difficult to simulate, a linear model is defined.

The linear model neglects the nonlinearity (NL_2) in the dynamics. This reduces the nonlinear model of Figure 54 to the linear model shown in Figure 59. The pupillary output P(t) can now be represented by Equation 3.

$$P(t)=P_s(D)+\frac{B_2K_2(B_2)}{a_2^3}U(t-T)[2-e^{-a_2(t-T)}(a_2^2(t-T)^2+2a_2(t-T)+2)] \qquad (3)$$

Since there are three experimental dilatative curves shown in Figures 18-20, three sets of data cards were punched for blur levels of 2.0D, 4.0D and 6.0D. The same procedures applied to the constrictive data were applied here.

Again, an arbitrary decision was made to obtain a fit for the 8.0D to 4.0D average response given in Figure 19. The minimization of the absolute error was the criterion used to achieve the best fit. The absolute error was a minimum when a_2=3.0 [1/second] and $K_2(B_2)$=5.0 [mm/D-second^3], B_2=4.0D. The maximum vertical error was +0.168 mm (the computed curve was above the experimental curve by this amount) and the endpoint error was -0.018 mm (the computed curve was below the experimental curve by this amount). A plot of the experimental curve and computed curves for dilatation is given in Figure 56. The computed curve is the dashed curve. The numbers appearing in parentheses are the computed values. The numbers without the parentheses are experimental values. The left-hand set of numbers represent the pupillary diameter in millimeters at 0.03 second. These values also represent $P_s(D)$. The right-hand values represent the pupillary diameter in millimeters for 3.99 seconds. All intermediate values are available in tabular form.

Equation 3 was not fitted to the experimental dilatative data having blurs of 2.0D and 6.0D. Equation 3 was fitted to the 7.0D to 5.0D experimental data by varying $K_2(B_2)$, B_2=2.0D, in the same fashion. For the given a_2, the value of $K_2(2)$ that minimized the endpoint error was K_2=5.0 [mm/D-second^3]. The maximum vertical error was -0.077 mm and the endpoint error was -0.052 mm. The computed curve is illustrated by the

dashed line in Figure 55.

Equation 3 was adjusted to the 9.0D to 3.0D experimental data by varying $K_2(B_2)$, B_2=6.0D, in the same fashion. For the given a_2, the value of $K_2(6)$ that minimized the endpoint error was K_2=5.0 [mm/D-second^3]. The maximum vertical error was +0.520 mm and the endpoint error was +0.232 mm. The computed curve is illustrated by the dashed line in Figure 57.

The dashed lines for the computed dilatative curves in Figures 55-57 are the result of fitting a linear equation (Equation 3) to nonlinear data. Again, the middle stimulus level of 8.0D to 4.0D was chosen for the best fit. For this level, the minimum absolute error resulted in values of a_2=3.0 [1/second] and $K_2(4)$=5.0 [mm/D-second^3]. The value of a_2 was then fixed and K_2 was varied to achieve a minimum endpoint error in the 7.0D to 5.0D and 9.0D to 3.0D experimental data. K_2 had a value of 5.0 for all three levels.

The errors again indicate that a better fit might be obtained if a_2 was a function of B_2. This would suggest that the gain and time constant of the dilatative dynamics are functions of blur level. A still better representation would be a piecewise nonlinear set of equations that would account for the changes in the dilatative dynamic parameters at approximately 2.0 seconds. Figure 59 indicates a linear model of the dilatative system. The model is proposed because of its simplicity. Only a nonlinear model will validly represent the dilatative data. Neither model accounts for the fact that retinal blur eventually returns to zero.

SUMMARY AND CONCLUSIONS

An infrared TV-Pupillometer was used to study the accommodative-pupillary system of the human eye. The stimulus to the eye was a series of accommodative steps which produced a retinal blur. The duration and amplitude of the accommodative steps were randomized. The blur was represented in diopters (D). Focusing of the eye reduced this blur and produced changes in the pupillary diameter. If an object was brought toward the eye, the dioptric power of the eye increased and the pupil constricted. This constriction altered the optical characteristics of the eye by increasing the depth of focus and decreasing spherical aberration.

Experimental data was presented showing an averaged pupillary response of the right eye to accommodative steps of 5.0D to 7.0D, 4.0D to 8.0D, 3.0D to 9.0D, 7.0D to 5.0D, 8.0D to 4.0D and 9.0D to 3.0D. One dark adapted, 20 year old male subject was permitted to use binocular vision throughout the experiments.

The duration of each response was 4.0 seconds. All constrictive and dilatative responses were observed to contain a time delay of approximately 0.4 second. The constrictive and dilatative responses were asymmetric. The constrictive responses were rapid and appeared to be exponential in form whereas the dilatative responses were more sluggish and complex. The properties of the dilatative dynamics changed approximately 2.0 seconds after the response began.

The experimental data indicated that a blur greater than 2.0D would cause increasing nonlinearities in the dynamics of the constrictive and

dilatative systems. These systems were analyzed as linear systems when the magnitude of the blur was less than or equal to 2.0D. Experimental data suggested that additional nonlinear mechanisms were recruited for small magnitudes of blur in order to maintain an accurate focus. The responses indicated that the constrictive dynamics ceased at about 3.0 seconds while the dilatative dynamics continued throughout the 4.0 second response. A static relationship between pupillary diameter and accommodative level was obtained.

Two separate nonlinear models were proposed for the constrictive accommodative-pupillary system and for the dilatative accommodative-pupillary system. Each model contained two inputs: blur in diopters (D) and static pupillary diameter in millimeters. Two linear models were also proposed. These models simulated the experimental responses. A mathematical function representing pupillary diameter as a function of time was presented for both linear models.

The responses of the linear models were compared to the experimental results. Modifications of the mathematical equations which would improve the simulated responses were suggested.

In summary, linear systems analysis was applied to the study of the static and dynamic nonlinearities of the accommodative-pupillary system.

BIBLIOGRAPHY

1. Adler, Francis H. Physiology of the eye: clinical application. 4th. ed. St. Louis, Mo., The C. V. Mosby Co., Inc. c1965.

2. Allen, Merrill J. An investigation of the time characteristics of accommodation and convergence of the eyes. American Journal of Optometry 30:78-83. 1953.

3. Allen, Merrill J. An investigation of the time characteristics of accommodation and convergence of the eyes. American Journal of Optometry 30:393-402. 1953.

4. Allen, Merrill J. The response of the intraocular muscles of the dog and cat to electrical stimulation. American Journal of Optometry 27:287-293. 1950.

5. Allen, Merrill J. The stimulus to accommodation. American Journal of Optometry 32:422-431. 1955.

6. Alpern, M. Accommodation. In Davson, H., ed. The eye. Vol. 3. Pp. 191-225. New York, N.Y., Academic Press, Inc. 1962.

7. Alpern, M. Variability of accommodation during steady fixation at various levels of illuminance. Optical Society of America Journal 48:193-197. 1958.

8. Alpern, M., Ellen, P., and Goldsmith, R. I. The electrical response of the human eye in far-to-near accommodation. Archives of Ophthalmology 60:592-602. 1958.

9. Alpern, M. and Jardinico, R. E. Vergence and accommodation. V. Pupil size changes associated with changes in accommodative vergence. American Journal of Ophthalmology 52:762-767. 1961.

10. Baker, F. H. Pupillary response to double-pulse stimulation: a study of nonlinearity in the human system. Optical Society of America Journal 53:1430-1436. 1963.

11. Bracewell, R. The Fourier transform and its applications. New York, N.Y., McGraw-Hill Book Co., Inc. c1965.

12. Brodkey, J. and Stark, L. Accommodative convergence: an adaptive nonlinear control system. Institute of Electrical and Electronics Engineers Transactions on Systems Science and Cybernetics 3:121-133. 1967.

13. Brodkey, J. and Stark, L. Feedback control analysis of accommodative convergence. American Journal of Surgery 114:150-158. 1967.

14. Brown, R. G. and Nilsson, J. W. Introduction to linear systems analysis. New York, N.Y., John Wiley and Sons, Inc. c1962.

15. Campbell, F. W. Correlation of accommodation between the two eyes. Optical Society of America Journal 50:738. 1960.

16. Campbell, F. W. The minimum quantity of light required to elicit the accommodation reflex in man. Journal of Physiology 123:357-366. 1954.

17. Campbell, F. W., Robson, J. G., and Westheimer, G. Fluctuations of accommodation under steady viewing conditions. Journal of Physiology 145:579-594. 1959.

18. Campbell, F. W. and Westheimer, G. Dynamics of accommodation responses of the human eye. Journal of Physiology 151:285-295. 1960.

19. Campbell, F. W. and Westheimer, G. Factors influencing accommodation responses of the human eye. Optical Society of America Journal 49:568-571. 1959.

20. Carter, J. H. A servoanalysis of the human accommodative mechanism. Unpublished Ph.D. thesis. Bloomington, Indiana, Library, Indiana University. 1962.

21. Clark, R. N. Introduction to automatic control systems. New York, N.Y., John Wiley and Sons, Inc. c1962.

22. Clynes, M. Computer dynamic analysis of the pupil light reflex. International Conference on Medical Electronics, London, Proceedings 3:356-358. 1960.

23. Cook, G., Stark, L. and Zuber, B. L. Horizontal eye movements studied with the on-line computer. Archives of Ophthalmology 76:589-595. 1966.

24. Cook, G. and Stark, L. Dynamics of the saccadic eye-movement mechanism. Presbyterian-St. Luke's Hospital (Chicago, Illinois) Medical Bulletin 6:44-45. 1967.

25. Crawford, B. H. The dependence of pupil size upon external light stimulus under static and variable conditions. Royal Society of London Proceedings 121B:376-395. 1937.

26. Davson, H., ed. The eye. Vol. 3. New York, N.Y., Academic Press, Inc. 1962.

27. Duke-Elder, W. S. Textbook of ophthalmology. Vol. I. St. Louis, Mo., The C. V. Mosby Co., Inc. 1938.

28. Electronic Associates, Inc. The human pupil servomechanism. Applications Reference Library Bulletin No. ALAC 64091. Long Branch, New Jersey, Electronic Associates, Inc. 1964.

29. Fincham, E. F. Accommodation and convergence in the absence of retinal images. Vision Research 1:425-440. 1962.

30. Fincham, E. F. The accommodation reflex and its stimulus. British Journal of Ophthalmology 35:381-393. 1951.

31. Fincham, E. F. The mechanism of accommodation. British Journal of Ophthalmology Monograph Supplement 8:7-80. 1937.

32. Fincham, E. F. The proportion of ciliary muscular force required for accommodation. Journal of Physiology 128:99-112. 1955.

33. Fry, G. A. The relation of pupil size to accommodation and convergence. American Journal of Optometry 22:451-465. 1945.

34. Gibson, J. E. Nonlinear automatic control. New York, N.Y., McGraw-Hill Book Co., Inc. c1963.

35. Gradle, H. S. and Ackerman, W. The reaction time of the normal pupil. American Medical Association Journal 99:1334-1336. 1932.

36. Guyton, A. C. Textbook of medical physiology. 3rd ed. Philadelphia, Pa., W. B. Saunders Co., Inc. 1966.

37. Heath, G. G. Accommodative responses of totally color blind observers. American Journal of Optometry 33:457-465. 1956.

38. Jones, R. W. Some properties of physiological regulators. International Congress of the International Federation of Automatic Control, Moscow, Proceedings 1:674-678. 1960.

39. Knoll, H. A. Pupillary changes associated with accommodation and convergence. American Journal of Optometry 26:346-357. 1949.

40. Kuo, B. D. Automatic control systems. Englewood Cliffs, N.Y., Prentice-Hall, Inc. c1962.

41. Lowenstein, O. and Lowenfeld, I. E. The pupil. In Davson, H., ed. The eye. Vol. 3. Pp. 231-267. New York, N.Y., Academic Press, Inc. 1962.

42. Marg, E. and Morgan, M. W. The pupillary near reflex: the relation of pupillary diameter to accommodation and the various elements of convergence. American Journal of Optometry 26:183-198. 1949.

43. Morgan, M. W. Accommodation and its relationship to convergence. American Journal of Optometry 21:183-195. 1944.

44. Morgan, M. W. The ciliary body in accommodation and accommodative-convergence. American Journal of Optometry 31:219-229. 1954.

45. Morgan, M. W. The nervous control of accommodation. American Journal of Optometry 21:87-93. 1944.

46. Morgan, M. W. A new theory for the control of accommodation. American Journal of Optometry 23:99-110. 1946.

47. Nadell, M. D. and Knoll, H. A. The effect of luminance, target configuration and lenses upon the refractive state of the eye. American Journal of Optometry 33:24-42. 1956.

48. Nadell, M. C. and Knoll, H. A. The effect of luminance, target configuration and lenses upon the refractive state of the eye. American Journal of Optometry 33:86-95. 1956.

49. Naquin, H. Argyll Robertson pupil. American Journal of Ophthalmology 38:23-33. 1954.

50. Nathan, P. W. and Turner, J. W. A. Efferent pathway for pupillary contraction. Brain 65:343-351. 1942.

51. O'Neill, W. D. and Stark, L. Triple-function ocular monitor. Optical Society of America Journal 58:570-573. 1968.

52. Ripps, H., Chin, N. B., Siegel, I. M., and Breinir, G. M. The effect of pupil size on accommodation, convergence, and the AC/A ratio. Investigative Ophthalmology 1:127-135. 1962.

53. Ruch, T. C. and Patton, H. D. Physiology and biophysics. 19th ed. Philadelphia, Pa., W. B. Saunders Co., Inc. c1965.

54. Russell, G. F. M. The nervous control of visual accommodation. Clinical Science 18:119-124. 1959.

55. Samoilov, A. Ya., Sokolova, O. N., and Shakhnovich, A. R. Pupillographic method in the study of the act of convergence. Biophysics 6:53-57. 1961.

56. Seifert, W. W. and Steeg, C. W., Jr. Control systems engineering. New York, N.Y., McGraw-Hill Book Co., Inc. 1960.

57. Sridhar, R. A general method for deriving the describing functions for a certain class of nonlinearities. Institute of Electrical and Electronics Engineers Transactions on Automatic Control 5:135-141. 1960.

58. Stanten, S. F. and Stark, L. A statistical analysis of pupil noise. Institute of Electrical and Electronics Engineers Transactions on Biomedical Engineering 13:140-152. 1966.

59. Stark, L. Oscillations of a neurological servomechanism predicted by the Nyquist stability criterion. In Selected papers in biophysics. New Haven, Conn., Yale University Press, Inc. 1959. Original not available; cited in Stark, L. Stability, oscillations, and noise in human servomechanism. Institute of Radio Engineers Proceedings 47:1932. 1959.

60. Stark, L. Stability, oscillations, and noise in the human pupil servomechanism. Institute of Radio Engineers Proceedings 47:1925-1939. 1959.

61. Stark, L. Vision: servoanalysis of pupil reflex to light. In Glasser, ed. Medical physics. Vol. 3. Pp. 702-719. Chicago, Ill., The Year Book Publishing Co., Inc. 1960.

62. Stark, L. and Baker, R. Stability and oscillations in a neurological servomechanism. Journal of Neurophysiology 22:156-164. 1959.

63. Stark, L., Campbell, F. W., and Atwood, J. Pupil unrest: an example of noise in a biological servomechanism. Nature 182:857-858. 1958.

64. Stark, L. and Cornsweet, T. N. Testing a servoanalytic hypothesis for pupil oscillations. Science 127:588. 1958.

65. Stark, L. and Sherman, P. M. A servoanalytic study of consensual pupil reflex to light. Journal of Neurophysiology 20:17-26. 1957.

66. Stark, L., Takahashi, Y. and Zames, G. Nonlinear servoanalysis of human lens accommodation. Institute of Electrical and Electronics Engineers Transactions on Systems Science and Cybernetics 1:75-83. 1965.

67. Truxal, J. G. Automatic feedback control system synthesis. New York, N. Y., McGraw-Hill Book Co., Inc. 1955.

68. Young, F. A. and Biersdorf, W. R. Pupillary contraction and dilatation in light and darkness. Journal of Comparative Psychology 47:264-268. 1954.

69. Wald, G. and Griffin, D. R. The change in refractive power of the human eye in dim and bright light. Optical Society of America Journal 37:321-336. 1947.

70. Warshawsky, J. The focusing servomechanism of the human eye. Unpublished Ph.D. thesis. Evanston, Ill., Library, Northwestern University. 1963.

71. Westheimer, G. Optical and motor factors in the formation of the retinal image. Optical Society of America Journal 53:86-88. 1963.

72. Wilkie, D. R. The mechanical properties of muscle. British Medical Bulletin 12:177-182. 1956.

ACKNOWLEDGEMENTS

This dissertation could not have been completed without the assistance and cooperation of Professors Neal R. Cholvin, D.V.M., Ph.D. and Lawrence Stark, M.D.

Dr. Cholvin acted as major professor and sponsor. His suggestions on the organization and writing of the dissertation were invaluable. He encouraged the author to pursue experimental eye research at the Biomedical Engineering Department, Presbyterian-St. Luke's Hospital, Chicago, Illinois. The research was supported by a predoctoral fellowship (5-F1-GM-25, 931-04) from the National Institute of General Medical Sciences.

Dr. Stark was most gracious in inviting the author to Chicago to use his TV-Pupillometer. The author is indebted to Dr. Stark for the many suggestions, discussions and the research experience obtained under his direction. The author is indebted to John L. Semmlow, the staff and the graduate students at the hospital for their help.

The author wishes to express his thanks to the faculty of the Electrical Engineering Department and the Biomedical Engineering Program at Iowa State University. Finally, the author wishes to thank his wife, Sandra, for her encouragement and patience throughout this project.

APPENDIX

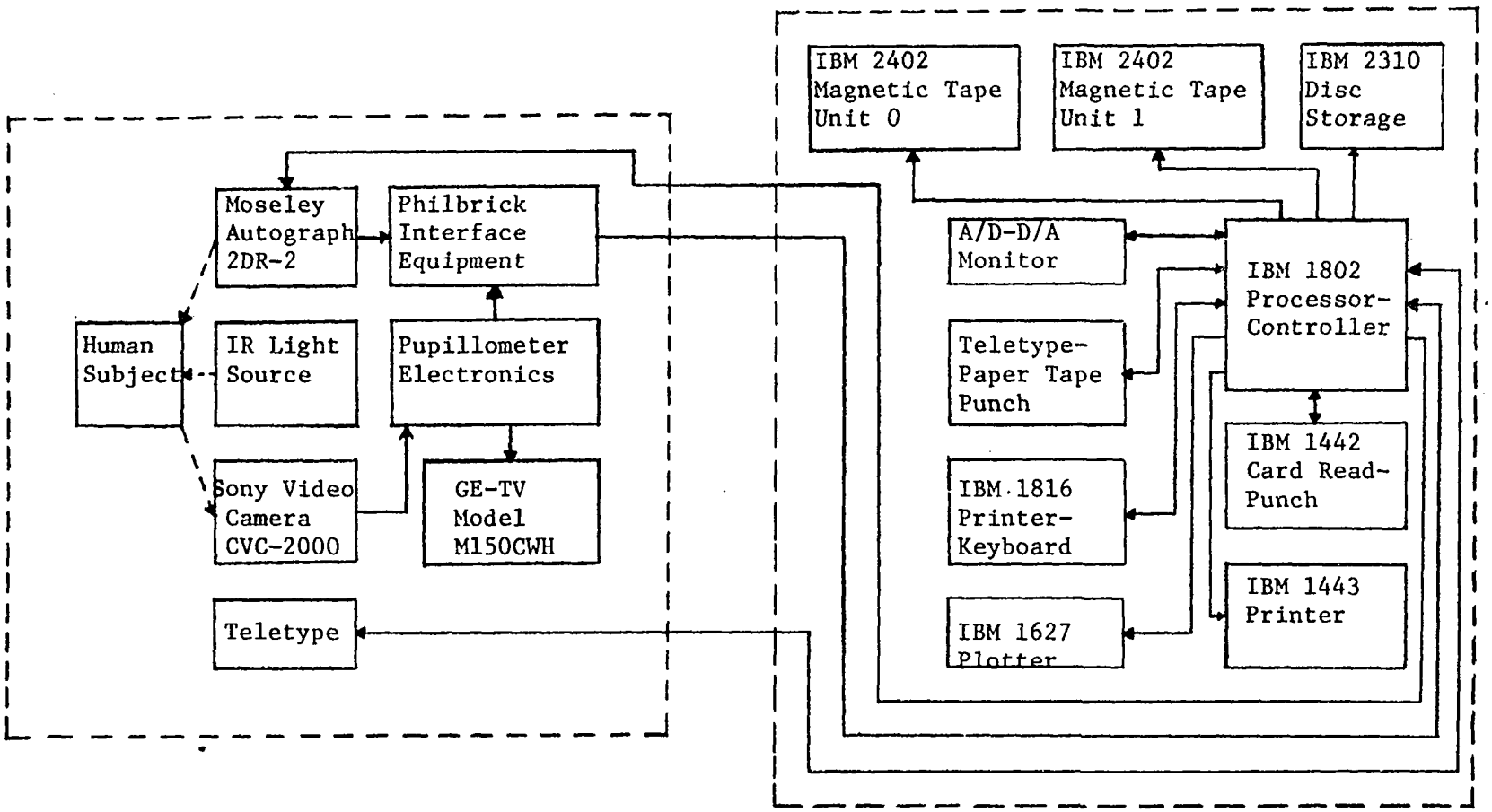

Figure 6. A block diagram illustrating the interrelationships between the TV Pupillometer and the IBM 1800 digital computer

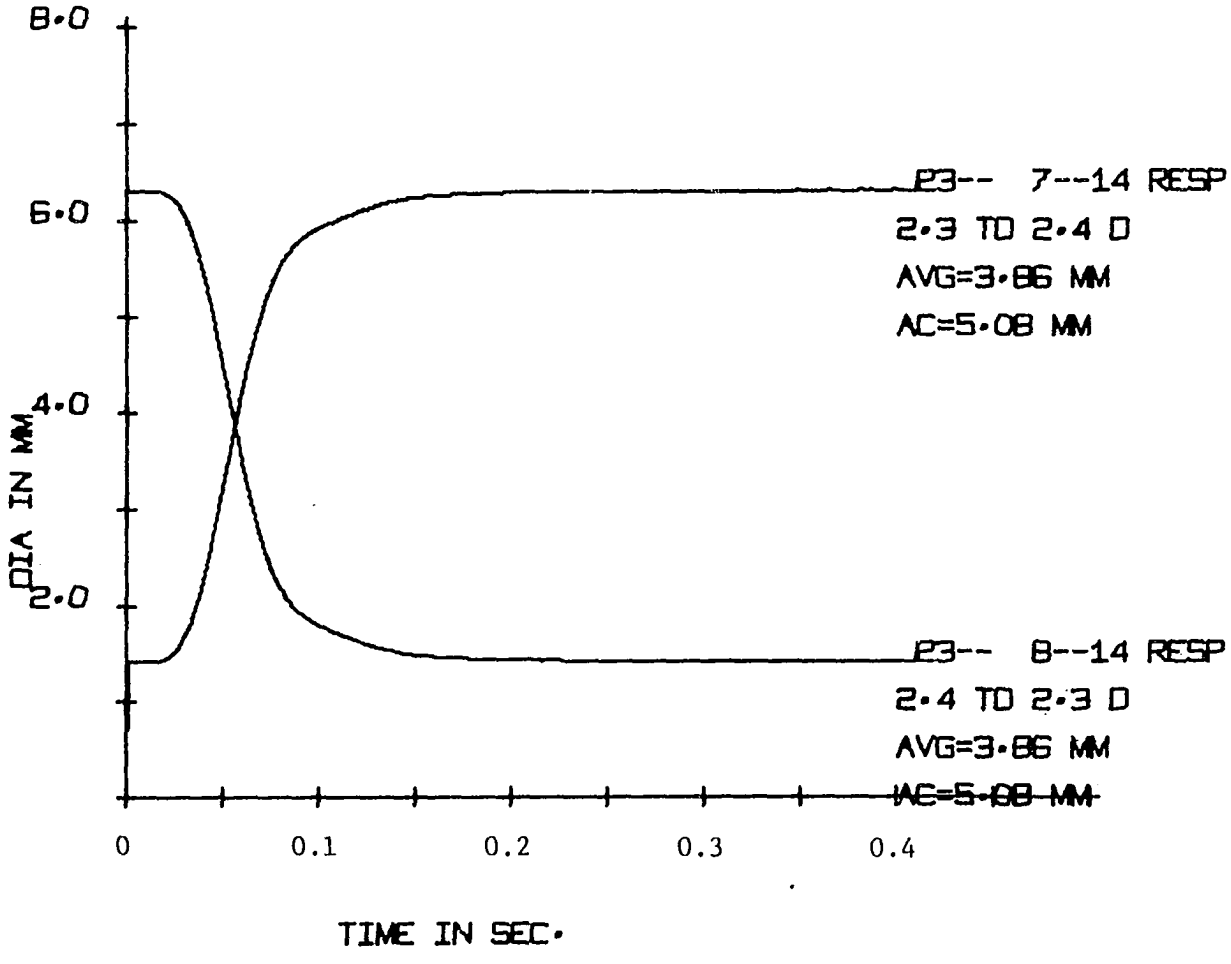

Figure 7. The time-response of the interface equipment to bidirectional steps

Figure 8. A Bode plot of the interface system responding to an increasing step function. Shown are the fundamental (0.625 Hz.) and odd harmonic frequencies

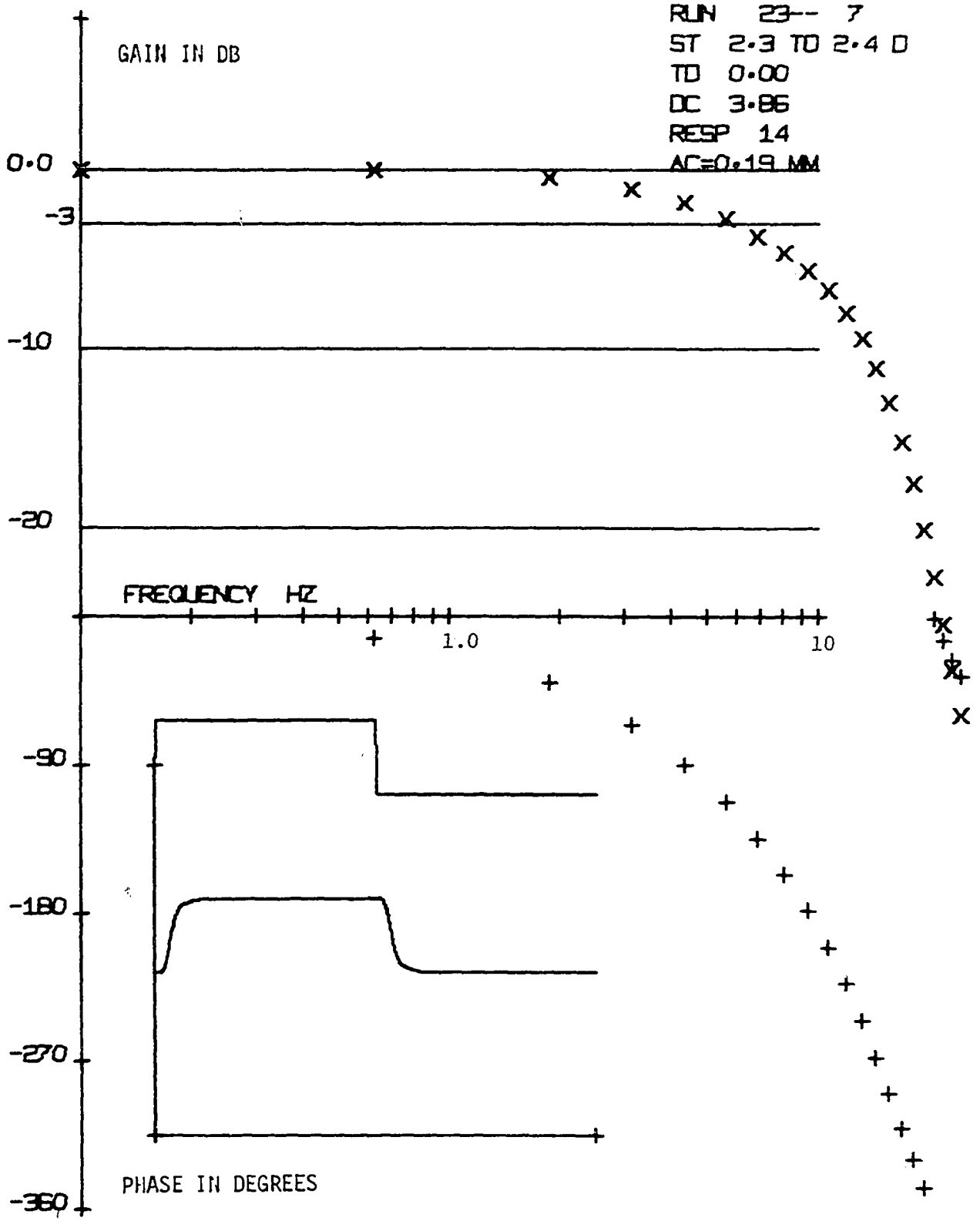
RUN 23-- 7
ST 2.3 TO 2.4 D
TD 0.00
DC 3.86
RESP 14
AC=0.19 MM
GAIN IN DB
0.0
-3
-10
-20
FREQUENCY HZ
1.0
10
-90
-180
-270
-360
PHASE IN DEGREES

Figure 9. A Bode plot of the interface system responding to a decreasing step function. This figure is identical to Figure 8 as it should be if the analysis technique is linear

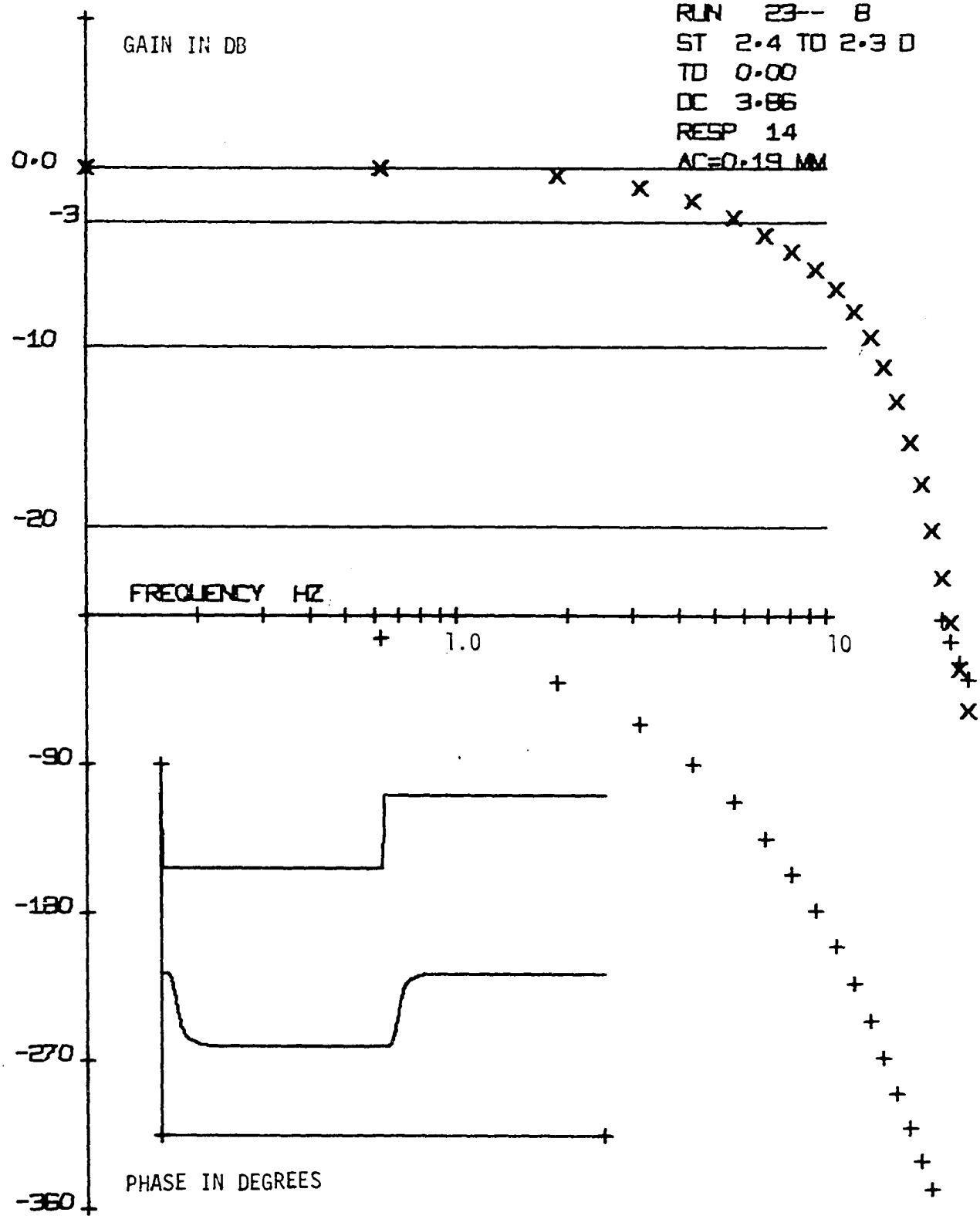
RUN 23-- 8
ST 2.4 TO 2.3 D
TD 0.00
DC 3.86
RESP 14
AC=0.19 MM
GAIN IN DB
0.0
-3
-10
-20
FREQUENCY HZ
1.0
10
-90
-180
-270
-360
PHASE IN DEGREES

Figure 10. A Bode plot of a digitally simulated first-order filter having a time constant of 0.333 second. An attenuation of -3db occurs at a frequency of 0.478 Hz. and the higher frequency terms approach an asymptote having a slope of -20db per decade. Shown are the fundamental (0.0625 Hz.) and odd harmonic frequencies. This test was performed to check the validity of the Bode analysis routine

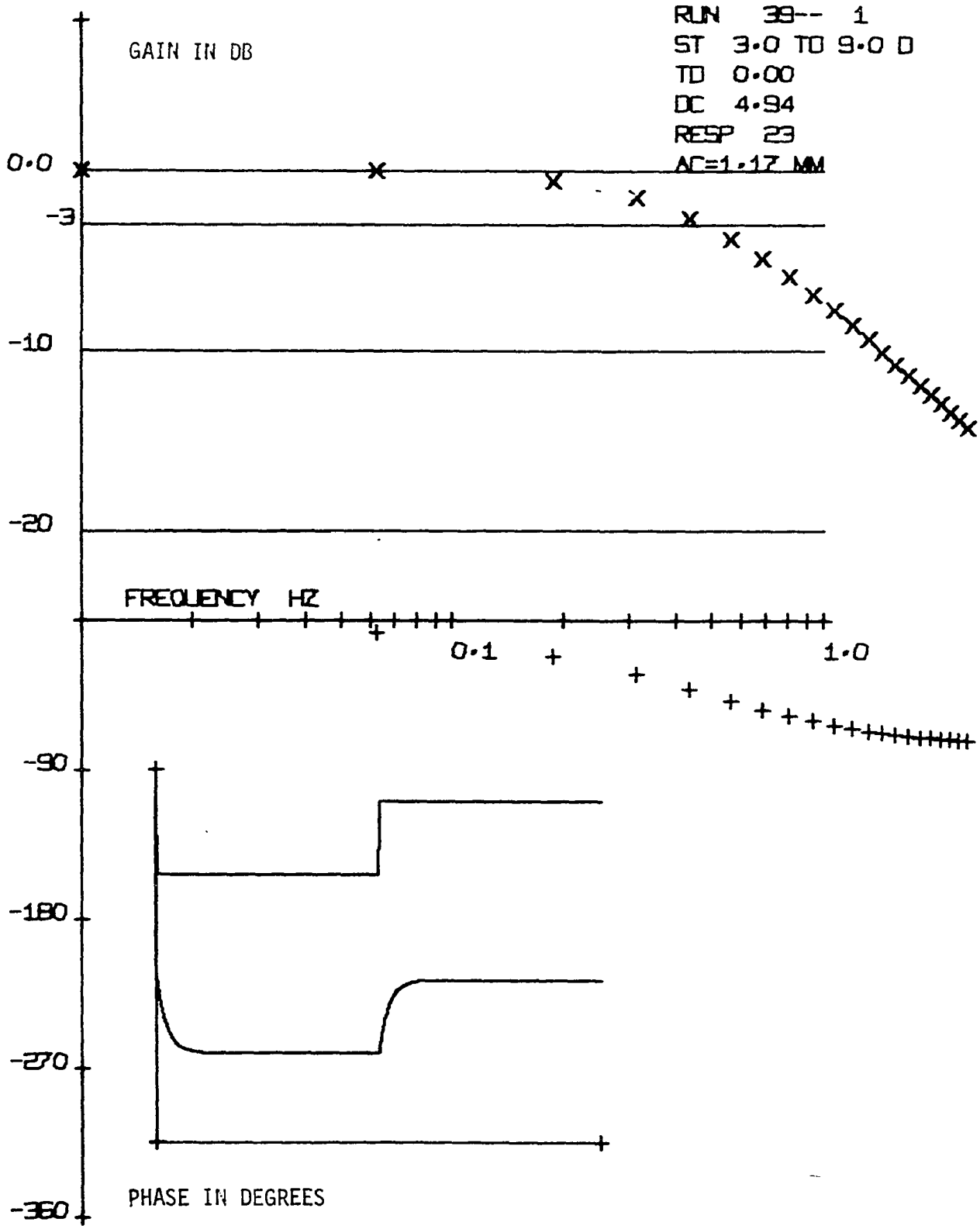
RUN 39-- 1
ST 3.0 TO 9.0 D
TD 0.00
DC 4.94
RESP 23
AC=1.17 MM
GAIN IN DB
0.0
-3
-10
-20
FREQUENCY HZ
0.1
1.0
-90
-180
-270
-360
PHASE IN DEGREES

Figure 11. This figure is identical to that of Figure 10 except that the input to the simulated filter was an increasing step function. Identical responses indicate that no asymmetry exists in the Bode analysis routine

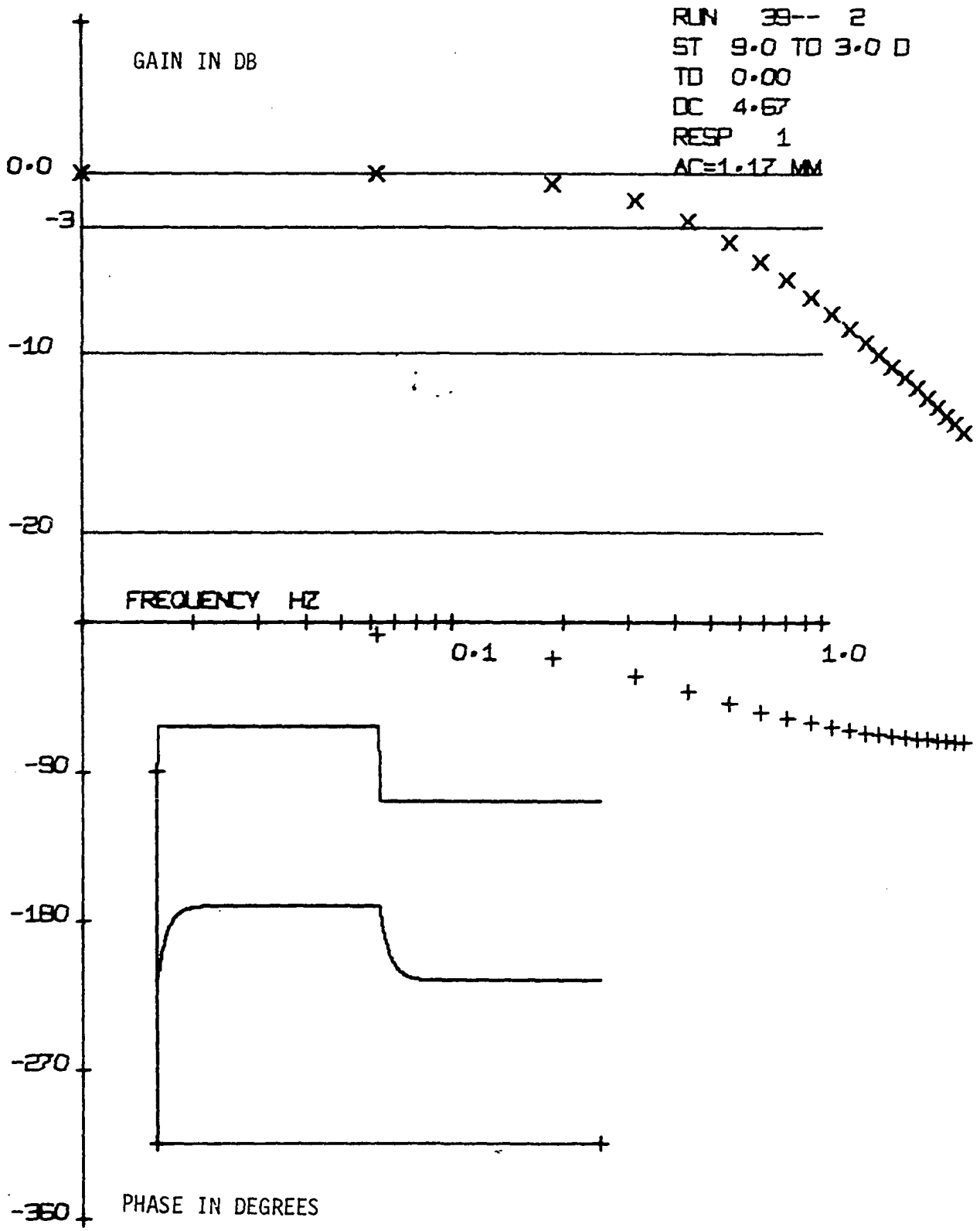
RUN 38-- 2
ST 9.0 TO 3.0 D
TD 0.00
DC 4.67
RESP 1
AC=1.17 MM
GAIN IN DB
0.0
-3
-10
-20
FREQUENCY HZ
0.1
1.0
-90
-180
-270
-360
PHASE IN DEGREES

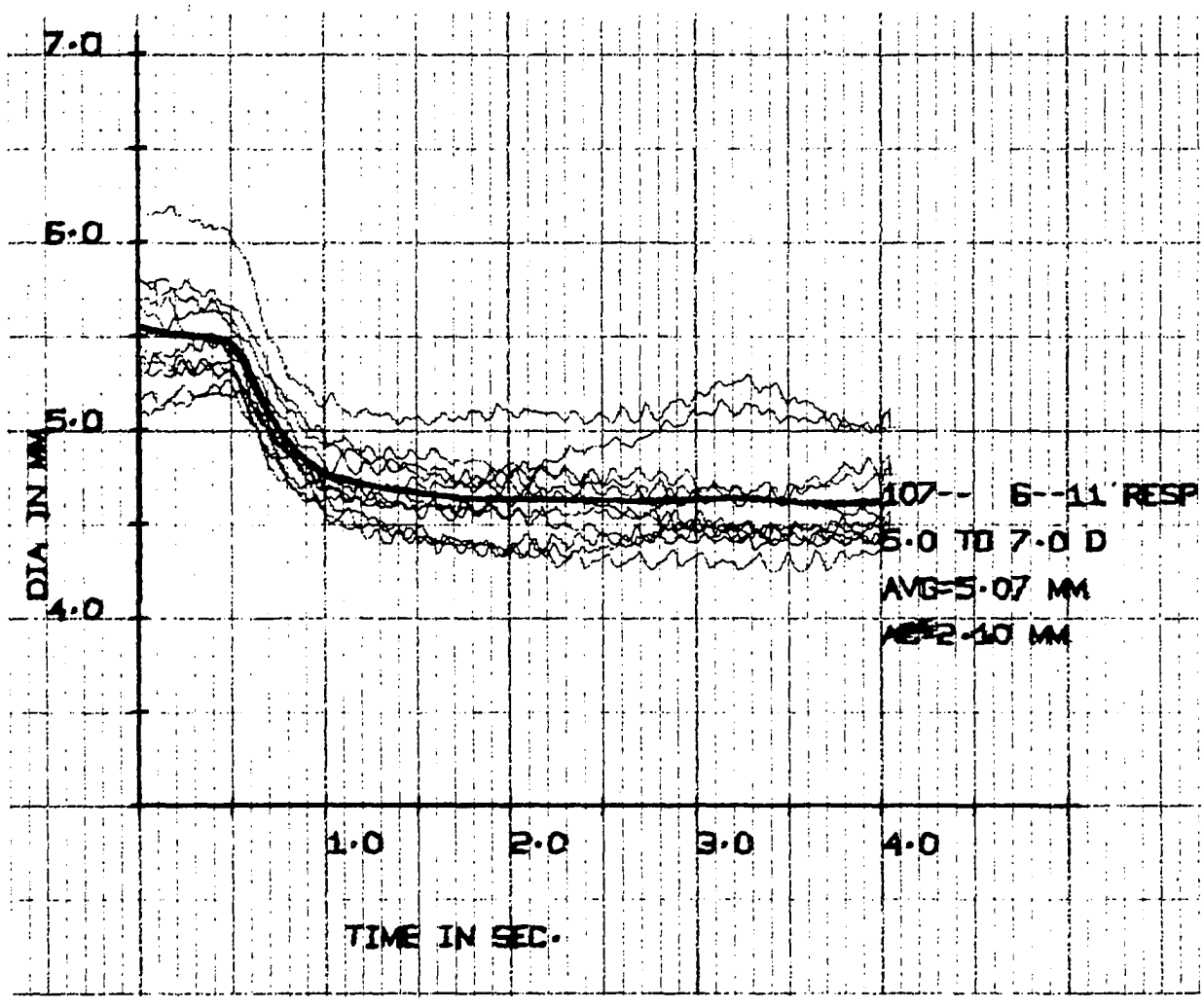

Figure 12. Responses of pupil diameter to eleven accommodative steps from 5.0D to 7.0D. The dark line indicates the average of the eleven responses

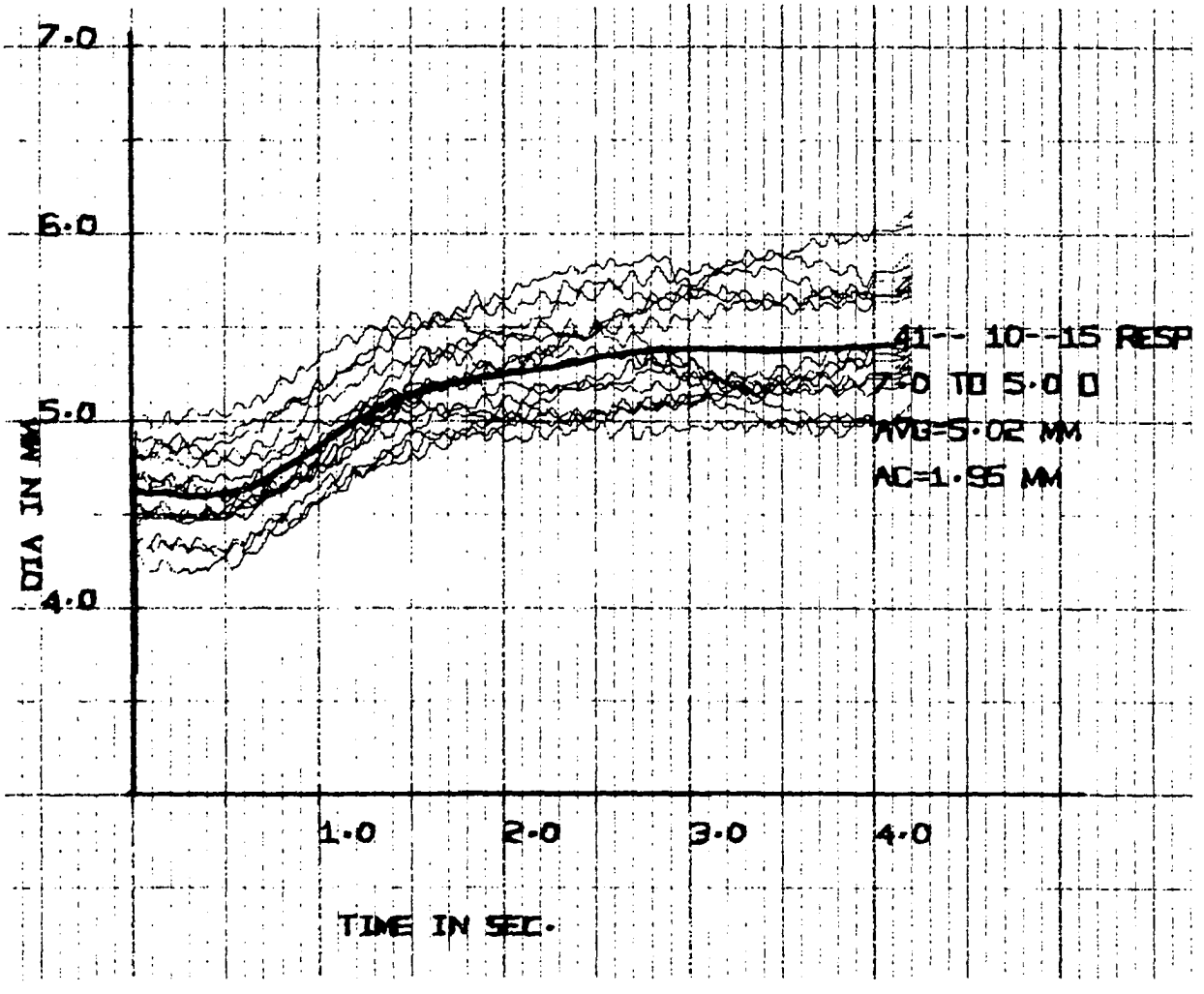

Figure 13. Responses of pupil diameter to fifteen accommodative steps from 7.0D to 5.0D. The dark line indicates the average of the fifteen responses

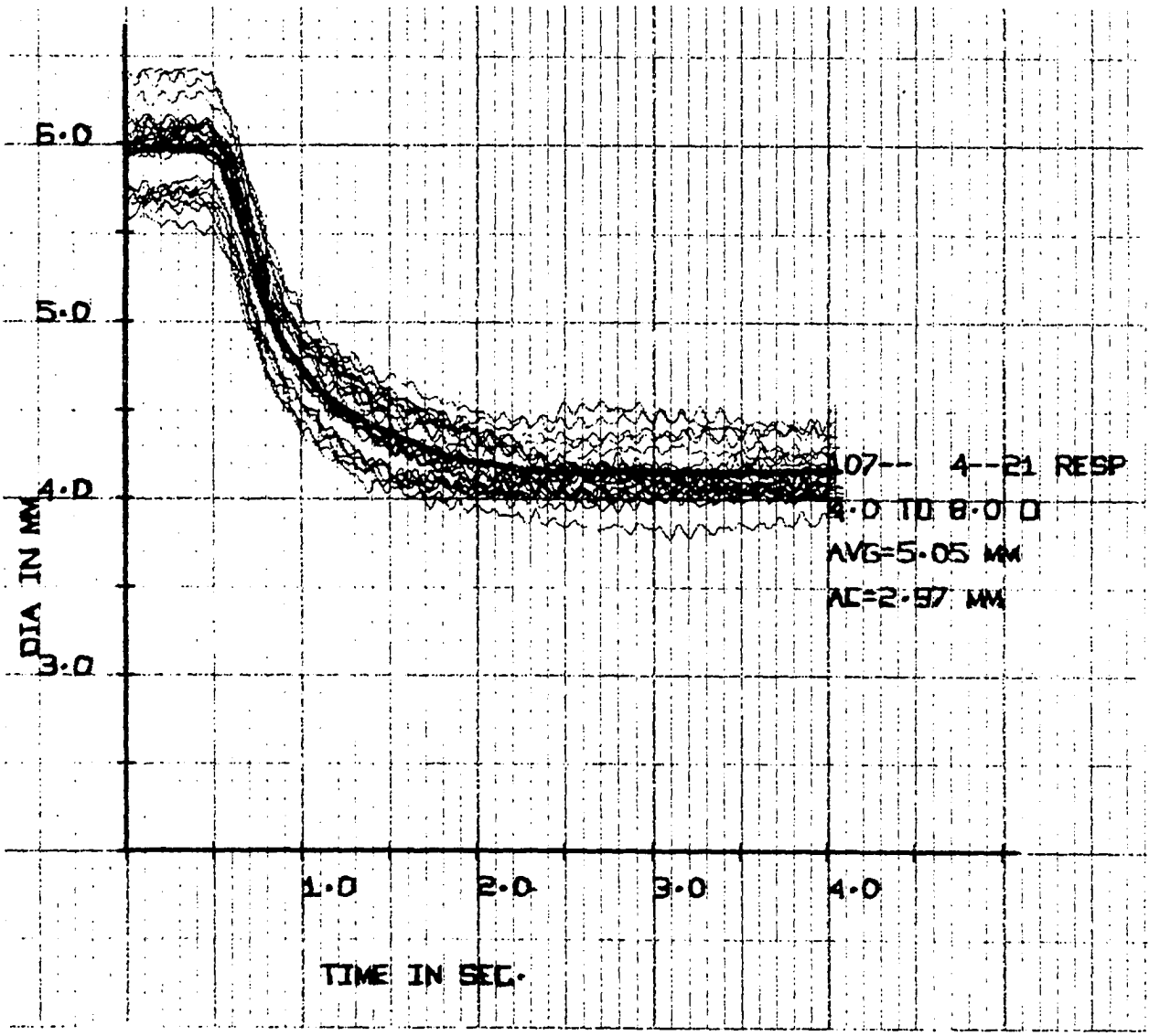

Figure 14. Responses of the pupil diameter to twenty-one accommodative steps from 4.0D to 8.0D. The dark line indicates the average of the twenty-one responses

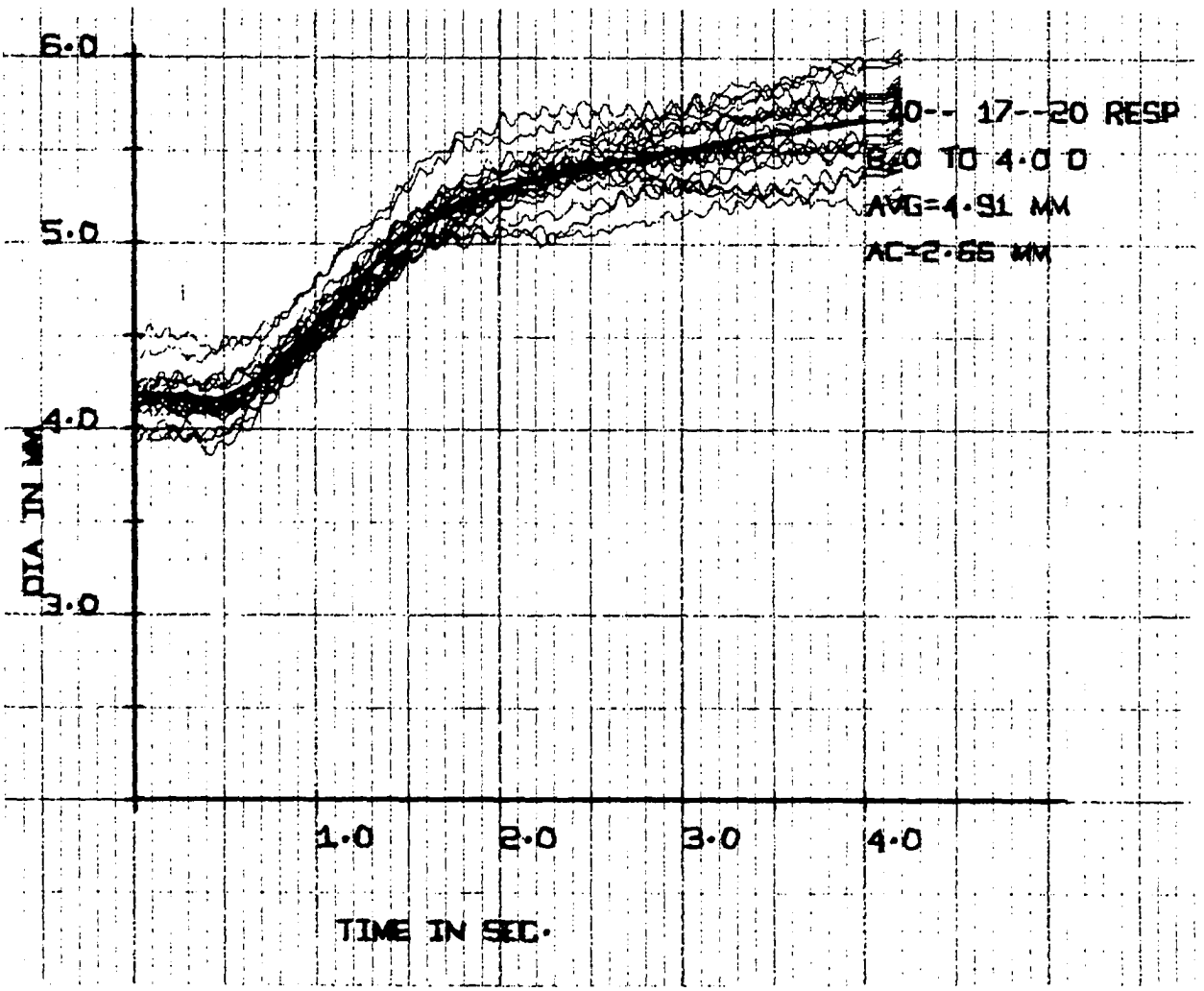

Figure 15. Responses of the pupil diameter to twenty accommodative steps from 8.0D to 4.0D. The dark line indicates the average of the twenty responses

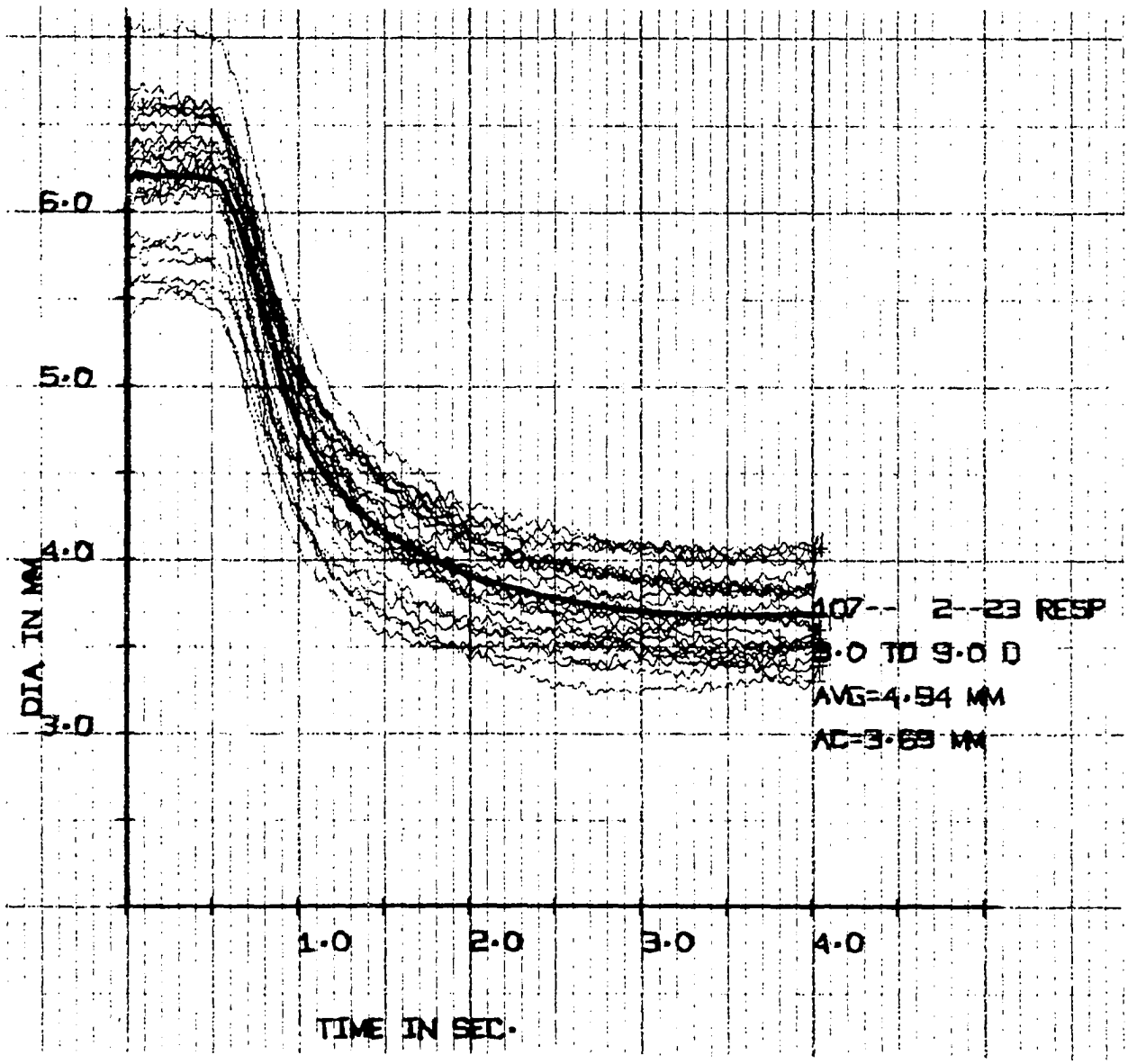

Figure 16. Responses of the pupil diameter to twenty-three accommodative steps from 3.0D to 9.0D. The dark line indicates the average of the twenty-three responses

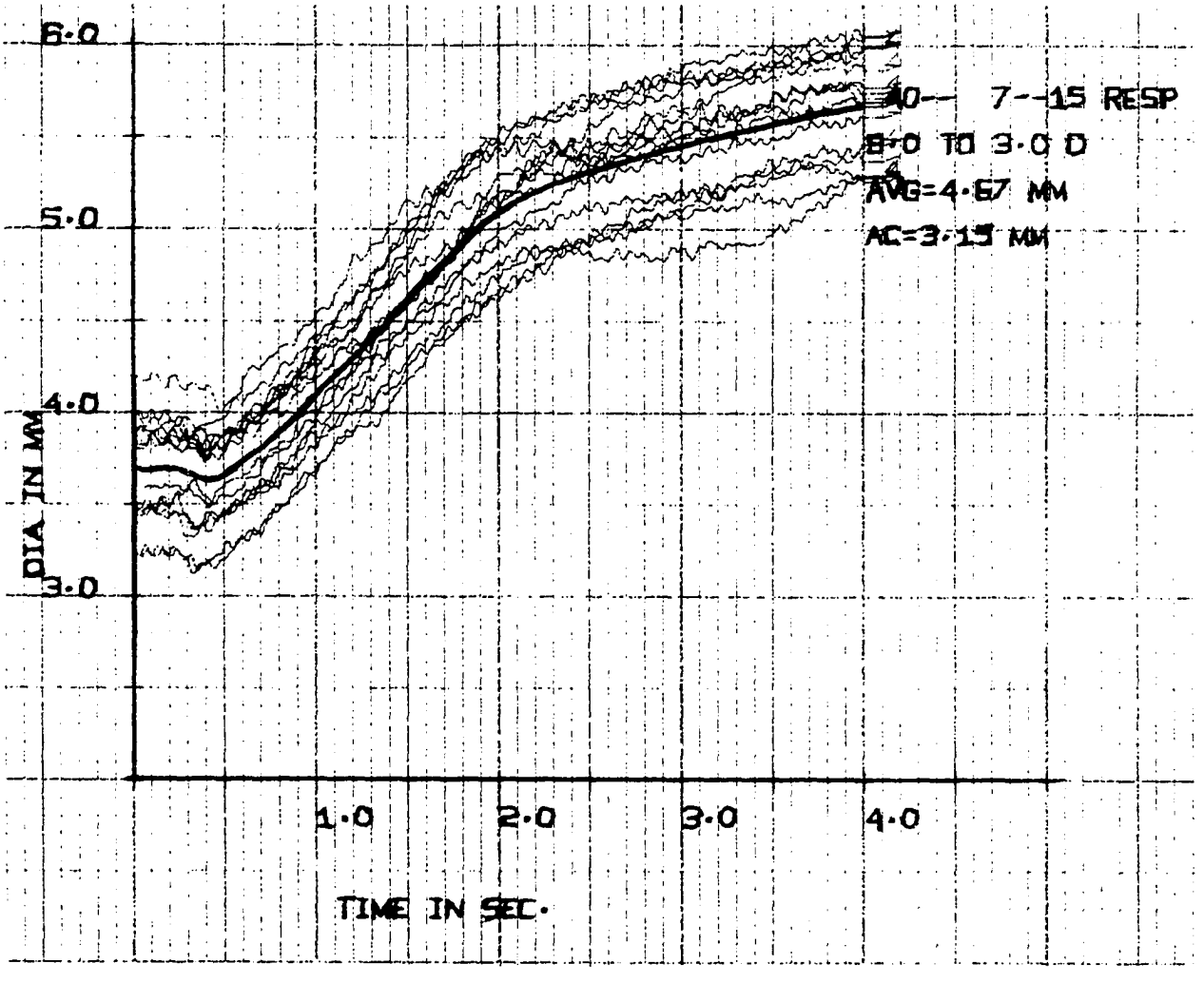

Figure 17. Responses of the pupil diameter to fifteen accommodative steps from 9.0D to 3.0D. The dark line indicates the average of the fifteen responses

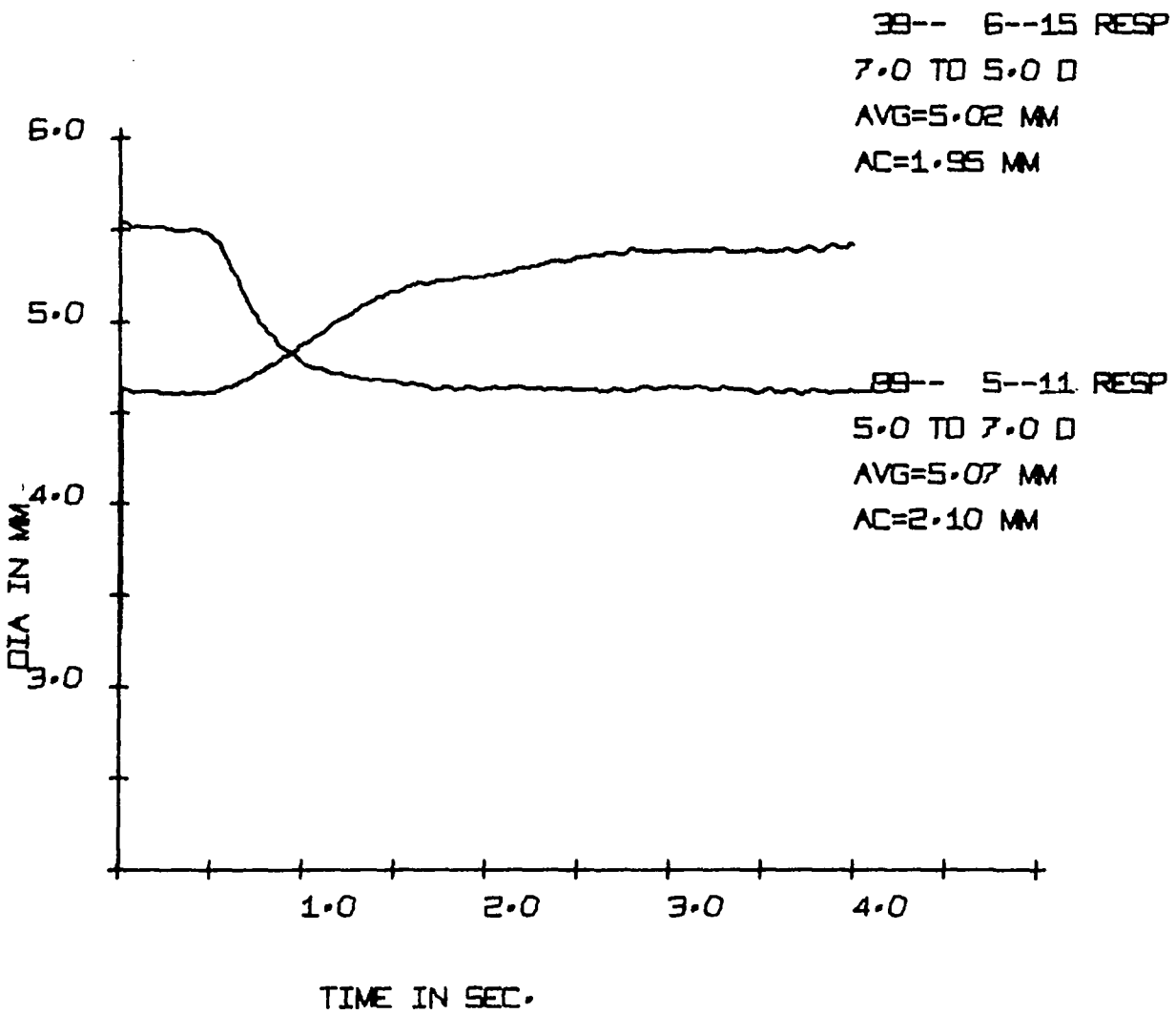

Figure 18. A plot of the average pupil diameter to accommodative steps from 5.0D to 7.0D and 7.0D to 5.0D

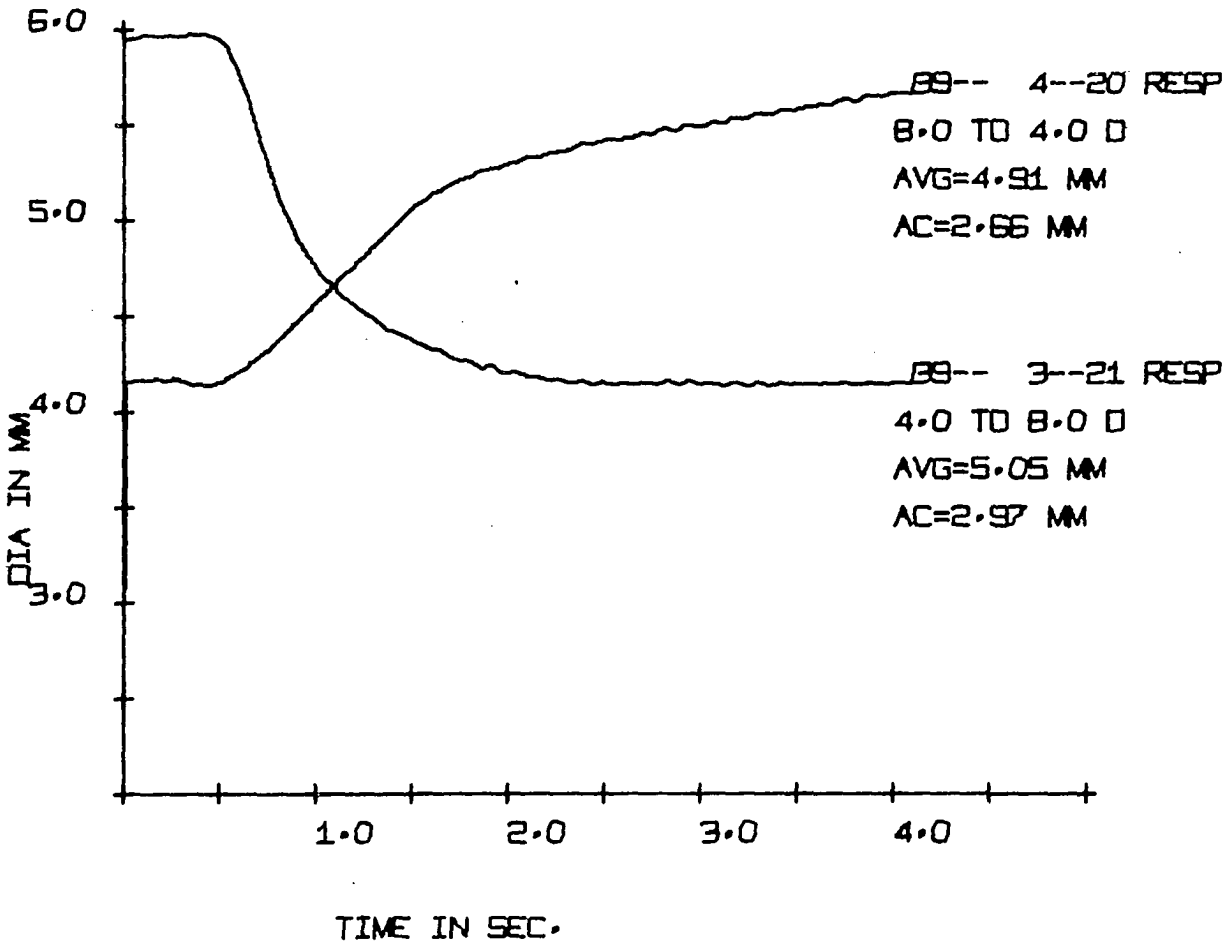

Figure 19. A plot of the average pupil diameter response to accommodative steps from 4.0D to 8.0D and 8.0D to 4.0D

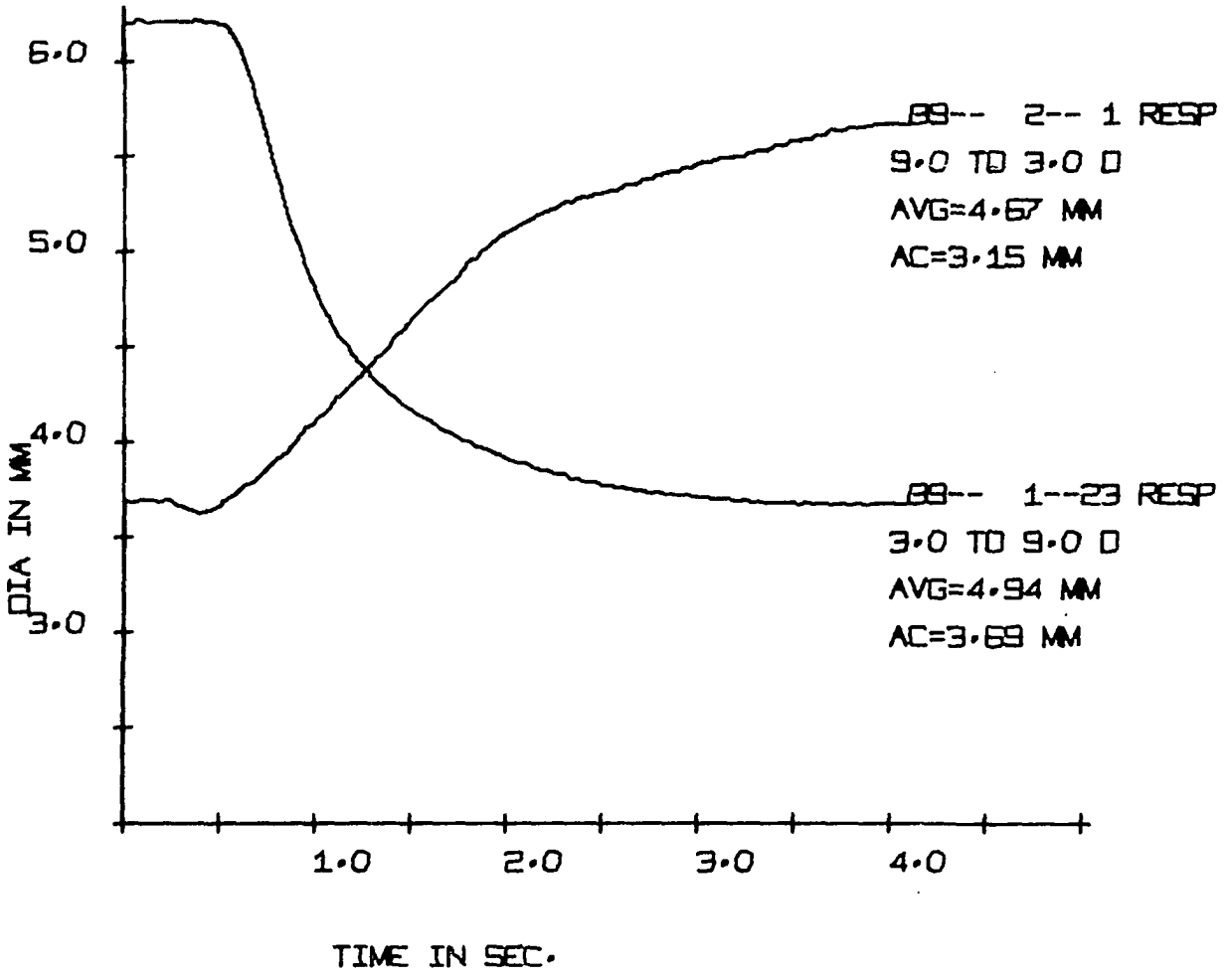

Figure 20. A plot of the average pupil diameter response to accommodative steps from 3.0D to 9.0D and 9.0D to 3.0D

Figure 21. A Bode plot of the accommodative-pupillary system responding to eleven accommodative steps (ST) from 5.0D to 7.0D. Shown are the fundamental (0.0625 Hz.) and odd harmonic frequencies. No time delay (TD) has been removed

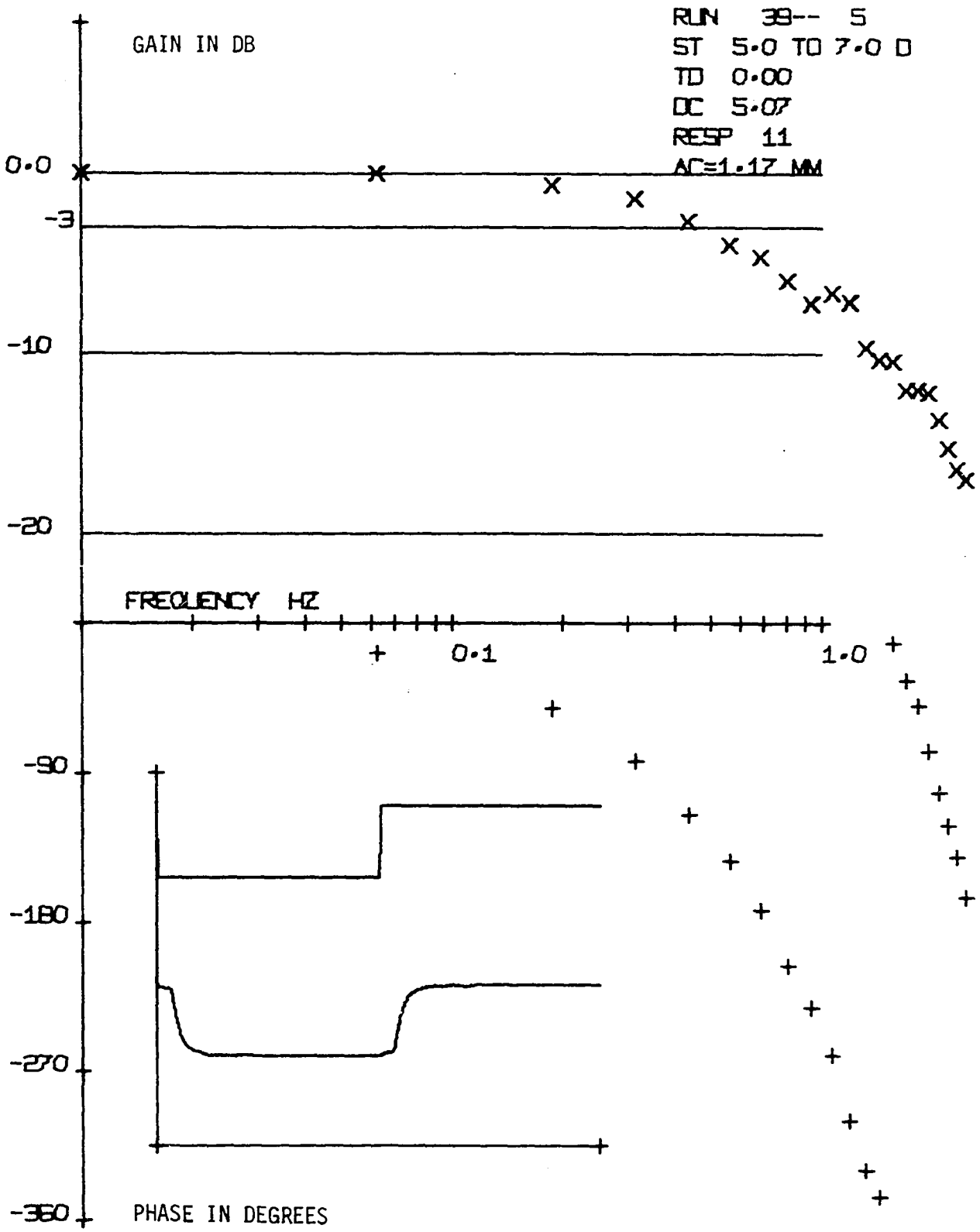
RUN 38-- 5
ST 5.0 TO 7.0 D
TD 0.00
DC 5.07
RESP 11
AC=1.17 MM
GAIN IN DB
0.0
-3
-10
-20
FREQUENCY HZ
0.1
1.0
-90
-180
-270
-360
PHASE IN DEGREES

Figure 22. This figure is the same as Figure 21 except that a time delay of 0.29 second has been removed

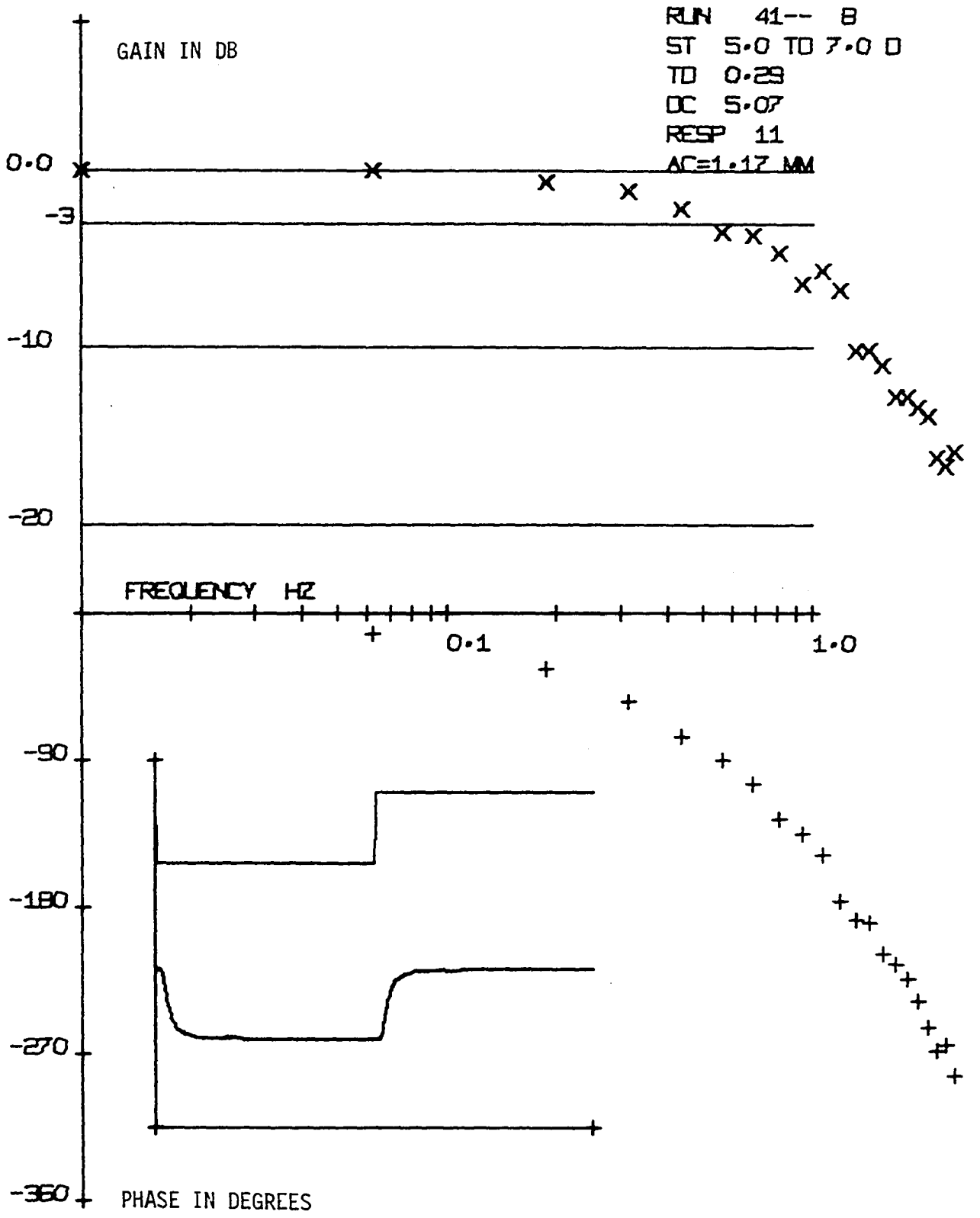
RUN 41-- B
ST 5.0 TO 7.0 D
TD 0.29
DC 5.07
RESP 11
AC=1.17 MM
GAIN IN DB
0.0
-3
-10
-20
FREQUENCY HZ
0.1
1.0
-90
-180
-270
-360
PHASE IN DEGREES

Figure 23. This figure is the same as Figure 21 except that a time delay of 0.41 second has been removed

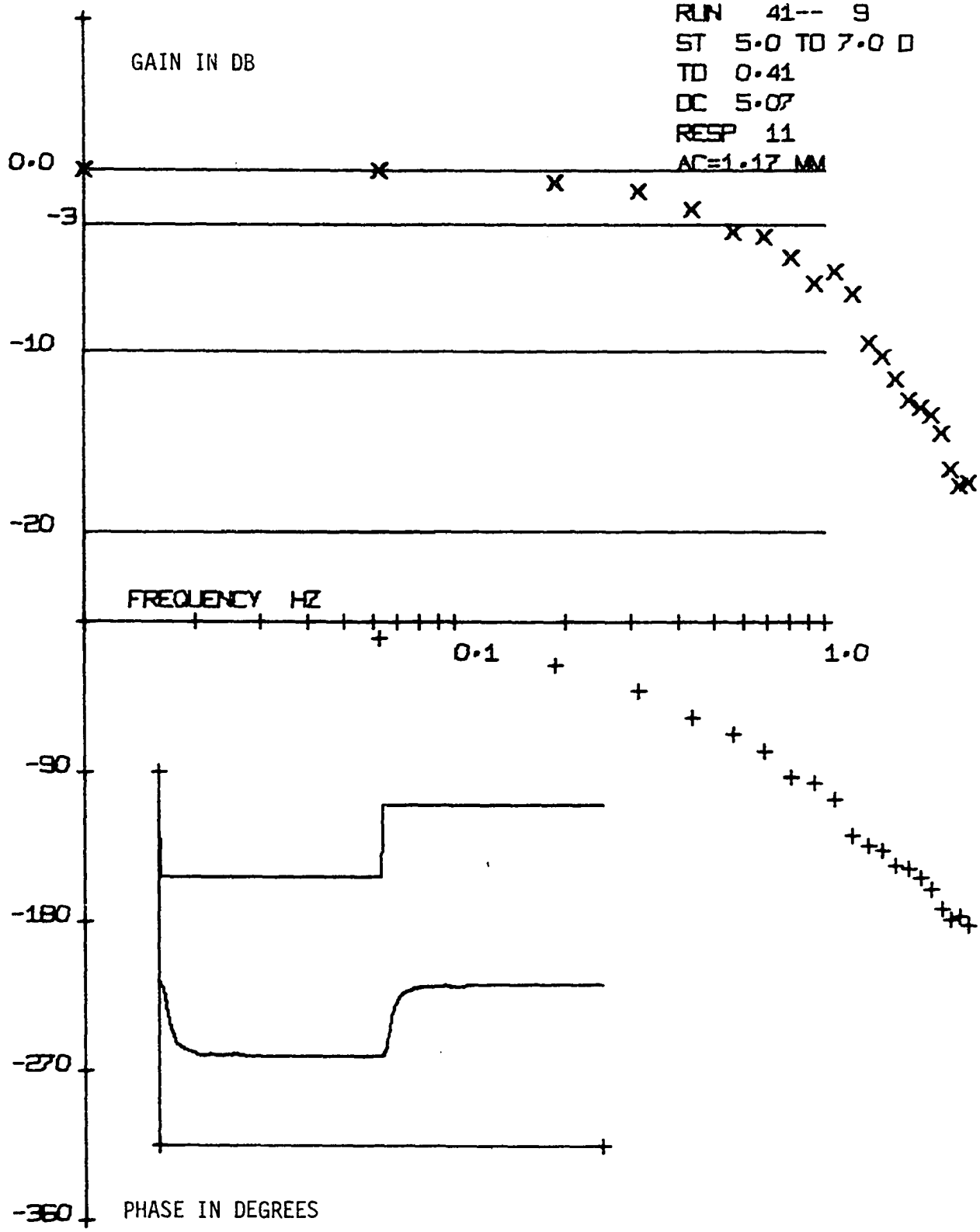
RUN 41-- 9
ST 5.0 TO 7.0 D
TD 0.41
DC 5.07
RESP 11
AC=1.17 MM
GAIN IN DB
0.0
-3
-10
-20
FREQUENCY HZ
0.1
1.0
-90
-180
-270
-360
PHASE IN DEGREES

Figure 24. This figure is the same as Figure 21 except that a time delay of 0.51 second has been removed

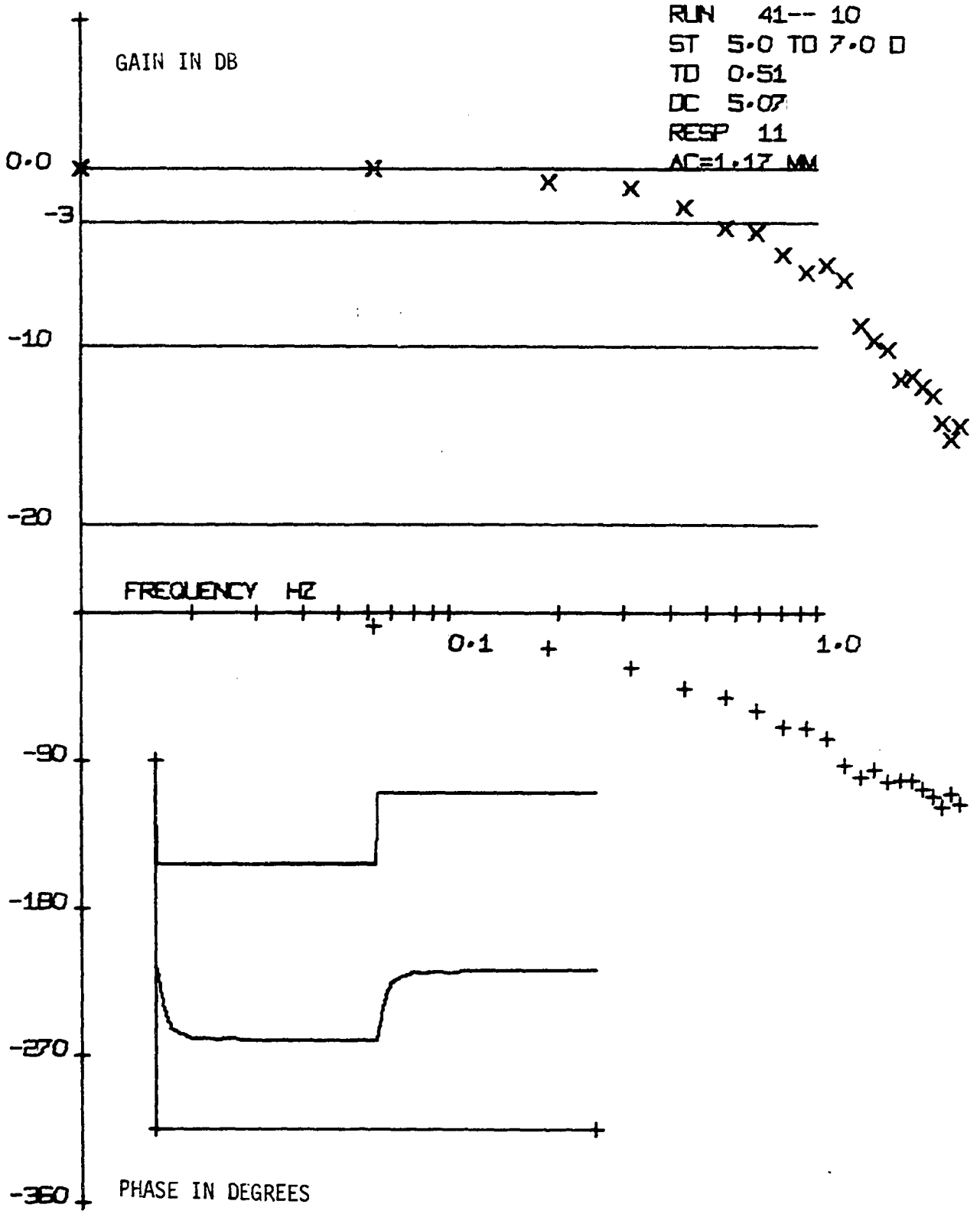
RUN 41-- 10
ST 5.0 TO 7.0 D
TD 0.51
DC 5.07
RESP 11
AC=1.17 MM
GAIN IN DB
0.0
-3
-10
-20
FREQUENCY HZ
0.1
1.0
-90
-180
-270
-360
PHASE IN DEGREES

Figure 25. A Bode plot of the accommodative-pupillary system responding to twenty-one accommodative steps (ST) from 4.0D to 8.0D. Shown are the fundamental (0.0625 Hz.) and odd harmonic frequencies. No time delay (TD) has been removed

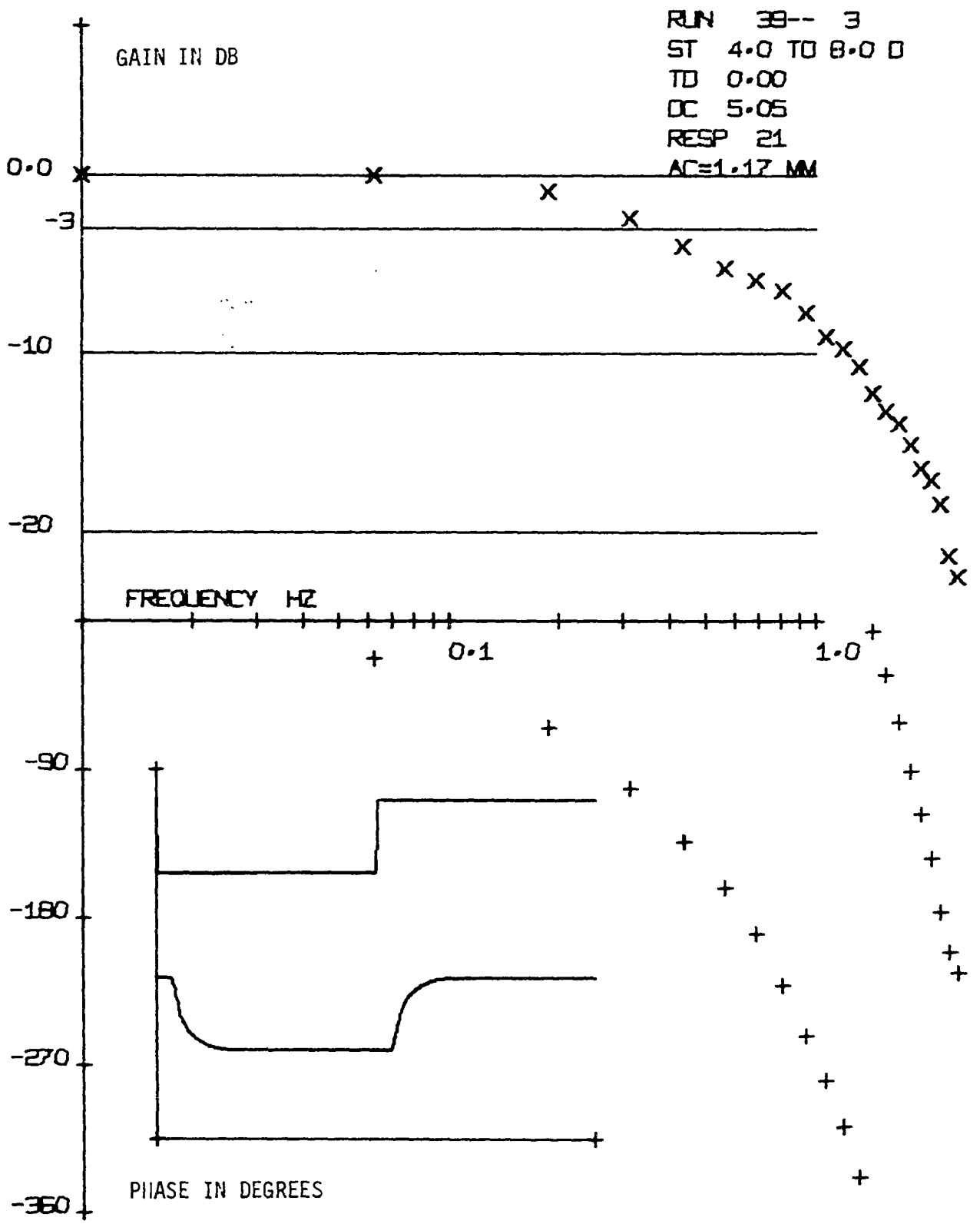
RUN 38-- 3
ST 4.0 TO 8.0 D
TD 0.00
DC 5.05
RESP 21
AC=1.17 MM
GAIN IN DB
0.0
-3
-10
-20
FREQUENCY HZ
0.1
1.0
-90
-180
-270
-360
PHASE IN DEGREES

Figure 26. This figure is the same as Figure 25 except that a time delay of 0.36 second has been removed

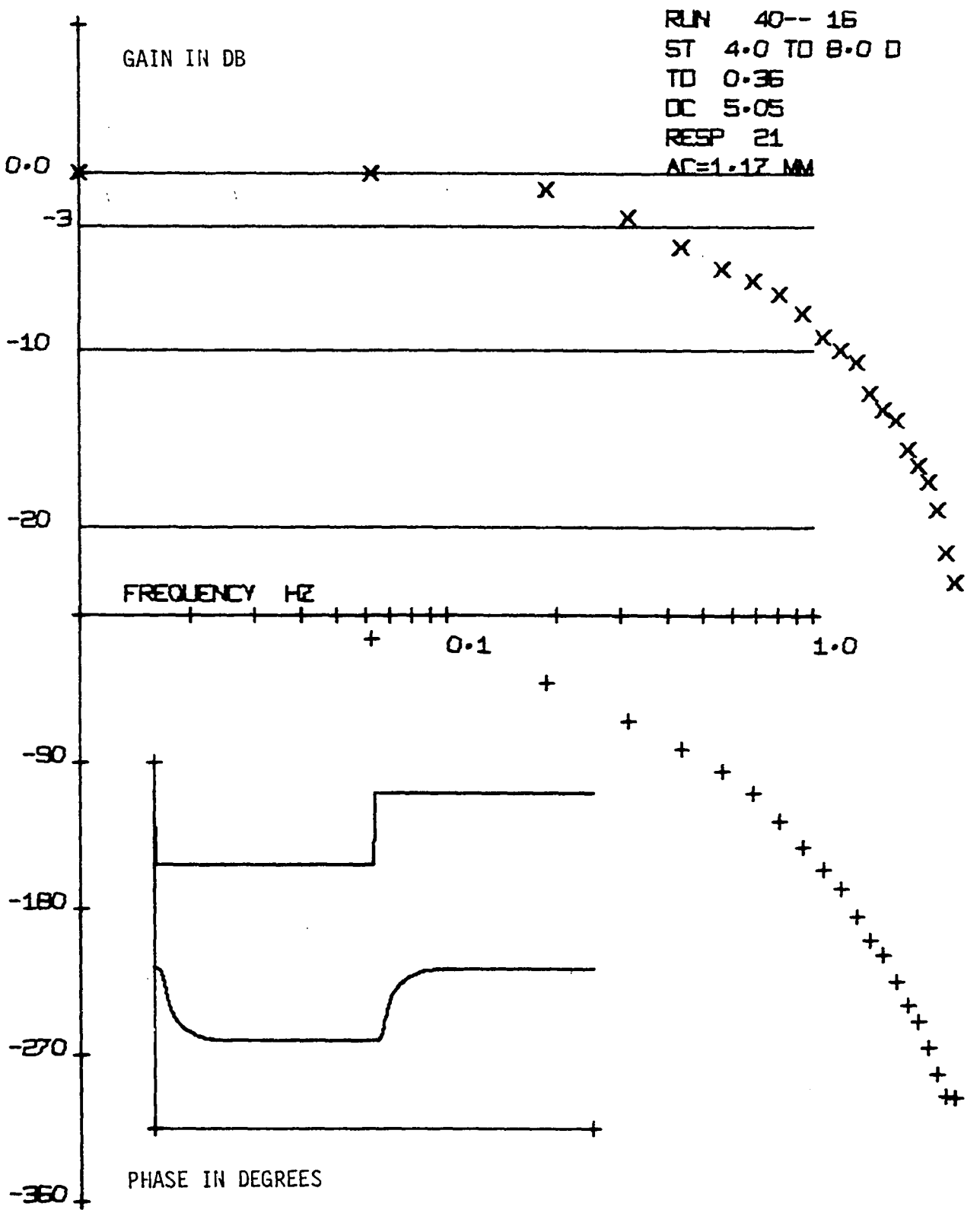
RUN 40-- 16
ST 4.0 TO 8.0 D
TD 0.36
DC 5.05
RESP 21
AC=1.17 MM
GAIN IN DB
0.0
-3
-10
-20
FREQUENCY HZ
0.1
1.0
-90
-180
-270
-360
PHASE IN DEGREES

Figure 27. This figure is the same as Figure 25 except that a time delay of 0.44 second has been removed

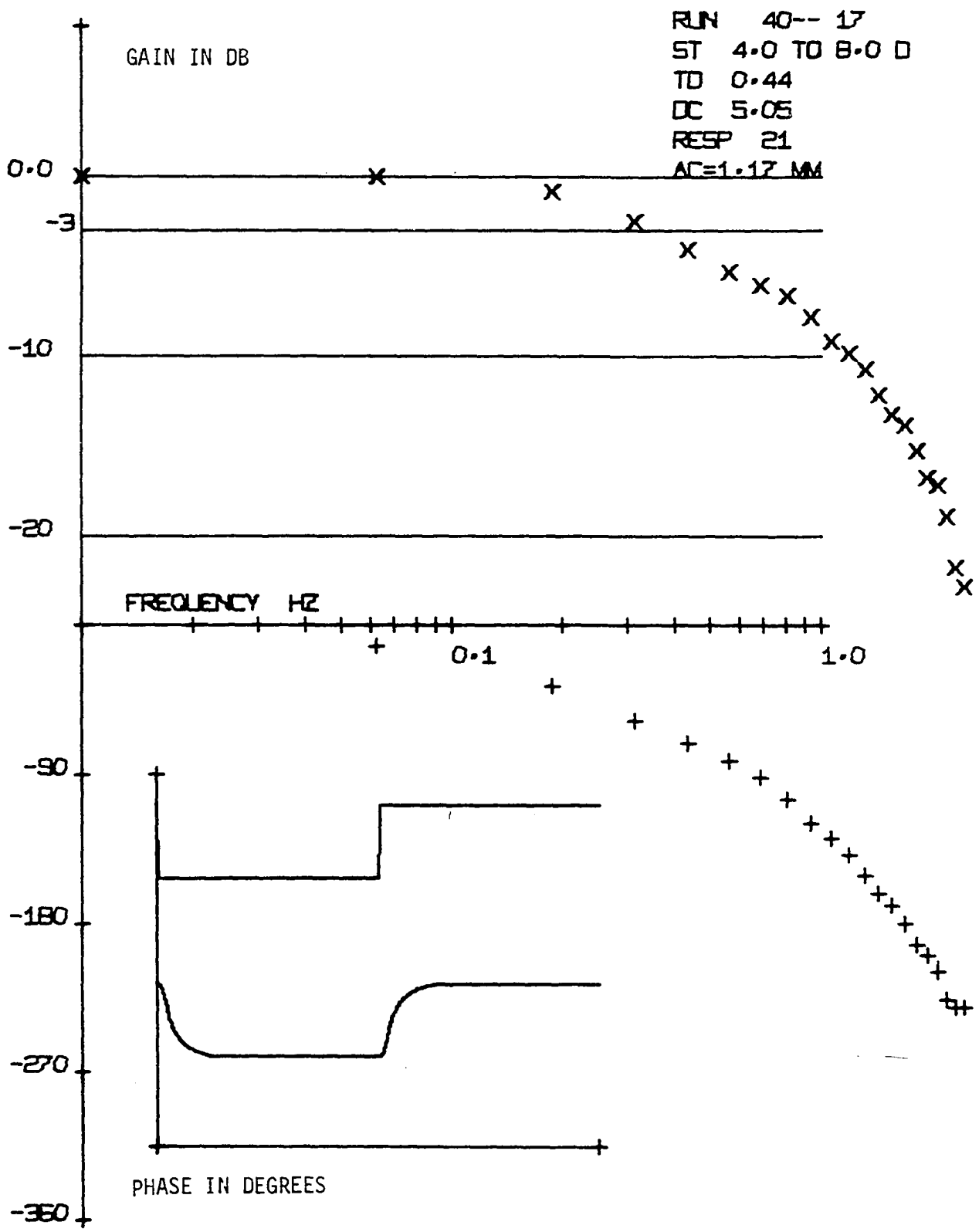
RUN 40-- 17
ST 4.0 TO 8.0 D
TD 0.44
DC 5.05
RESP 21
AC=1.17 MM
GAIN IN DB
0.0
-3
-10
-20
FREQUENCY HZ
0.1
1.0
-90
-180
-270
-360
PHASE IN DEGREES

Figure 28. A Bode plot of the accommodative-pupillary system responding to twenty-three accommodative steps (ST) from 3.0D to 9.0D. Shown are the fundamental (0.0625 Hz.) and odd harmonic frequencies. No time delay (TD) has been removed

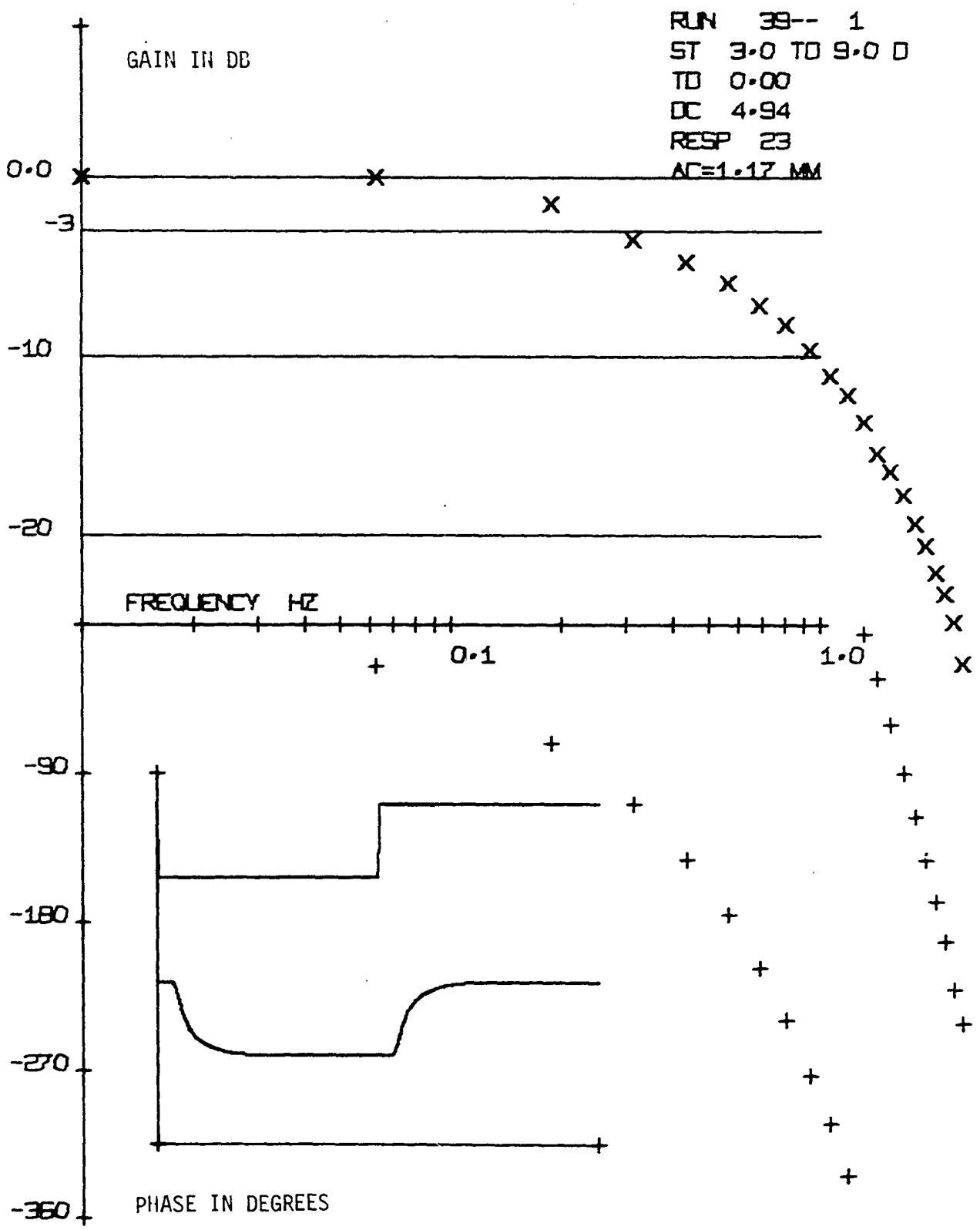
RUN 38-- 1
ST 3.0 TO 9.0 D
TD 0.00
DC 4.94
RESP 23
AC=1.17 MM
GAIN IN DB
0.0
-3
-10
-20
FREQUENCY HZ
0.1
1.0
-90
-180
-270
-360
PHASE IN DEGREES

Figure 29. This figure is the same as Figure 28 except that a time delay of 0.33 second has been removed

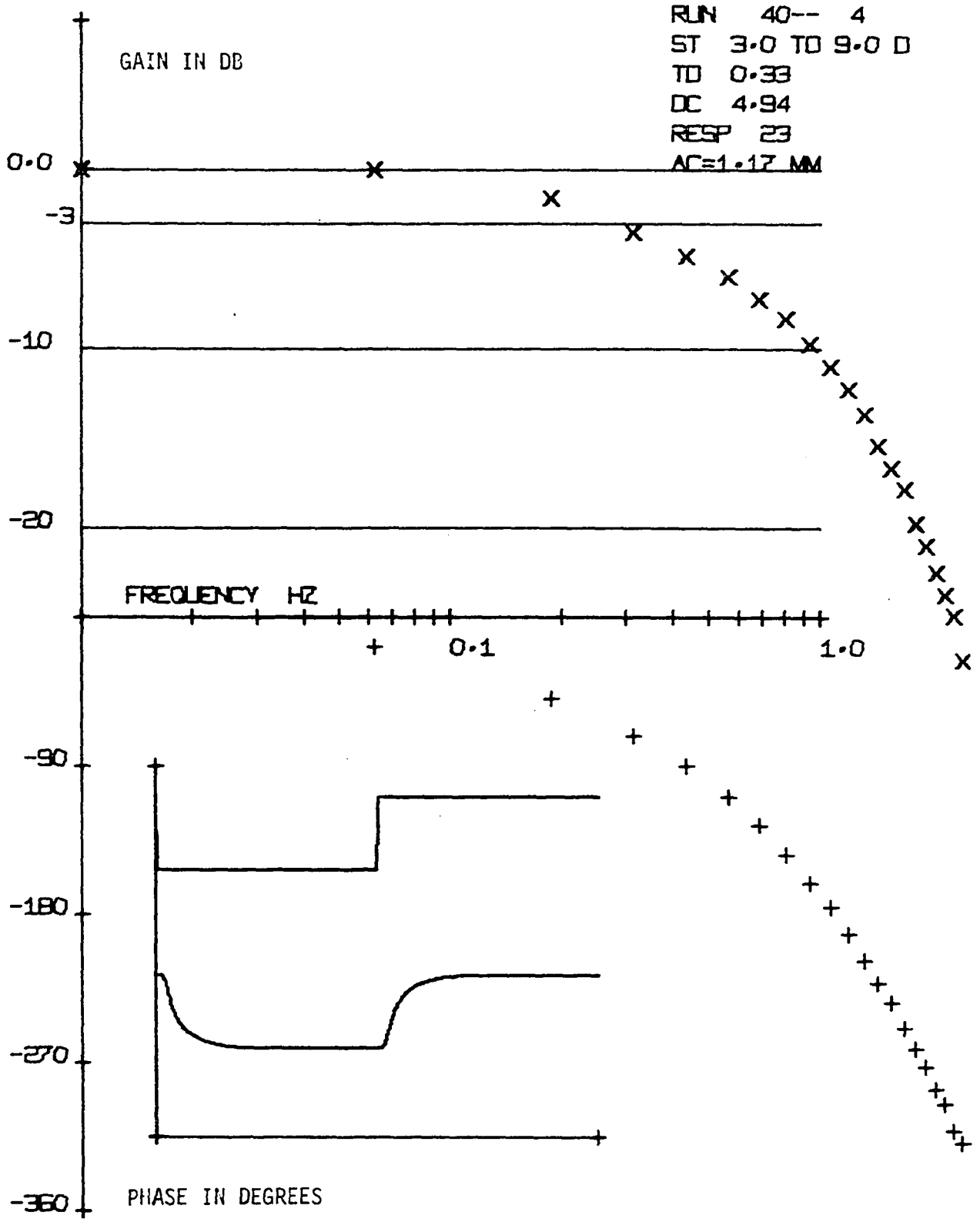
RUN 40-- 4
ST 3.0 TO 9.0 D
TO 0.33
DC 4.94
RESP 23
AC=1.17 MM
GAIN IN DB
0.0
-3
-10
-20
FREQUENCY HZ
0.1
1.0
-90
-180
-270
-360
PHASE IN DEGREES

Figure 30. This figure is the same as Figure 28 except that a time delay of 0.41 second has been removed

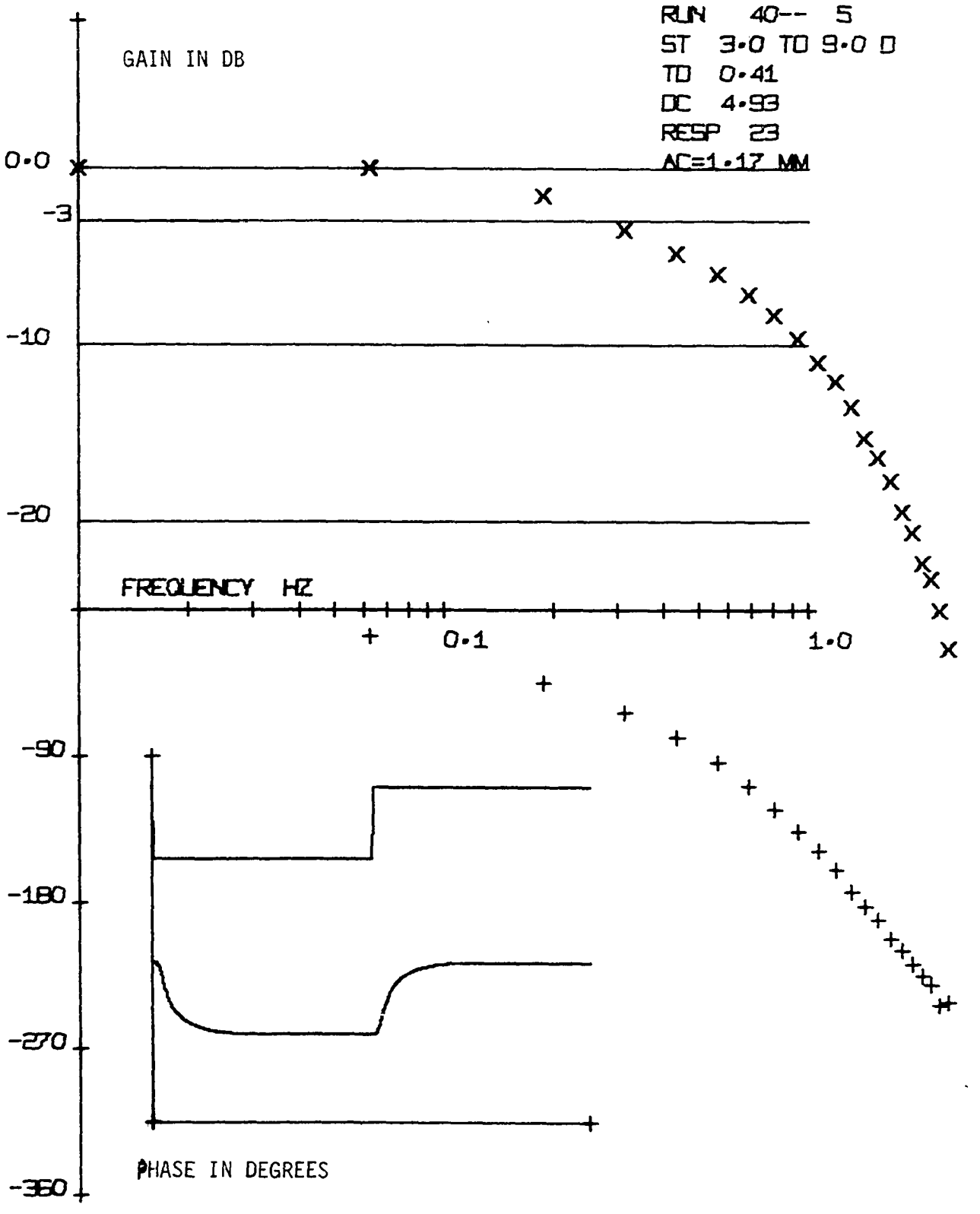
RUN 40-- 5
ST 3.0 TO 9.0 D
TD 0.41
DC 4.93
RESP 23
AC=1.17 MM
GAIN IN DB
0.0
-3
-10
-20
FREQUENCY HZ
0.1
1.0
-90
-180
-270
-360
PHASE IN DEGREES

Figure 31. This figure is the same as Figure 28 except that a time delay of 0.49 second has been removed

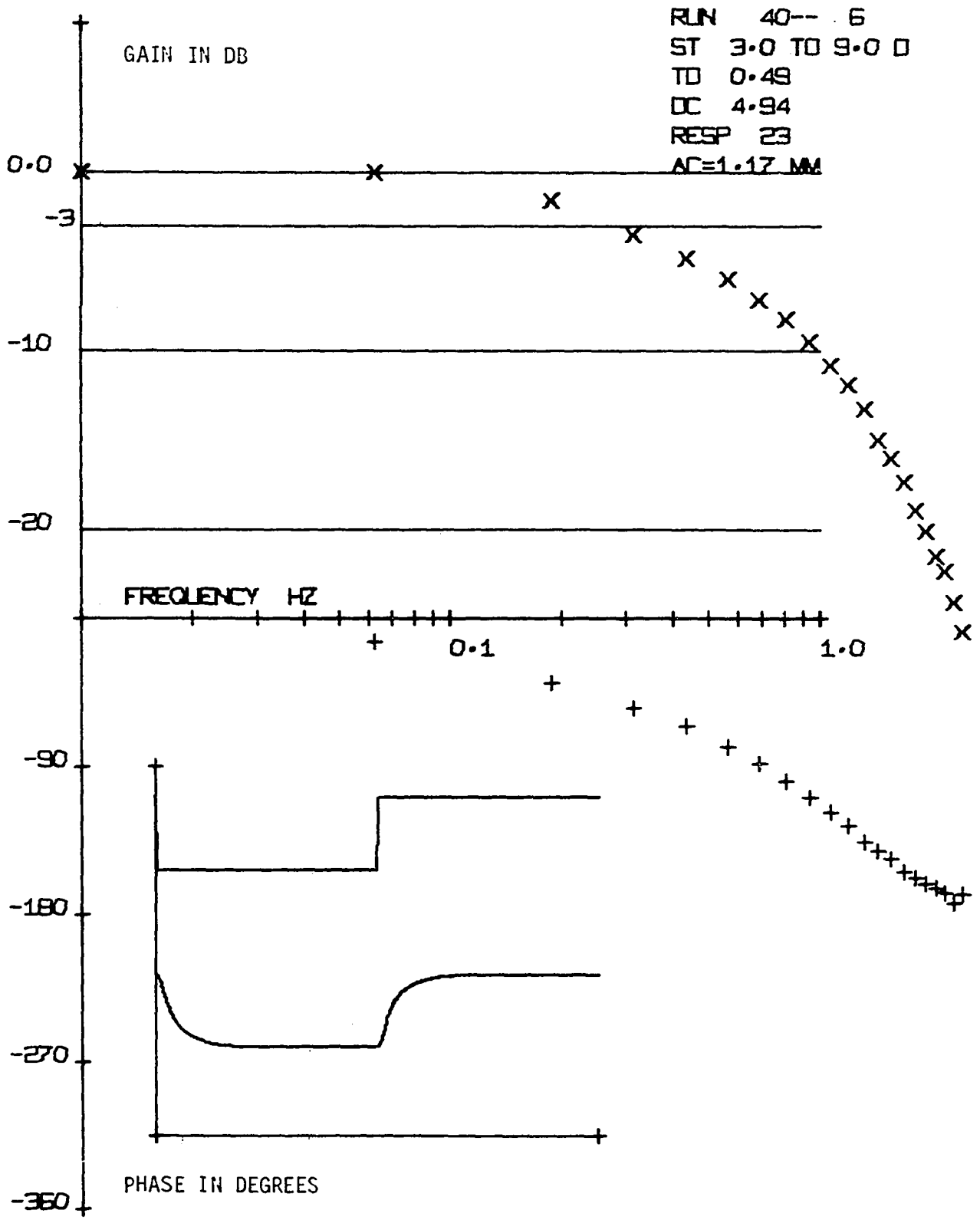
RUN 40-- 6
ST 3.0 TO 9.0 D
TD 0.49
DC 4.94
RESP 23
AC=1.17 MM
GAIN IN DB
0.0
-3
-10
-20
FREQUENCY HZ
0.1
1.0
-90
-180
-270
-360
PHASE IN DEGREES

Figure 32. A Bode plot of the accommodative-pupillary system responding to fifteen accommodative steps (ST) from 7.0D to 5.0D. Shown are the fundamental (0.0625 Hz.) and odd harmonic frequencies. No time delay (TD) has been removed

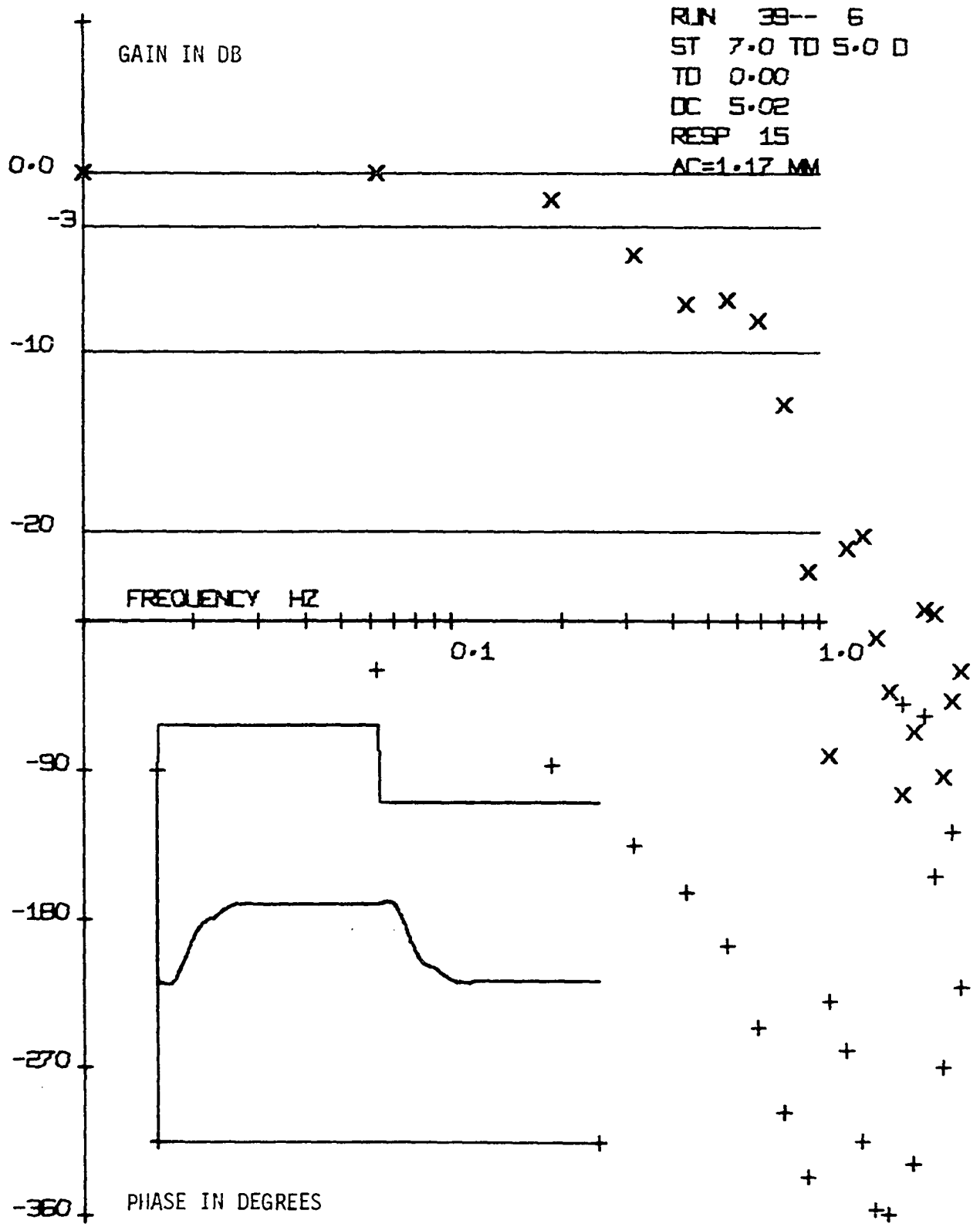
RUN 39-- 6
ST 7.0 TO 5.0 D
TO 0.00
DC 5.02
RESP 15
AC=1.17 MM
GAIN IN DB
0.0
-3
-10
-20
FREQUENCY HZ
0.1
1.0
-90
-180
-270
-360
PHASE IN DEGREES

Figure 33. This figure is the same as Figure 32 except that a time delay of 0.29 second has been removed

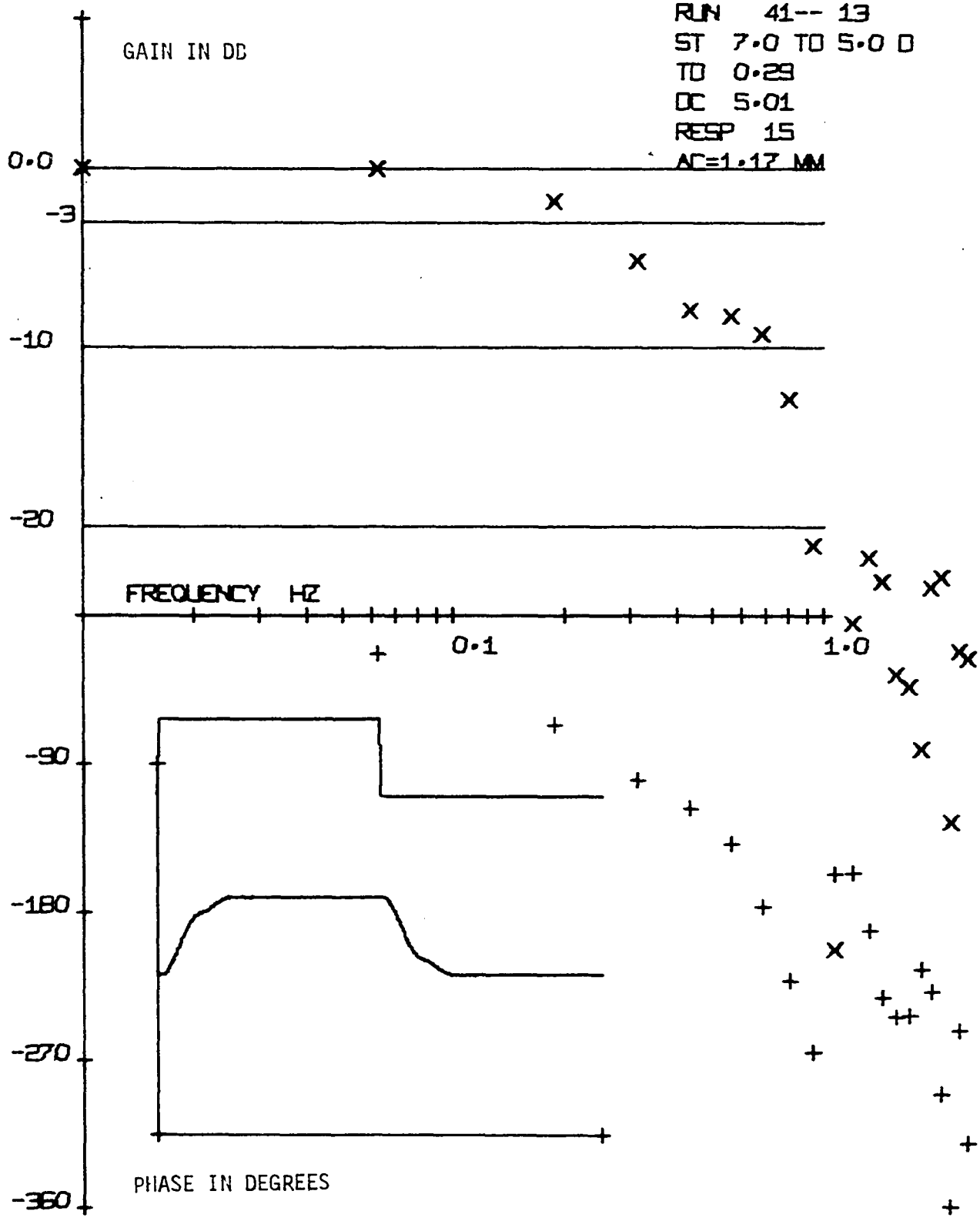
RUN 41-- 13
ST 7.0 TO 5.0 D
TO 0.29
DC 5.01
RESP 15
AC=1.17 MM
GAIN IN DB
0.0
-3
-10
-20
FREQUENCY HZ
0.1
1.0
-90
-180
-270
-360
PHASE IN DEGREES

Figure 34. This figure is the same as Figure 32 except that a time delay of 0.41 second has been removed

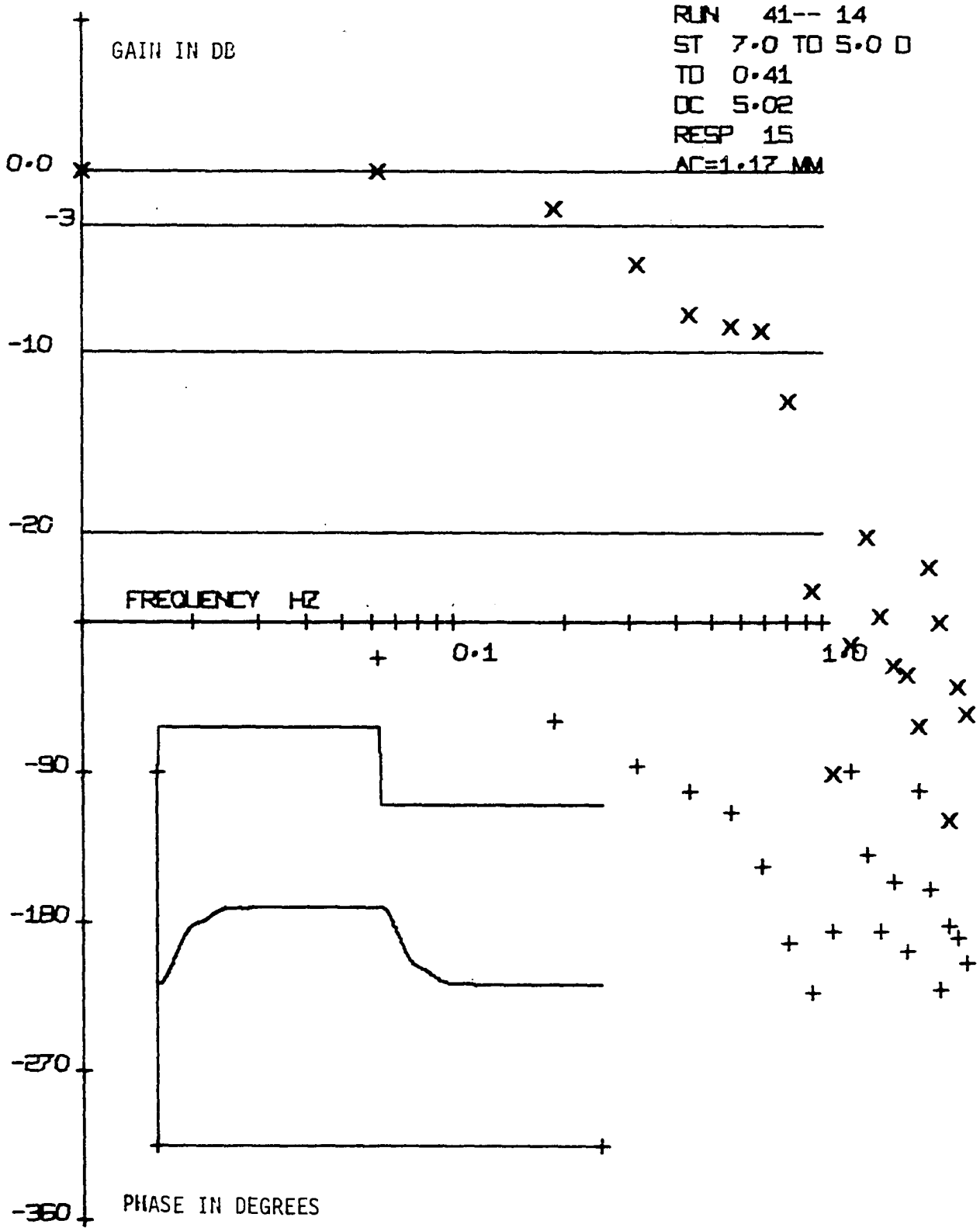
RUN 41-- 14
ST 7.0 TO 5.0 D
TD 0.41
DC 5.02
RESP 15
AC=1.17 MM
GAIN IN DB
0.0
-3
-10
-20
FREQUENCY HZ
0.1
1.0
-90
-180
-270
-360
PHASE IN DEGREES

Figure 35. This figure is the same as Figure 32 except that a time delay of 0.49 second has been removed

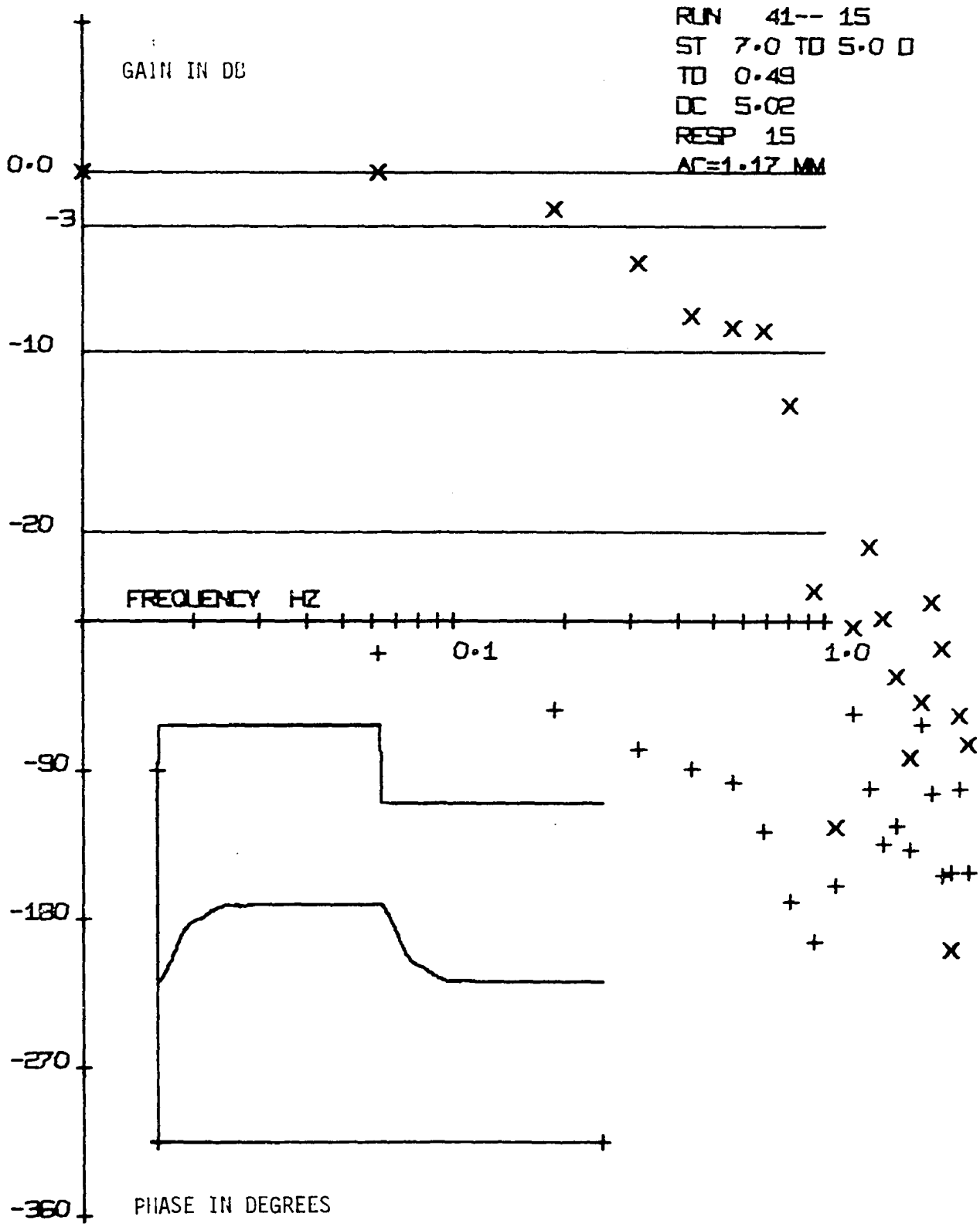
RUN 41-- 15
ST 7.0 TO 5.0 D
TO 0.49
DC 5.02
RESP 15
AC=1.17 MM
GAIN IN DB
0.0
-3
-10
-20
FREQUENCY HZ
0.1
1.0
-90
-180
-270
-360
PHASE IN DEGREES

Figure 36. A Bode plot of the accommodative-pupillary system responding to twenty accommodative steps (ST) from 8.0D to 4.0D. Shown are the fundamental (0.0625 Hz.) and odd harmonic frequencies. No time delay (TD) has been removed

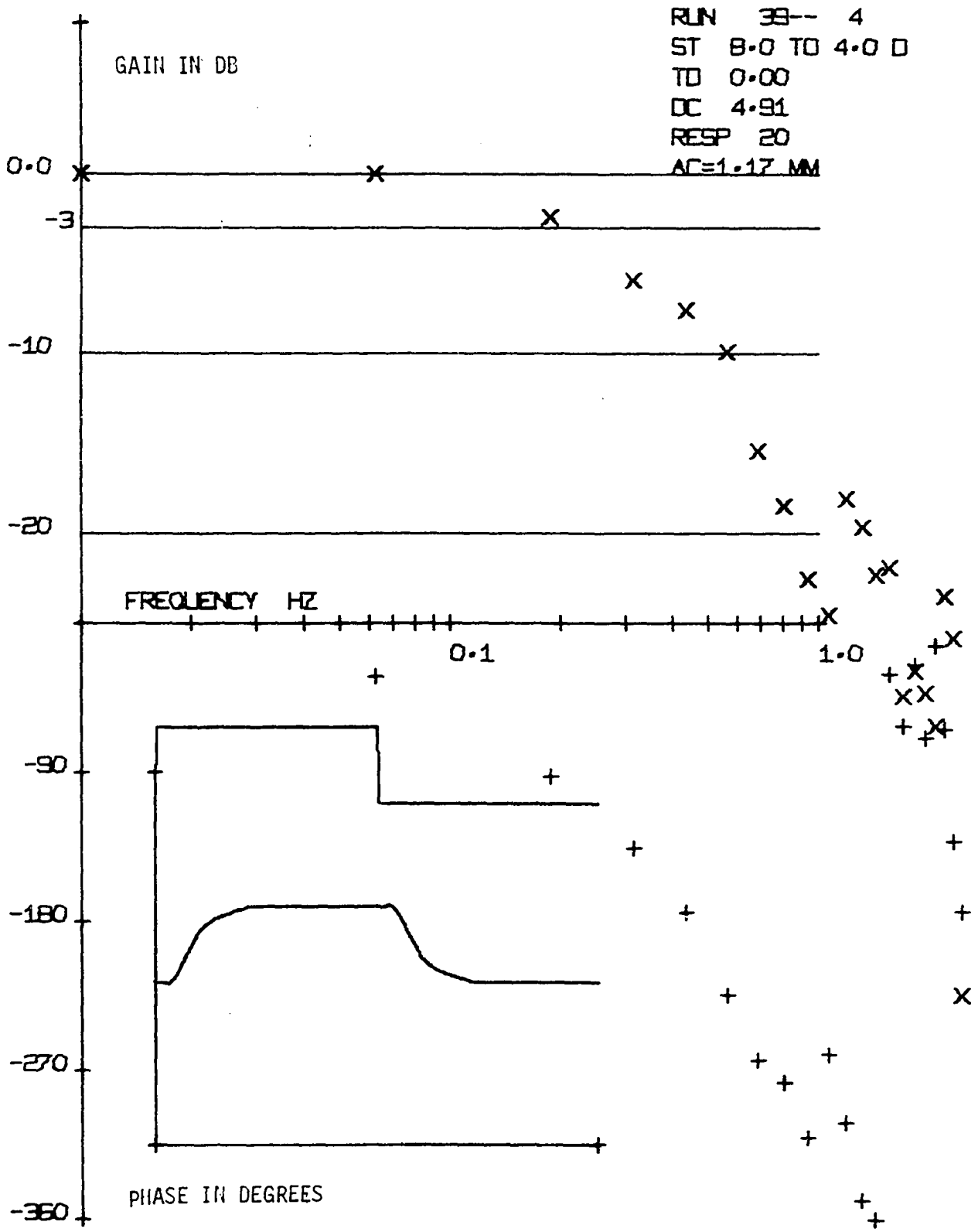
RUN 39-- 4
ST 8.0 TO 4.0 D
TD 0.00
DC 4.91
RESP 20
AC=1.17 MM
GAIN IN DB
0.0
-3
-10
-20
FREQUENCY HZ
0.1
1.0
-90
-180
-270
-360
PHASE IN DEGREES

Figure 37. This figure is the same as Figure 36 except that a time delay of 0.32 second has been removed

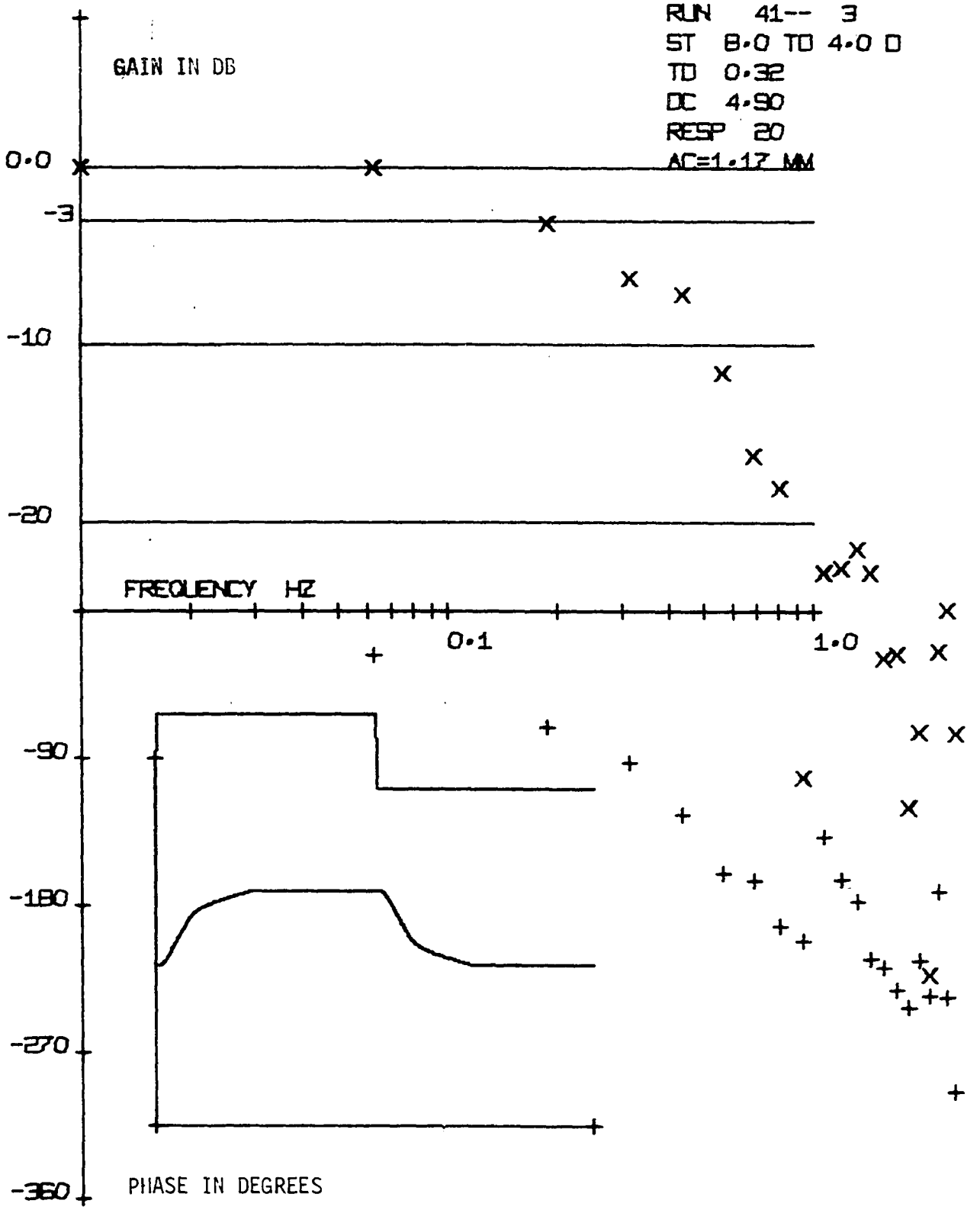
RUN 41-- 3
ST 8.0 TO 4.0 D
TO 0.32
DC 4.90
RESP 20
AC=1.17 MM
GAIN IN DB
0.0
-3
-10
-20
FREQUENCY HZ
0.1
1.0
-90
-180
-270
-360
PHASE IN DEGREES

Figure 38. This figure is the same as Figure 36 except that a time delay of 0.42 second has been removed

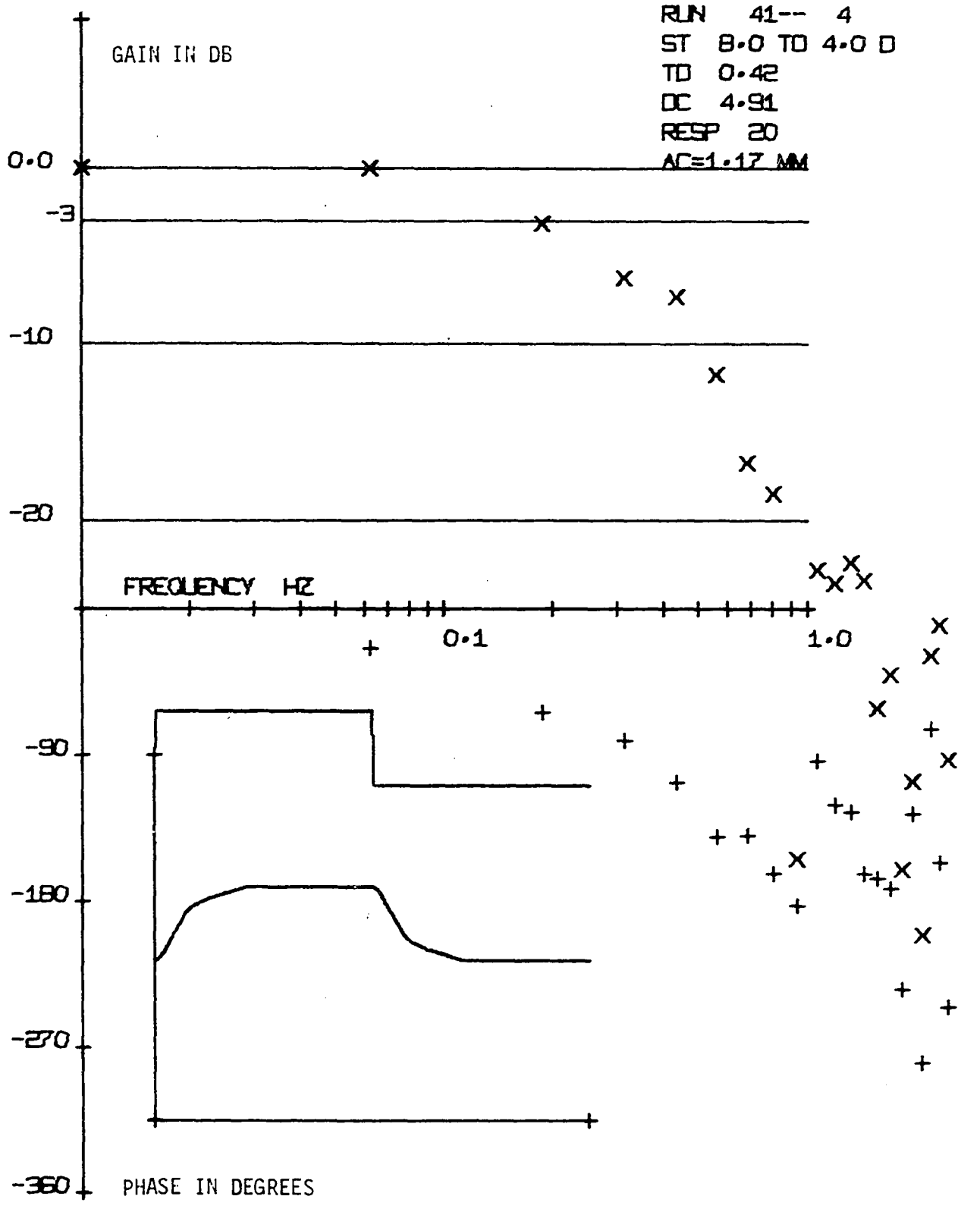
RUN 41-- 4
ST 8.0 TO 4.0 D
TD 0.42
DC 4.91
RESP 20
AC=1.17 MM
GAIN IN DB
0.0
-3
-10
-20
FREQUENCY HZ
0.1
1.0
-90
-180
-270
-360
PHASE IN DEGREES

Figure 39. This figure is the same as Figure 36 except that a time delay of 0.54 second has been removed

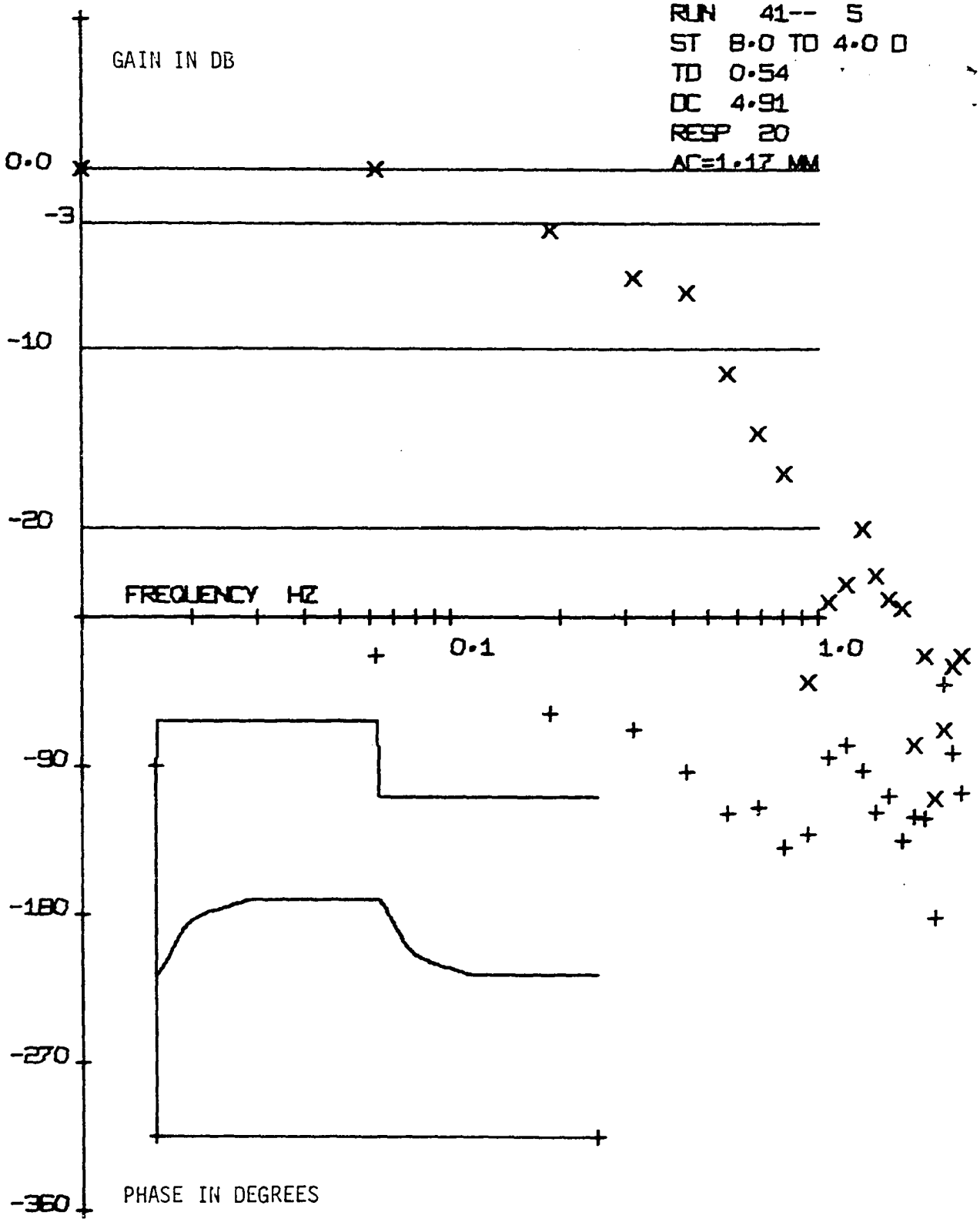
RUN 41-- 5
ST 8.0 TO 4.0 D
TD 0.54
DC 4.91
RESP 20
AC=1.17 MM
GAIN IN DB
0.0
-3
-10
-20
FREQUENCY HZ
0.1
1.0
-90
-180
-270
-360
PHASE IN DEGREES

Figure 40. A Bode plot of the accommodative-pupillary system responding to fifteen accommodative steps (ST) from 8.0D to 4.0D. Shown are the fundamental (0.0625 Hz.) and odd harmonic frequencies. No time delay (TD) has been removed

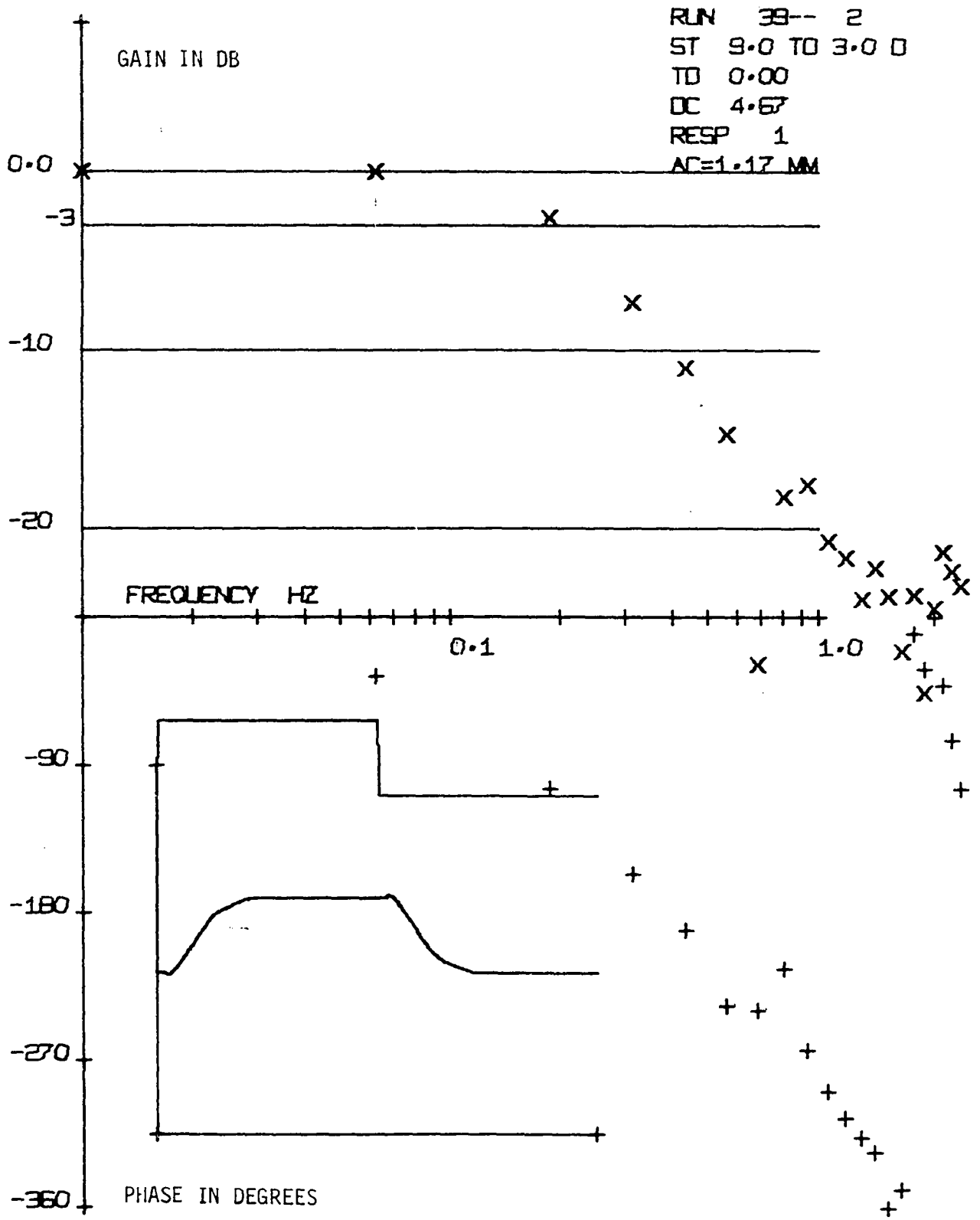
RUN 38-- 2
ST 9.0 TO 3.0 D
TD 0.00
DC 4.67
RESP 1
AC=1.17 MM
GAIN IN DB
0.0
-3
-10
-20
FREQUENCY HZ
0.1
1.0
-90
-180
-270
-360
PHASE IN DEGREES

Figure 41. This figure is the same as Figure 40 except that a time delay of 0.32 second has been removed

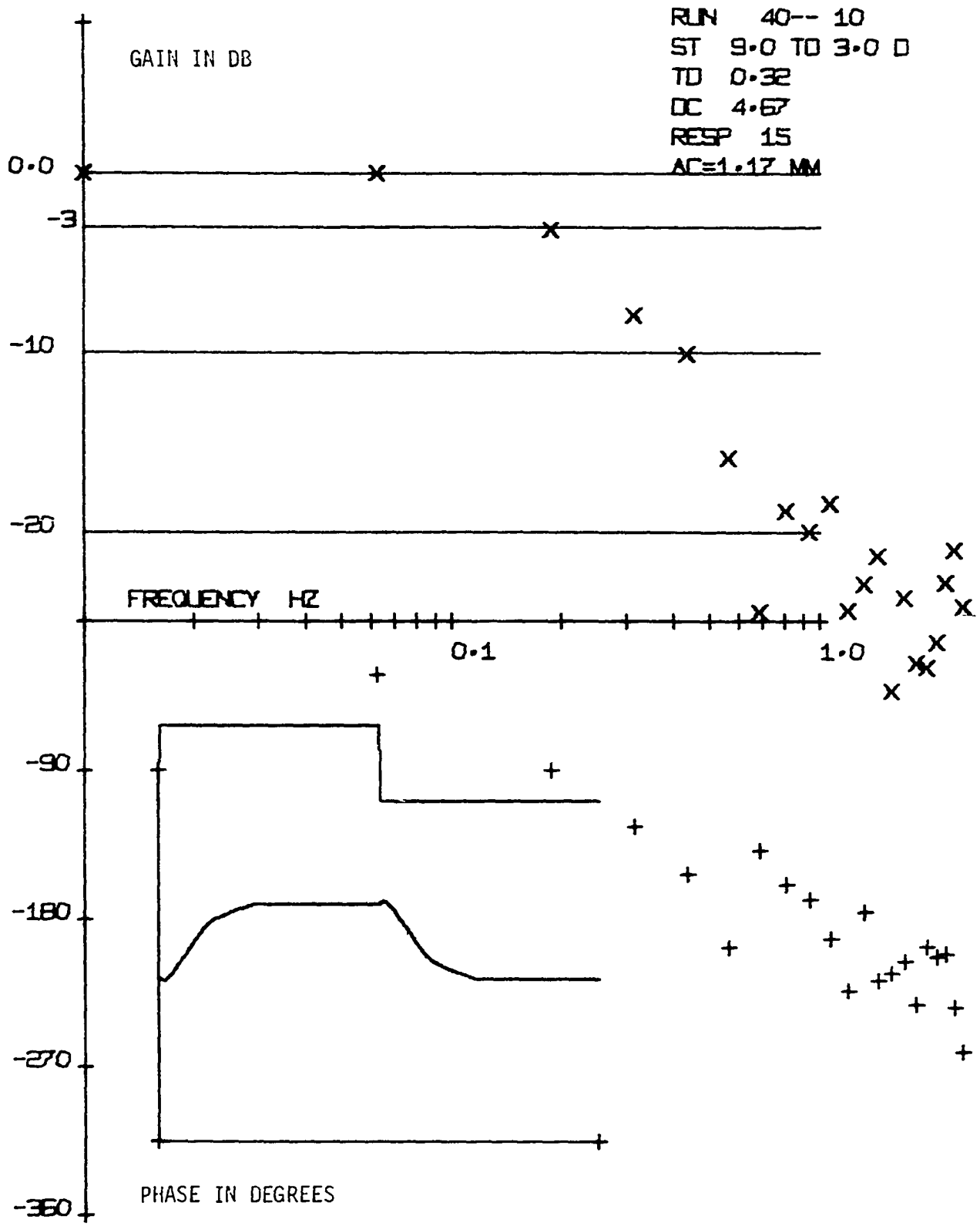
RUN 40-- 10
ST 9.0 TO 3.0 D
TD 0.32
DC 4.67
RESP 15
AC=1.17 MM
GAIN IN DB
0.0
-3
-10
-20
FREQUENCY HZ
0.1
1.0
-90
-180
-270
-360
PHASE IN DEGREES

Figure 42. This figure is the same as Figure 40 except that a time delay of 0.43 second has been removed

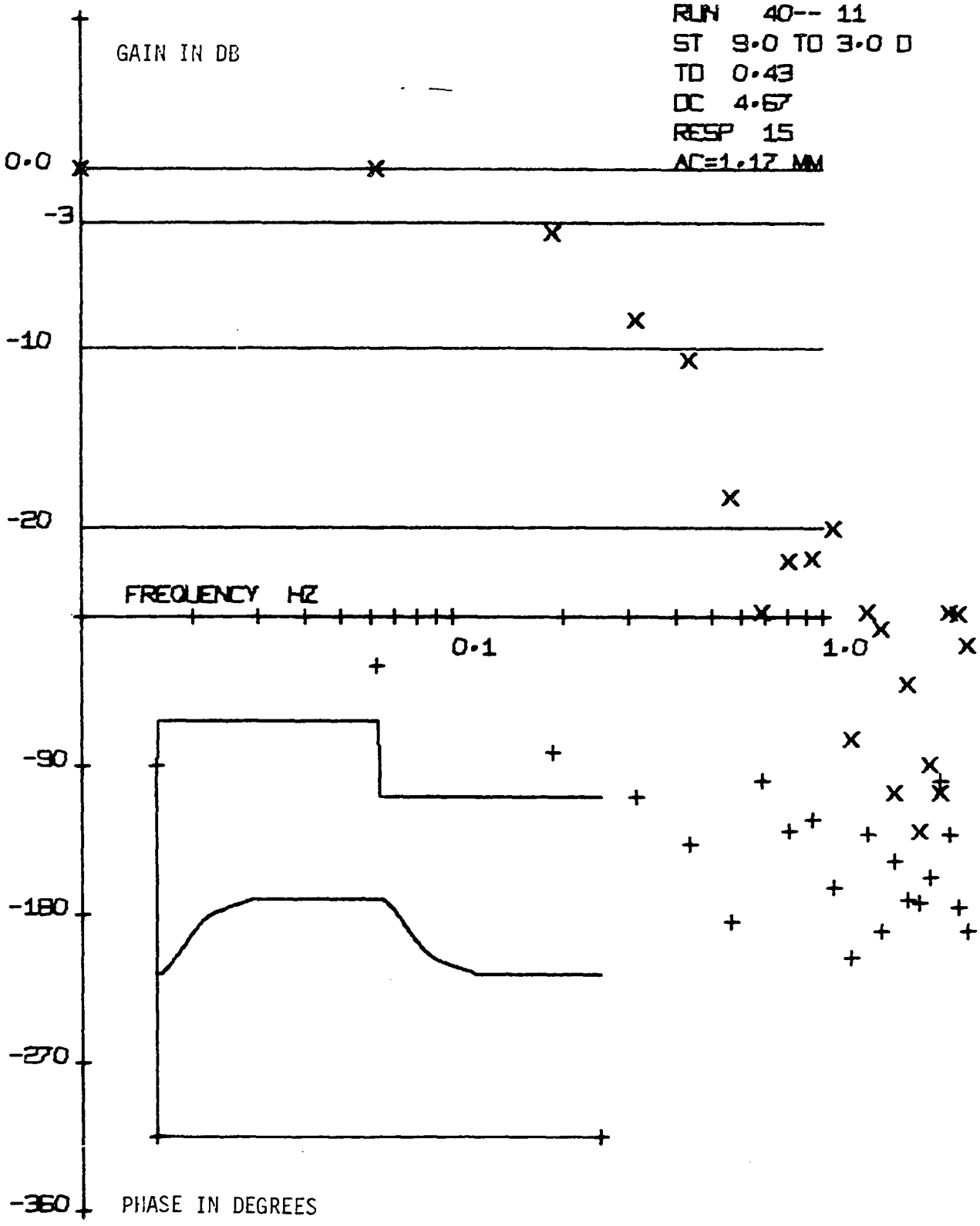
RUN 40-- 11
ST 9.0 TO 3.0 D
TD 0.43
DC 4.67
RESP 15
AC=1.17 MM
GAIN IN DB
0.0
-3
-10
-20
FREQUENCY HZ
0.1
1.0
-90
-180
-270
-360
PHASE IN DEGREES

Figure 43. This figure is the same as Figure 40 except that a time delay of 0.51 second has been removed

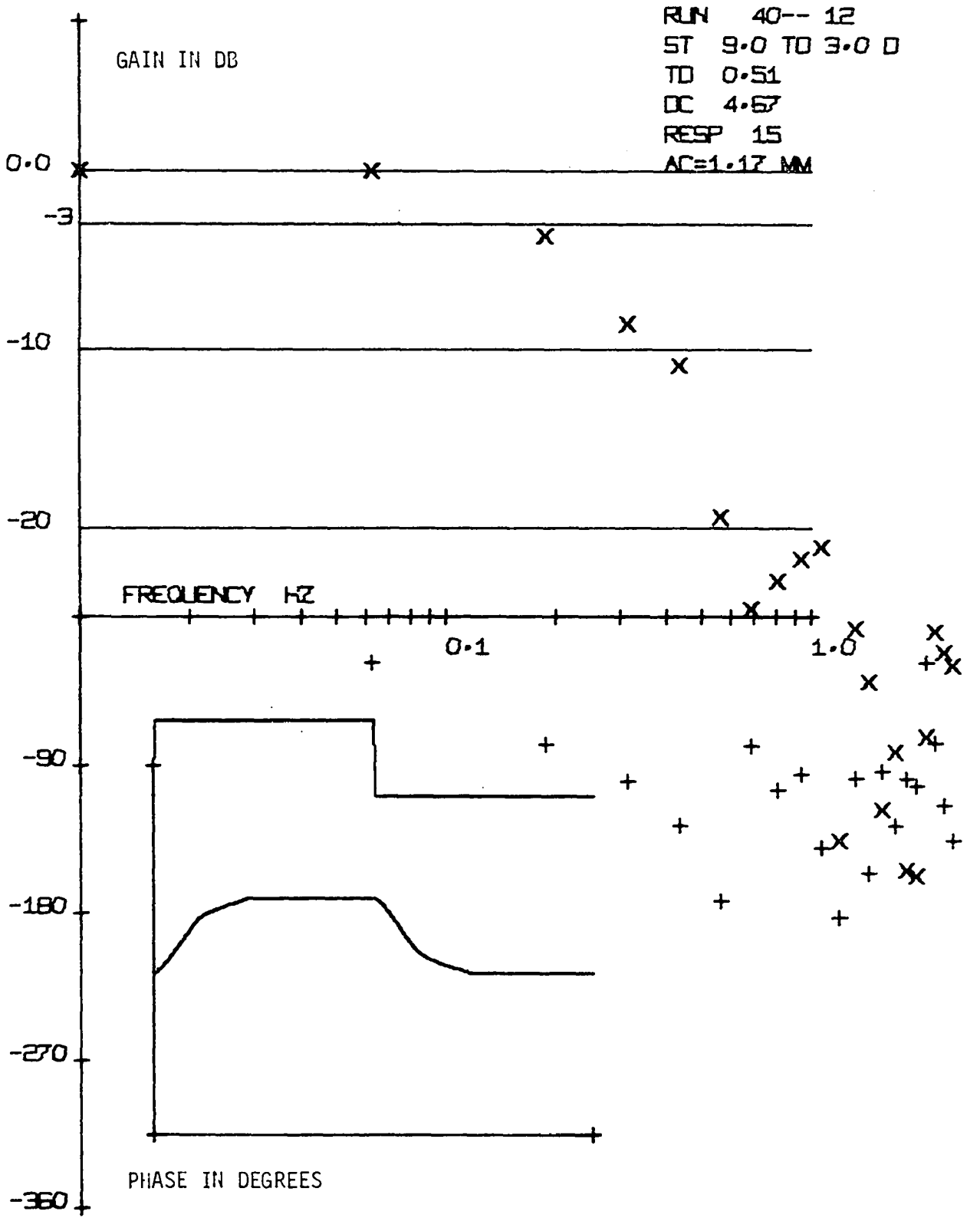
RUN 40-- 12
ST 9.0 TO 3.0 D
TD 0.51
DC 4.57
RESP 15
AC=1.17 MM
GAIN IN DB
0.0
-3
-10
-20
FREQUENCY HZ
0.1
1.0
-90
-180
-270
-360
PHASE IN DEGREES

Figure 44. A Bode plot of the accommodative-pupillary system after a time delay of 0.41 second was removed. The curved dark line in the gain portion of the figure is for a second-order system of the form $1/(s+a)^2$ where a=6.28 [1/sec.]. The dark line plotted in the phase section represents the phase curve of this transfer function. Correction for the interface phase error results in the same phase curve as that of the second-order system. The interface phase error is shown in Figure 8. A correction in the gain curve due to the interface equipment is not necessary. Since the 5.0D to 7.0D stimulus produces the smallest blur of 2.0D, it is assumed that the system will respond in a linear fashion at this level and that larger levels will exhibit nonlinearities

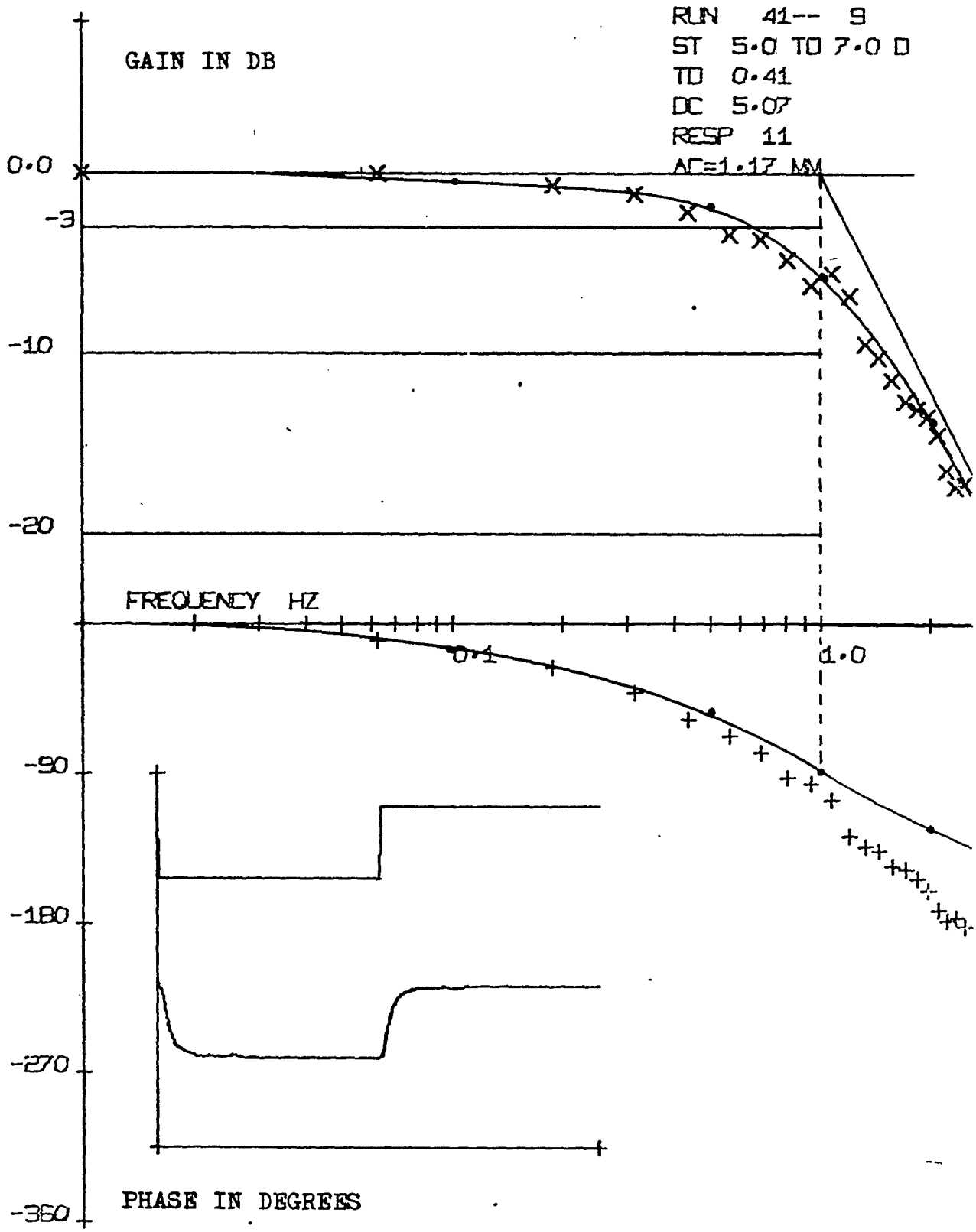
RUN 41-- 9
ST 5.0 TO 7.0 D
TD 0.41
DC 5.07
RESP 11
AC=1.17 MV
GAIN IN DB
0.0
-3
-10
-20
FREQUENCY HZ
0.1
1.0
-90
-180
-270
-360
PHASE IN DEGREES

Figure 45. The curved-dashed lines represent the second-order system of Figure 44. The solid lines represent the phase corrected and gain data for the 4.0D to 8.0D diopter accommodative stimulus. The spacing between the dashed and solid lines for each frequency is an indication of the nonlinearity in the dynamics

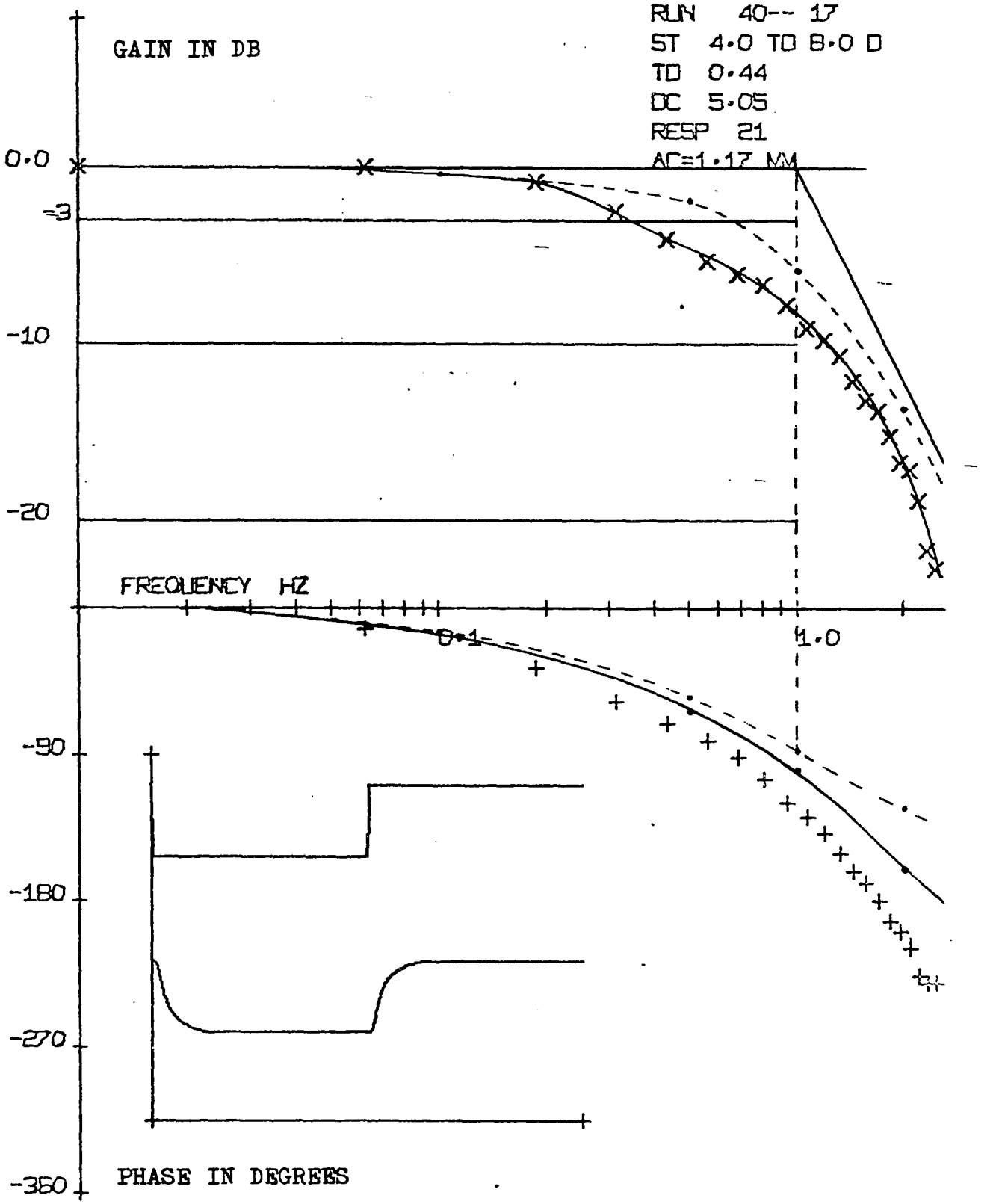
RUN 40-- 17
ST 4.0 TO 8.0 D
TD 0.44
DC 5.05
RESP 21
AC=1.17 MM
GAIN IN DB
0.0
-3
-10
-20
FREQUENCY HZ
0.1
1.0
-90
-180
-270
-360
PHASE IN DEGREES

Figure 46. The curved-dashed lines represent the second-order system of Figure 44. The solid lines represent the phase corrected and gain data for the 3.0D to 9.0D accommodative stimulus. The spacing between the dashed and solid lines for each frequency is an indication of the nonlinearity in the dynamics

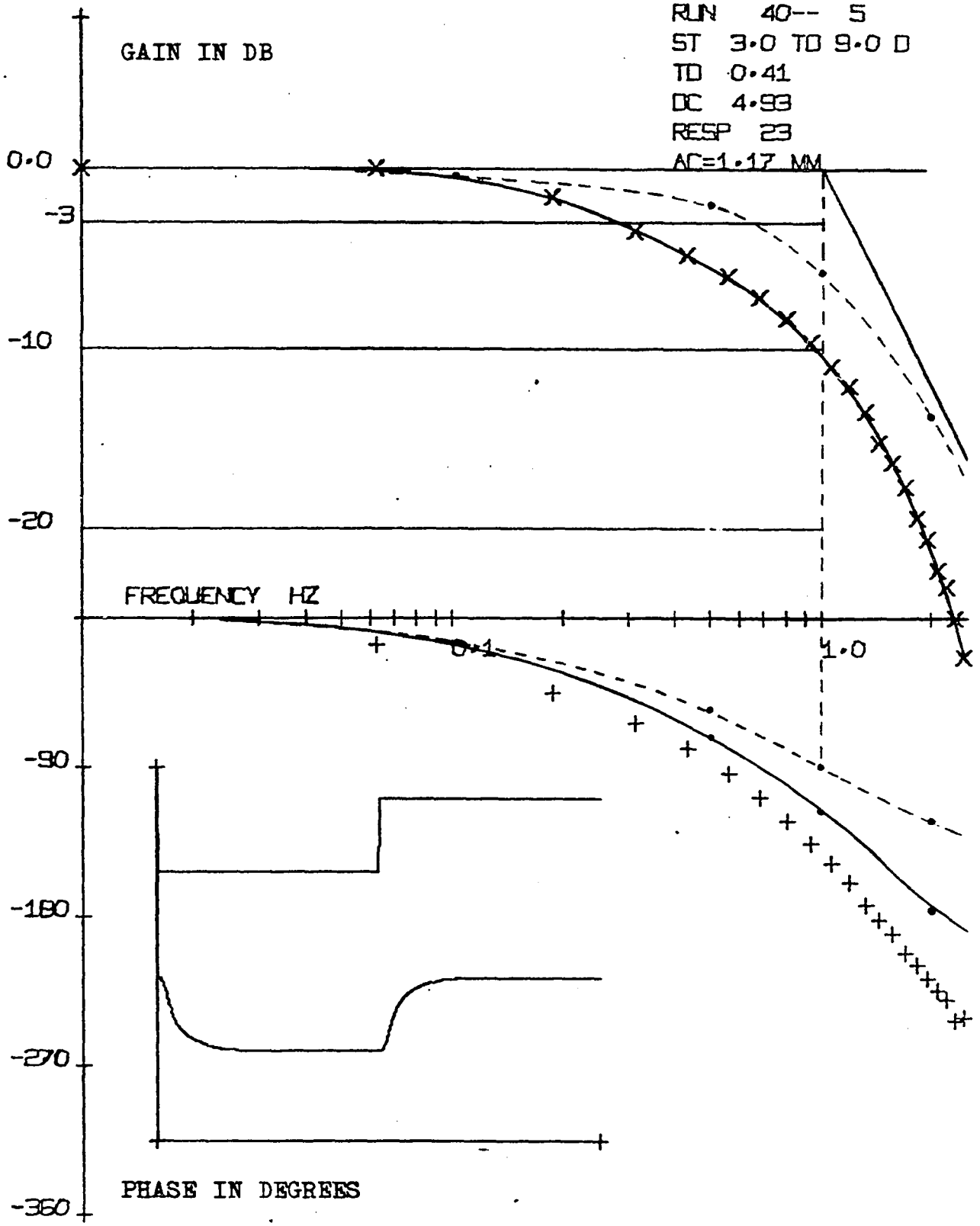
RUN 40-- 5
ST 3.0 TO 9.0 D
TD 0.41
DC 4.93
RESP 23
AC=1.17 MM
GAIN IN DB
0.0
-3
-10
-20
FREQUENCY HZ
0.1
1.0
-90
-180
-270
-360
PHASE IN DEGREES

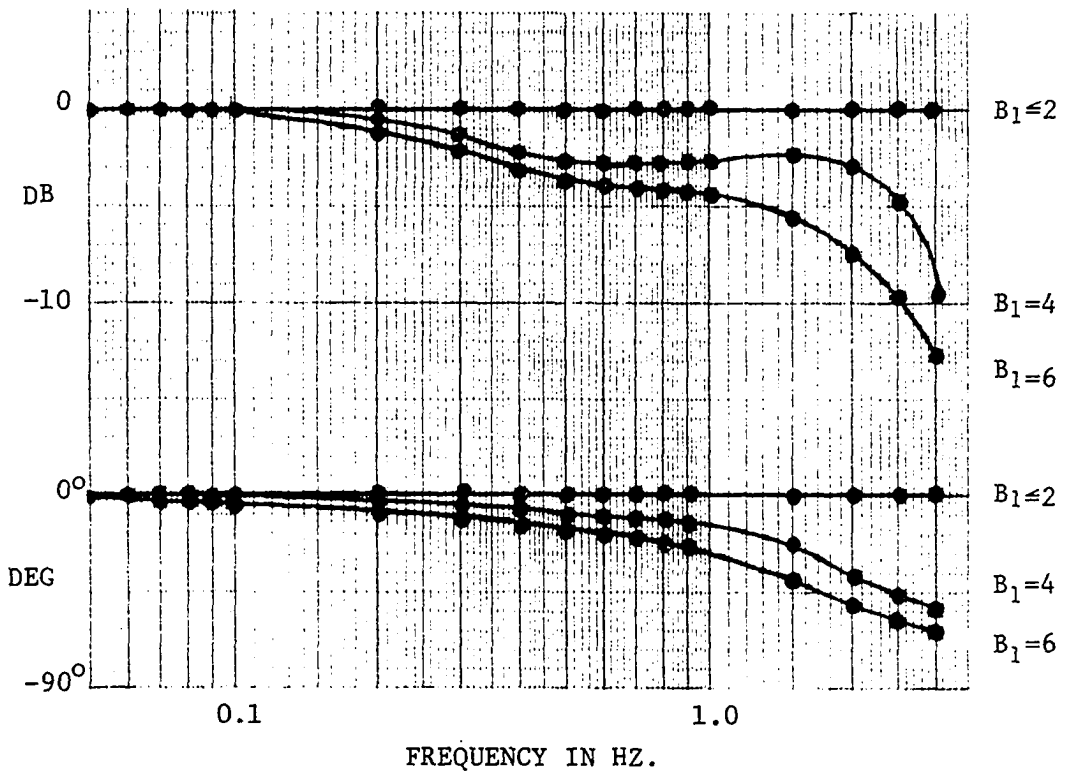

Figure 47. A plot of the nonlinearities resulting when Figures 45 and 46 are adjusted to the linear system indicated in Figure 44. It can be seen that a blur (B_1) of 2.0D or less does not involve a nonlinearity in the dynamics. It should be noted that a stimulus of 5.0D to 7.0D produces a blur of 2.0D. A stimulus of 4.0D to 8.0D produces a blur of 4.0D and a stimulus of 3.0D to 9.0D produces a blur of 6.0D

Figure 48. A Bode plot of the accommodative-pupillary system after a time delay of 0.41 second was removed. Both curved solid lines represent the gain and phase plots for a third-order linear system of the form $1/(s+a)^3$ where a=3.0 [1/sec.]. No corrections for interface phase error were used. The dilatative system is assumed linear for blurs of 2.0D or less

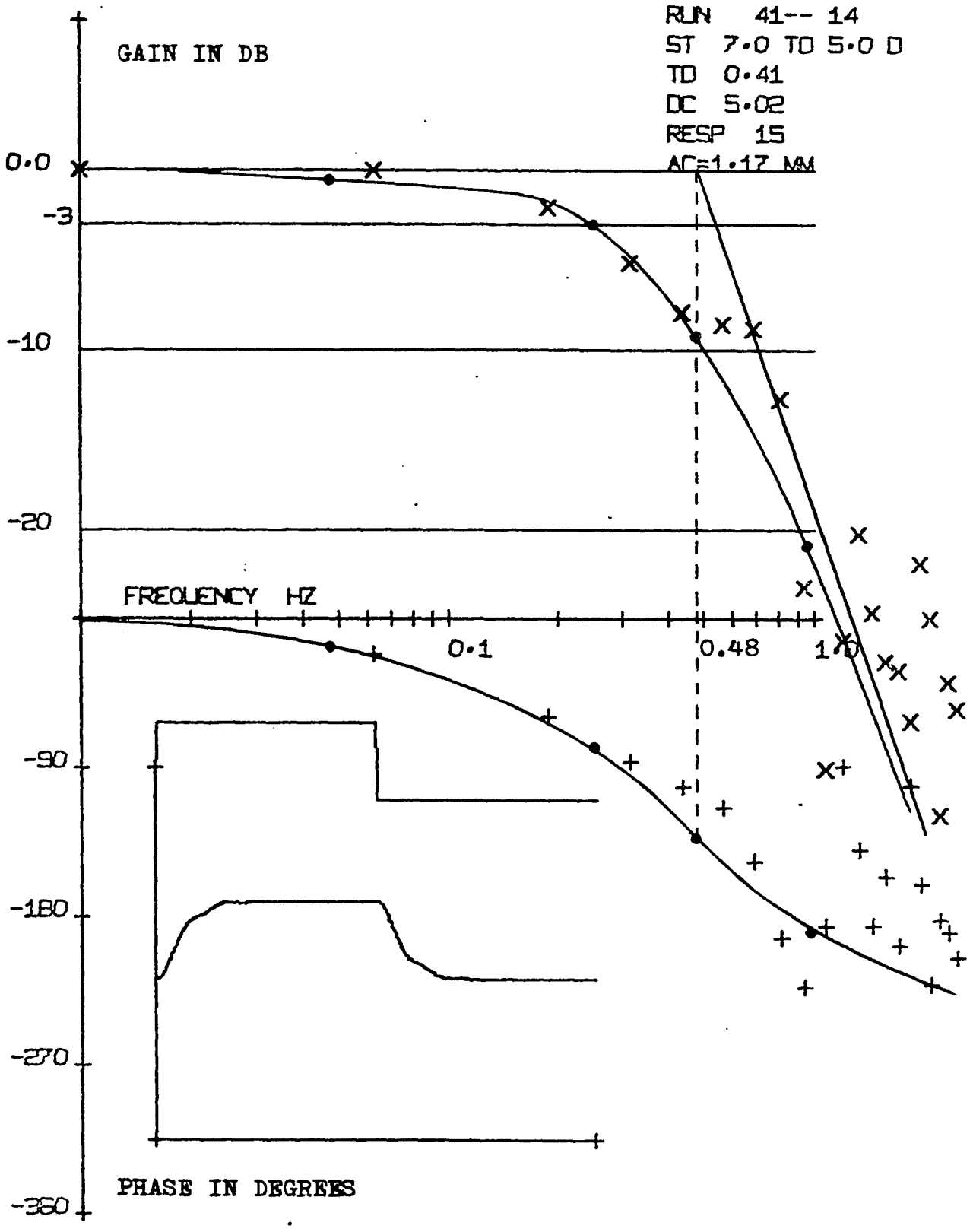
RUN 41-- 14
ST 7.0 TO 5.0 D
TD 0.41
DC 5.02
RESP 15
AC=1.17 MM
GAIN IN DB
0.0
-3
-10
-20
FREQUENCY HZ
0.1
0.48
1.0
-90
-180
-270
-360
PHASE IN DEGREES

Figure 49. The curved-dashed lines represent the third-order linear system of Figure 48. The solid lines represent the gain and phase data for the 8.0D to 4.0D accommodative stinulus. There appears to be little error in the phase, but the gain exhibits a nonlinearity in the dynamics

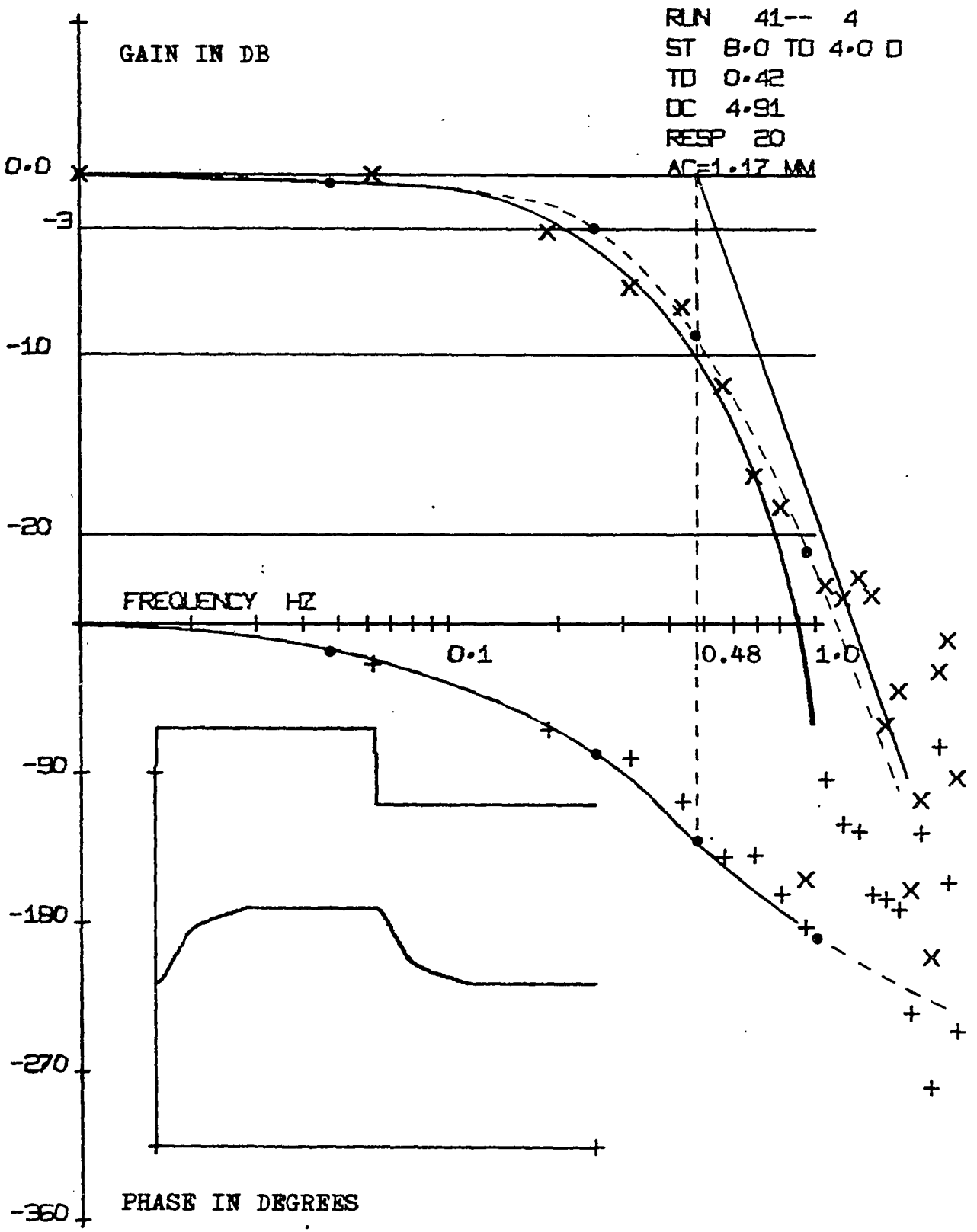
RUN 41-- 4
ST 8.0 TO 4.0 D
TD 0.42
DC 4.91
RESP 20
AC=1.17 MM
GAIN IN DB
0.0
-3
-10
-20
FREQUENCY HZ
0.1
0.48
1.0
-90
-180
-270
-360
PHASE IN DEGREES

Figure 50. The curved-dashed lines represent the third-order linear system of Figure 48. The solid lines represent the experimental gain and phase data for the 9.0D to 3.0D accommodative stimulus. A nonlinearity in both the gain and phase is noted

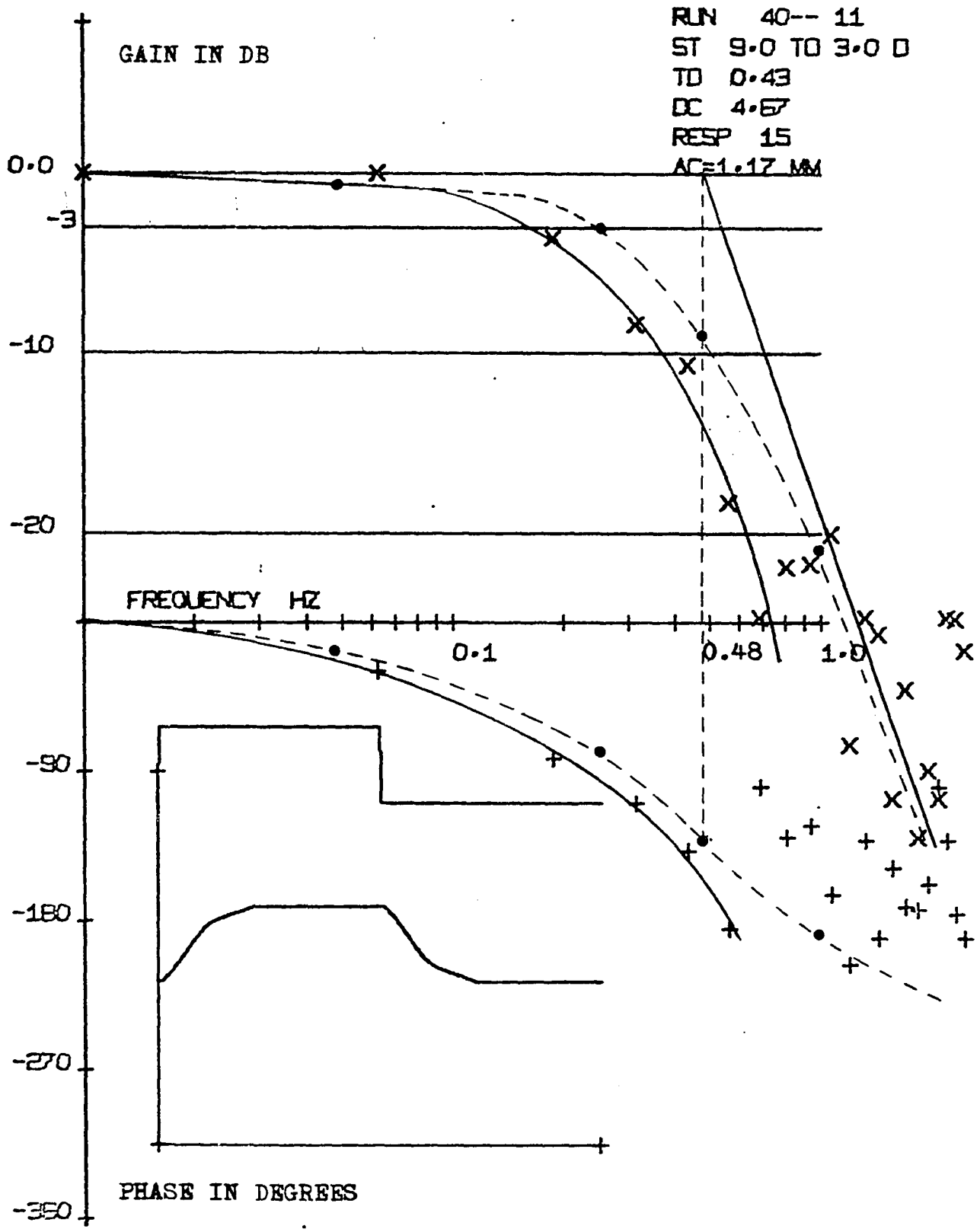
RUN 40-- 11
ST 9.0 TO 3.0 D
TD 0.43
DC 4.67
RESP 15
AC=1.17 MM
GAIN IN DB
0.0
-3
-10
-20
FREQUENCY HZ
0.1
0.48
1.0
-90
-180
-270
-360
PHASE IN DEGREES

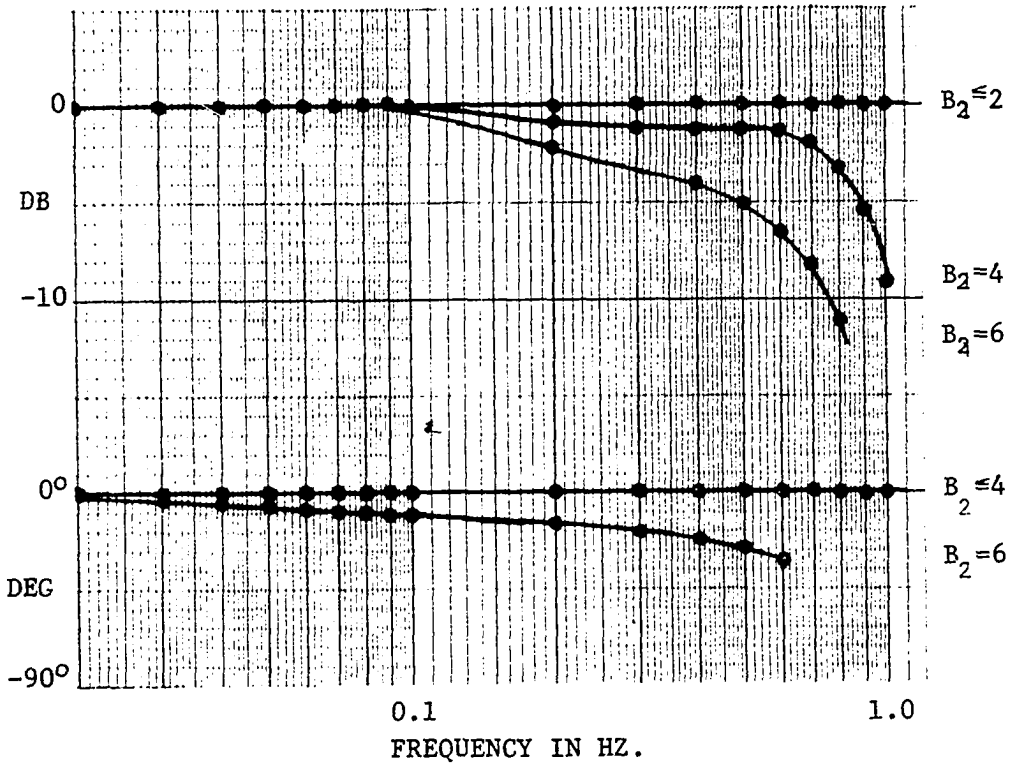

Figure 51. A plot of the nonlinearities resulting when Figures 49 and 50 are adjusted to the linear system indicated in Figure 48. It can be seen that a blur of 2.0D or less does not produce a nonlinearity in the gain and that a blur of 4.0D or less does not produce a nonlinearity in the phase

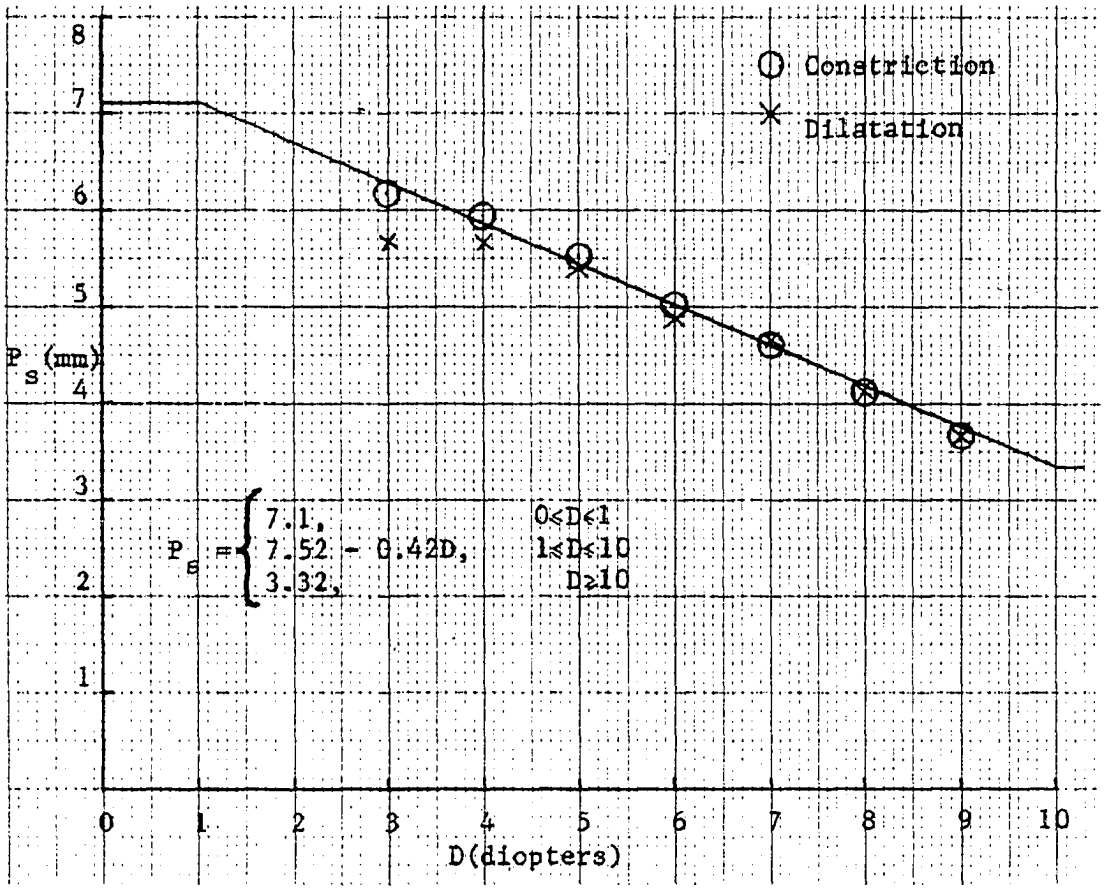

Figure 52. The static pupil diameter as a function of accommodation. This curve was established after the subject had undergone dark adaptation to a low level of red light. The curve was obtained from Figures 18-20 by measuring the static levels of pupil diameter as a function of accommodative level

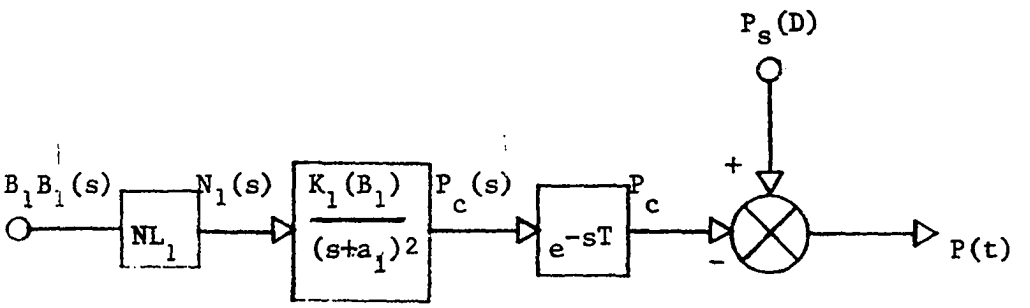

Figure 53. A nonlinear model for the constrictive accommodative-pupillary dynamics. The inputs to the system are blur, B_1[diopters], and static pupil diameter as a function of dioptric level, $P_s(D)$ [mm]. The Bode plot of the input-output relation for the nonlinearity NL_1 is given in Figure 47. The arbitrary output of the nonlinearity is $N_1(s)$. The nonlinearity is a function of the blur, B_1. The value for the time delay is T=0.4 second and a_1=6.28 [1/sec.]. A curve for the static pupil diameter as a function of dioptric level is given in Figure 52. B_1 is assumed zero until a change in accommodative level takes place. P(t) is the dynamic pupil response. This nonlinear model has not been simulated. The constant K_1 may be a function of the blur and has not been determined

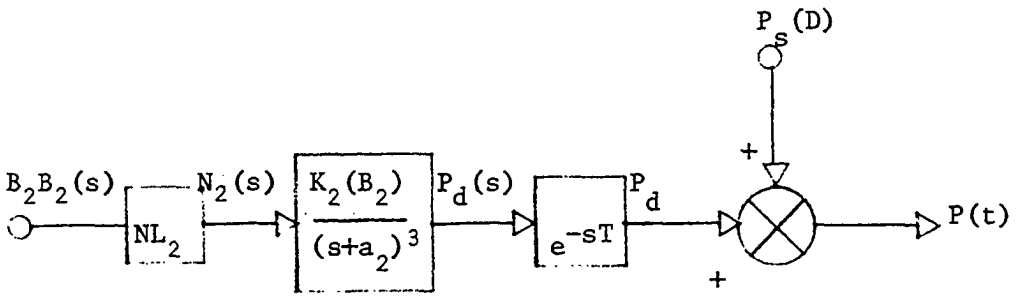

Figure 54. A nonlinear model for the dilatative accommodative-pupillary dynamics. The inputs to the system are blur, B_2[diopters], and static pupil diameter as a function of dioptric level D, $P_s(D)$[mm]. The Bode plot of the input-output relation for the nonlinearity NL_2 is given in Figure 51. The arbitrary output of the nonlinearity is $N_2(s)$. The nonlinearity is a function of the blur, B_1. The value for the time delay is T=0.4 second and a_2=3[1/sec.]. A curve for the static pupil diameter as a function of dioptric level D is given in Figure 52. B_2 is assumed zero until a change in accommodative level takes place. P(t) is the dynamic pupil response. This nonlinear model has not been simulated. The constant K_2 may be a function of the blur and has not been determined

Figure 55. The experimental (dark curves) and computed (dashed) curves for 5.0D to 7.0D and 7.0D to 5.0D pupillary responses. The values in parentheses are computed values. The values not in parentheses are experimental values. They represent the initial and final values of the constrictive and dilatative responses

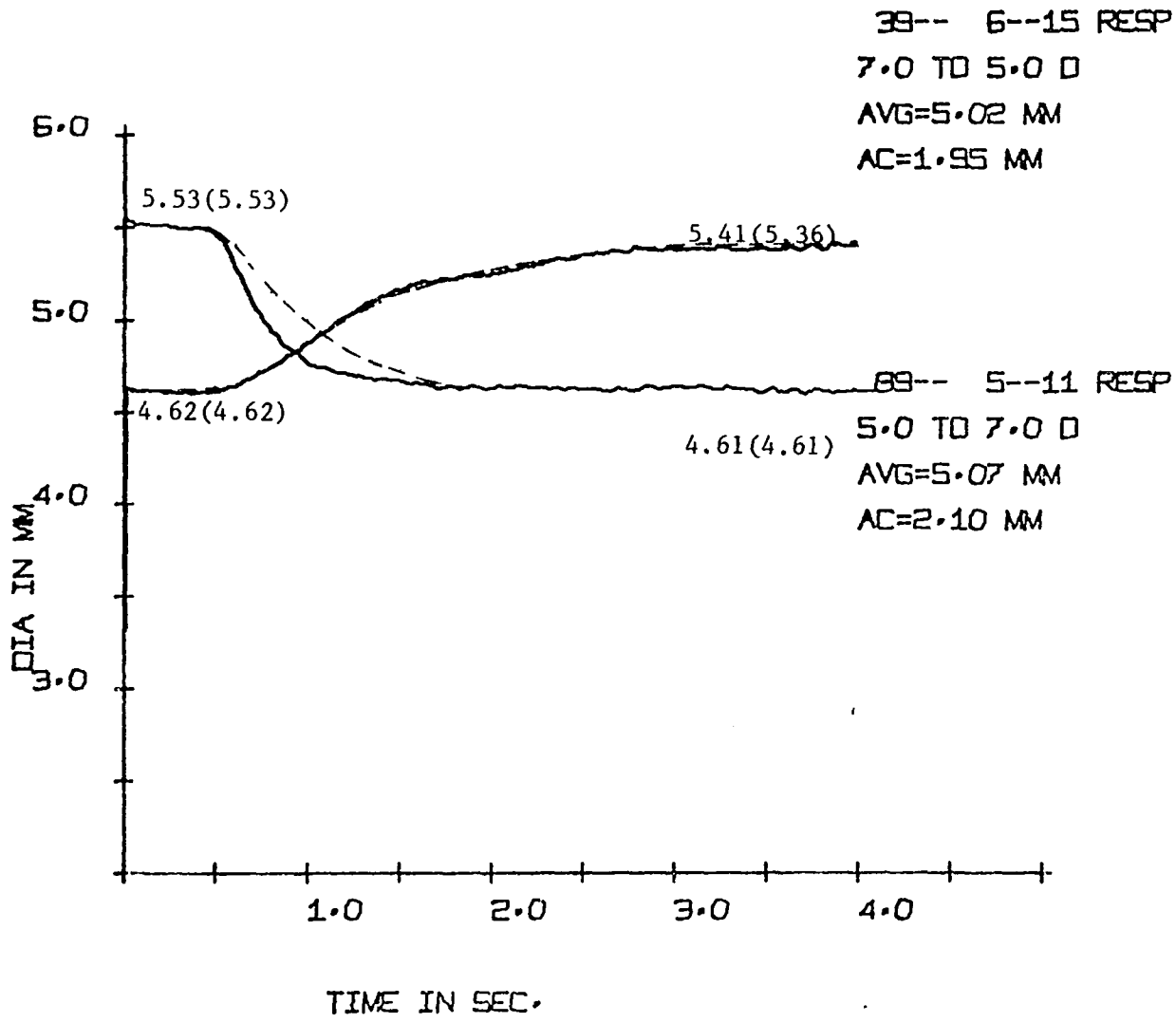
38-- 6--15 RESP
7.0 TO 5.0 D
AVG=5.02 MM
AC=1.95 MM
6.0
5.0
4.0
3.0
DIA IN MM
5.53(5.53)
5.41(5.36)
4.62(4.62)
4.61(4.61)
89-- 5--11 RESP
5.0 TO 7.0 D
AVG=5.07 MM
AC=2.10 MM
1.0
2.0
3.0
4.0
TIME IN SEC.

Figure 56. The experimental (dark curves) and computed (dashed) curves for 4.0D to 8.0D and 8.0D to 4.0D pupillary responses. The values in parentheses are computed values. The values not in parentheses are experimental values. They represent the initial and final values of the constrictive and dilatative responses

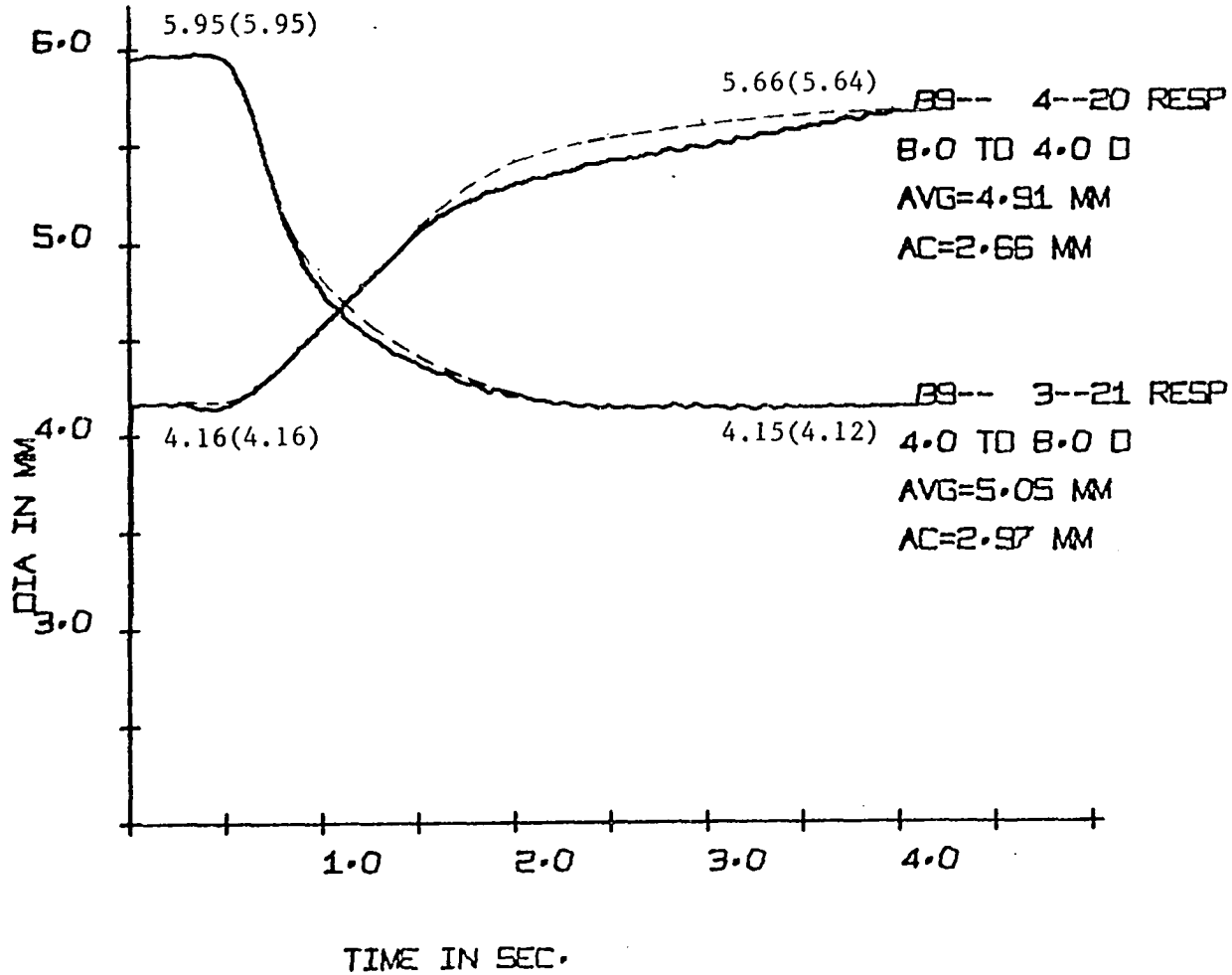
6.0
5.0
4.0
3.0
DIA IN MM
5.95(5.95)
5.66(5.64)
4.16(4.16)
4.15(4.12)
B9-- 4--20 RESP
8.0 TO 4.0 D
AVG=4.91 MM
AC=2.66 MM
B9-- 3--21 RESP
4.0 TO 8.0 D
AVG=5.05 MM
AC=2.97 MM
1.0
2.0
3.0
4.0
TIME IN SEC.

Figure 57. The experimental (dark curves) and computed (dashed) curves for 3.0D to 9.0D and 9.0D to 3.0D pupillary responses. The values in parentheses are computed values. The values not in parentheses are experimental values. They represent the initial and final values of the constrictive and dilatative responses

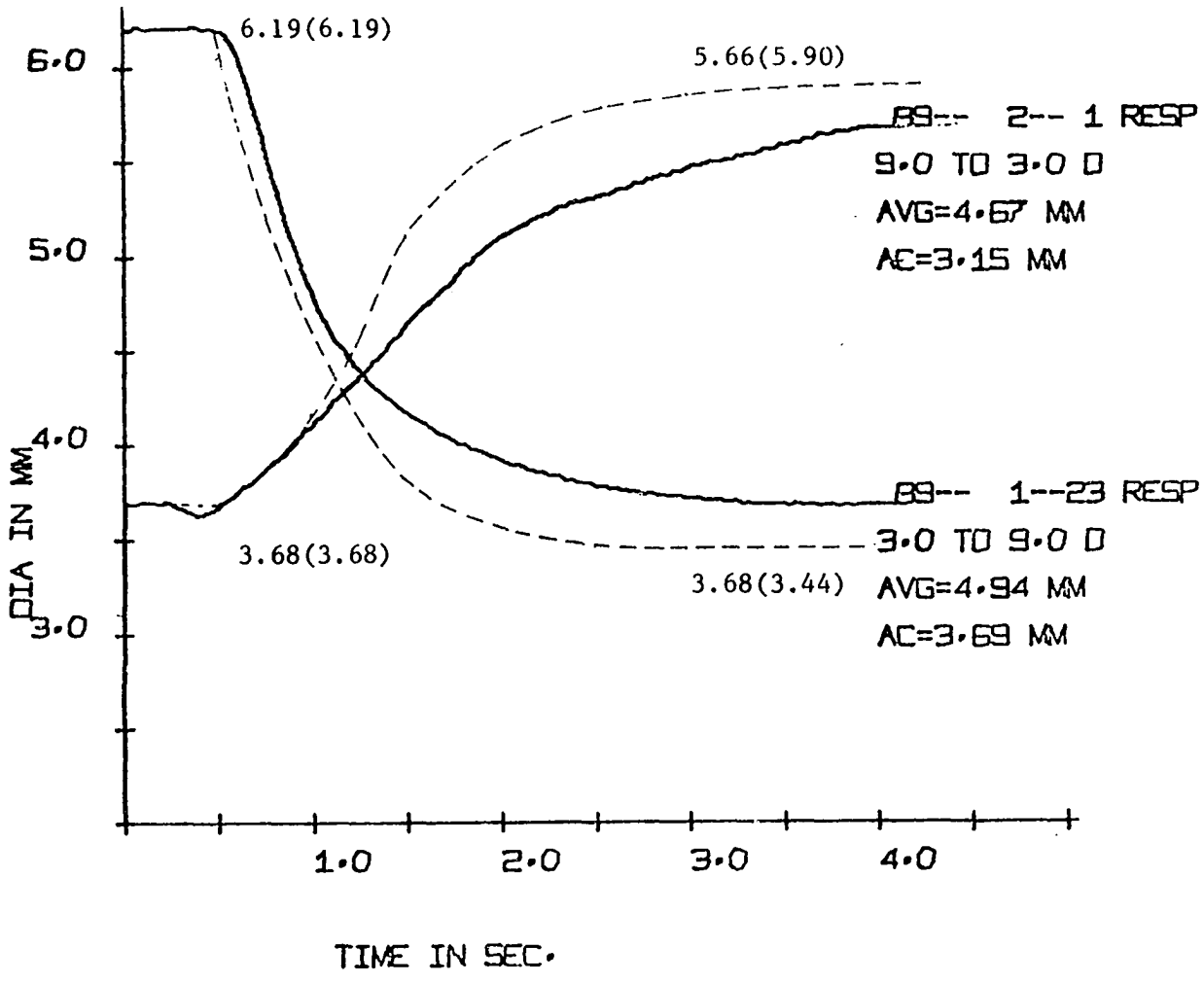
6.19(6.19)
5.66(5.90)
89-- 2-- 1 RESP
9.0 TO 3.0 D
AVG=4.67 MM
AC=3.15 MM
6.0
5.0
4.0
3.0
DIA IN MM
89-- 1--23 RESP
3.0 TO 9.0 D
AVG=4.94 MM
AC=3.69 MM
3.68(3.68)
3.68(3.44)
1.0
2.0
3.0
4.0
TIME IN SEC.

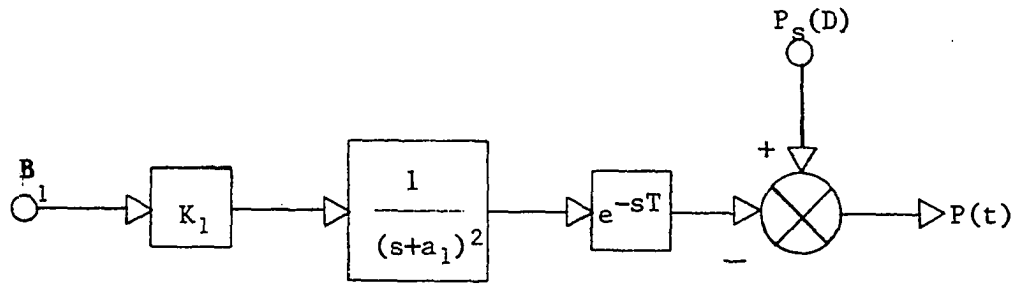

Figure 58. A linear model for the constrictive accommodative-pupillary dynamics. The inputs to the system are blur, B_1 [diopters], and static pupil diameter as a function of dioptric level, $P_s(D)$ [mm]. P(t) is the dynamic pupil response and is described by Equation 2 in the text. The value for the time delay is T=0.4 second and a_1=3.3 [1/sec.]. A curve for the static pupil diameter as a function of accommodative level is given in Figure 52. B_1 is positive and assumed zero until a step change in accommodation takes place. The constant has a value of K_1=5.0 [mm/D-sec.^{2}] for the blur levels of 2.0D, 4.0D and 6.0D. A comparison between the response of the model and the experimental data is given in Figures 55-57. The model response is shown by the dashed lines

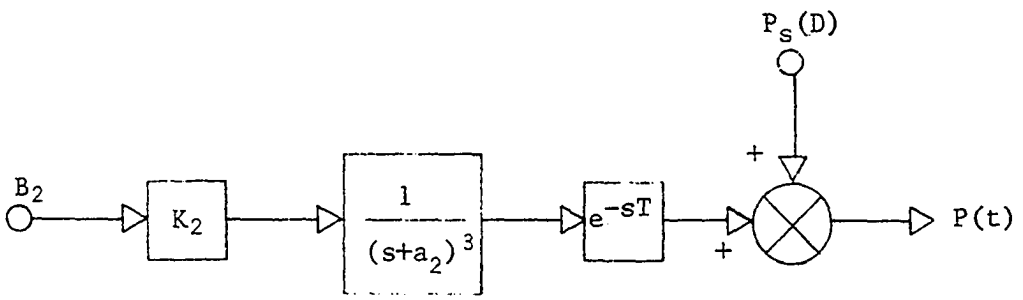

Figure 59. A linear model for the dilatative accommodative-pupillary dynamics. The inputs to the system are blur, B_2 [diopters], and static pupil diameter as a function of dioptric level, $P_s(D)$ [mm]. P(t) is the dynamic pupil response and is described by Equation 3 in the text. The value for the time delay is T=0.4 second and a_2=3.0 [1/sec.]. A curve for the static pupil diameter as a function of accommodative level is given in Figure 52. B_2 is positive and assumed zero until a step change in accommodation takes place. The constant has a vlue of K_2=5.0 [mm/D-sec.^{3}] for the blur levels of 2.0D, 4.0D and 6.0D. A comparison between the response of the model and the experimental data is given in Figures 55-57. The model response is shown by the dashed lines